

Daptomycin: studies on its action mode and on bacterial resistance with model membranes

by

Bradley I. Scott

A thesis
presented to the University of Waterloo
in fulfillment of the
thesis requirement for the degree of
Master of Science
in
Chemistry

Waterloo, Ontario, Canada, 2016

© Bradley I. Scott 2016

Author's Declaration

I hereby declare that I am the sole author of this thesis. This is a true copy of the thesis, including any required final revisions, as accepted by my examiners.

I understand that my thesis may be made electronically available to the public.

Abstract

Bacterial resistance to antibiotics is one of the most serious problems facing medicine today. Recently, reports have appeared describing bacteria that are resistant to daptomycin (dap), an important antibiotic used against systemic infections caused by various Gram-positive (Gram+) bacteria, including methicillin-resistant *Staphylococcus aureus* (MRSA). This has caused considerable concern amongst the medical community. With few medicines being developed to replace them, research on antibiotics of last resort is imperative.

Dap is a branched, cyclic lipodepsipeptide consisting of a 10-amino acid macrolactone ring to which is attached an exocyclic tripeptide bearing a decanoyl acyl tail. Its activity is calcium-dependent. The action mode best substantiated involves the killing of bacteria through specific interaction with phosphatidylglycerol (PG) in their cell membranes, followed by the formation of oligomeric, cation-selective pores and dissipation of membrane potential. The successive steps of the action mode have been investigated using fluorescence-based assays in model membranes. The steps include, 1) calcium-mediated binding of monomers to PG at the outer leaflet; 2) formation of oligomers; 3) formation of pores through equilibration and alignment of oligomers across both membrane leaflets. The assay fluorophores include the intrinsically fluorescent kynurenine residue in dap, and various environmentally sensitive labels attached to dap by chemical modification.

The objective of this work was to investigate three topics: the means by which lysyl-phosphatidylglycerol (LPG) disrupts the action mode of dap, the means through which dap induces toxicity in humans, and the characterization of synthetic dap analogs, including an acyl-linked dimer. LPG is of interest because its increased formation is a known resistance mechanism for many cationic antimicrobial peptides (CAMPs); it is also correlated to resistance to dap specifically. A potential component in dap-induced toxicity is presence of phosphatidylserine (PS) in mammalian tissues. PS is a major phospholipid, and was investigated due to its anionic properties, which may emulate bacterial PG. The characterization of synthetic dap analogs allows for the study of the structure-activity relationship (SAR) of dap. The LPG, PS and characterization studies were pursued using the aforementioned fluorescence assays on a model membrane system using large unilamellar vesicles (LUV; liposomes), and antibacterial activity assays as needed. LUVs may be substituted with *Bacillus subtilis* L-forms (cell wall deficient bacteria) when necessary. Deviations in the assay results on LPG liposomes give insight into the action mode step(s) impeded in LPG-mediated bacterial resistance. The

success or failure of the assays on PS membranes gives insight into the mechanism of toxicity via potential PS-mediated dap binding and permeabilization of mammalian cells. Characterization of the SAR of dap may lead to potential pharmacological improvements. Understanding these topics may also result in lipopeptides with improved activity on dap-resistant bacteria, modifications to the established mechanism of action, and suggestions for further investigations into dap toxicity.

In parallel and in combination with these experiments, it was investigated whether secondary interactions between peptidoglycan precursors and dap are of importance in its action mode; the macromolecular synthesis of the cell wall has long been suspected to play a part in the mechanism of action of dap, either through inhibition of peptidoglycan synthesis or binding of teichoic acids. The investigation was pursued using minimum inhibitory concentration (MIC) tests on *B. subtilis* L-forms. The MIC tests incorporate two antibiotics: one being dap, and the other to up- or down-regulate the abundance of a peptidoglycan precursor. *B. subtilis* L-forms are capable of growth in the absence of peptidoglycan, therefore its presence as a model organism is essential. The regulation of the abundance of the peptidoglycan precursors should increase or decrease the MIC of dap depending on its reliance on that precursor. Understanding the reliance of dap on cellular binding sites, may result in lipopeptides with improved activity on dap-resistant bacteria and modifications to the established mechanism of action.

Acknowledgements

Thank you to my supervisors, Dr. Scott Taylor and Dr. Michael Palmer for sharing their knowledge and supporting my research. The Taylor and Palmer labs have both been welcoming; thank you to all present and past members. I would like to give special thanks to Robert Taylor, Braden Kralt, Oscar Zhang and Eric Brefo-Mensah.

I also appreciate the input and time my committee members, Dr. Guy Guillemette and Dr. John Honek, have contributed to my project.

Finally, I would thank my family for their support and encouragement.

Table of Contents

Author's Declaration	ii
Abstract	iii
Acknowledgements	v
Table of Contents	vi
List of Figures	viii
List of Tables	xiv
List of Abbreviations	xv
Chapter 1 Introduction: antibiotics, daptomycin and L-forms	1
1.1 The history of antibiotics	1
1.1.1 Action modes of select antibiotics	3
1.1.2 Mechanisms of resistance	11
1.2 Daptomycin.....	13
1.2.1 Clinical use.....	14
1.2.2 The acidic lipopeptides	15
1.2.3 Biosynthesis	16
1.2.4 Mechanism of action.....	17
1.2.5 Daptomycin analogs.....	25
1.2.6 Mechanisms of resistance	27
1.3 Discovery of bacterial L-forms	31
1.3.1 Creation of <i>B. subtilis</i> PDC 134, an efficient producer of L-forms	31
Chapter 2 Characterizing an acyl-linked dimer of daptomycin	33
2.1 Introduction.....	33
2.2 Materials and Methods.....	34
2.2.1 Preparation of liposomes.....	34
2.2.2 Preparation of <i>B. subtilis</i> PDC 134 L-forms for fluorescence studies	35
2.2.3 Fluorescence studies	35
2.2.4 Determining the antibacterial activity of antibiotics	36
2.3 Results.....	36
2.4 Discussion.....	40
Chapter 3 Characterizing synthetic analogs of daptomycin.....	42
3.1 Introduction.....	42

3.2 Material and Methods.....	44
3.3 Results	44
3.3.1 Dap-E12-W13 and dap-E12-Y13 membrane binding	46
3.3.2 Dap-E12-Y13 oligomer formation	49
3.3.3 Dap-A7-E12-W13 antibacterial activity and membrane binding	51
3.3.4 Dap-E12-W13 surfactant sequestration.....	51
3.4 Discussion	53
Chapter 4 Characterizing lysyl-phosphatidylglycerol-mediated daptomycin resistance.....	56
4.1 Introduction	56
4.2 Materials and Methods	57
4.2.3 Measurement of membrane permeabilization with pyranine-loaded liposomes	58
4.3 Results	58
4.4 Discussion	65
Chapter 5 Investigating the role of phosphatidylserine in daptomycin-induced toxicity	67
5.1 Introduction	67
5.2 Materials and Methods	68
5.3 Results	68
5.4 Discussion	72
Chapter 6 Characterizing the reliance of daptomycin on peptidoglycan precursors	73
6.1 Introduction	73
6.2 Materials and Methods	75
6.2.1 Isolation of <i>B. subtilis</i> PDC 134 N-forms.....	75
6.2.2 Isolation of <i>B. subtilis</i> PDC 134 L-forms	76
6.2.4 Determining the antibacterial activity of daptomycin in the presence of other antibiotics	77
6.3 Results	78
6.3.1 The difference in antibacterial activity between <i>B. subtilis</i> L-forms and N-forms	78
6.3.2 The reliance of daptomycin and nisin on <i>B. subtilis</i> PDC 134 peptidoglycan precursors... ..	79
6.4 Discussion	82
6.5 Conclusion.....	83
Permissions.....	84
References	85
Appendix A Raw fluorescence figures.....	98

List of Figures

Figure 1.1: The progress of antibacterial development. Each antibiotic represents a new drug class at the date of their initial discoveries. ¹³	2
Figure 1.2: Cell wall and membrane structure of Gram ⁺ and Gram ⁻ bacteria, and mycobacteria.	4
Figure 1.3: Simplified biosynthesis of peptidoglycan.....	5
Figure 1.4: Fosfomycin, PEP, and glycerophosphate structures. Uptake of fosfomycin and PEP are mediated by the glycerophosphate transporter.....	6
Figure 1.5: Cycloserine inhibits the two enzymes which successively produce the D-alanyl-D-alanine dipeptide used in the production of the precursors to lipid I.....	6
Figure 1.6: Deactivation of peptidoglycan transpeptidases by ampicillin occurs through covalent bond formation with the active site serine residue.....	7
Figure 1.7: Sequestration of D-alanyl-D-alanine dipeptide by vancomycin.....	8
Figure 1.8: Structure of chloramphenicol, and its binding position within the peptidyl transferase site of the ribosome.	9
Figure 1.9: Structure of the lantibiotic nisin.	10
Figure 1.10: The structures of dap and A21978C ₁₋₃ at physiological pH.....	14
Figure 1.11: The structure of A5 Factor D at physiological pH.	16
Figure 1.12: Structures of phosphatidylglycerol (PG) and phosphatidylcholine (PC).	17
Figure 1.13: The structures of A5 and dap analogs used in the demonstration of oligomer formation on liposome model membranes.	19
Figure 1.14: Schematic of the pyranine-based liposome permeabilization assay.	21
Figure 1.15: Model of dap on liposomes, with and without CL.	22
Figure 1.16: NBD-dap fluorescence quenching assay, using dithionite.	23
Figure 1.17: Fluorescence spectra of tryptophan from A5 (<i>left</i>) and acrylodan from A5-acrylodan (<i>right</i>) in the presence of 70:30 PC:PG liposomes and increasing Ca ²⁺ concentration (mM) at 37 °C.....	24
Figure 1.18: Mean tryptophan wavelength emission of A5 compared to maximum fluorescence intensity of A5-acrylodan emission (I ₄₇₂), each as a function of Ca ²⁺ concentration. Liposome composition is 50:50 PC:PG. Legend: A5A refers to A5-acrylodan.	24
Figure 1.19: Model for the mode of MprF-mediated bacterial CAMP resistance. ⁹⁶	29
Figure 1.20: Structures of cardiolipin (CL) and lysyl-phosphatidylglycerol (LPG).....	30
Figure 2.1: Structure of the acyl-linked dap dimer.	34

Figure 2.2: Kynurenine fluorescence spectra of dap and the dap dimer in the presence of 70:30 PC:PG liposomes and increasing Ca^{2+} concentration (mM) at 37 °C.	37
Figure 2.3: Kynurenine fluorescence of dap and dap dimer on liposomes of varying composition at 37 °C.....	37
Figure 2.4: Kynurenine fluorescence of dap and dap dimer on PDC 134 L-forms at 30 °C.....	39
Figure 3.1: Initial dap analogs synthesized through SPPS: dap-E12-W13, dap-E12-Y13, and dap-A7-E12-W13.	43
Figure 3.2: Kynurenine fluorescence of Dap and Dap-SPPS on liposomes of varying composition at 37 °C.....	45
Figure 3.3: Tryptophan fluorescence spectra of dap-E12-W13 and dap-E12-Y13 in the presence of 70:30 PC:PG liposomes and increasing Ca^{2+} concentration (mM) at 37 °C.	46
Figure 3.4: Mean tryptophan wavelength emission of dap-E12-W13 (left) and Dap-E13-Y13 (right) compared to maximum fluorescence intensity of dap emission (I_{442}), each as a function of Ca^{2+} concentration.	47
Figure 3.5: Tryptophan fluorescence spectrum of A5 in the presence of 70:30 PC:PG liposomes and increasing Ca^{2+} concentration (mM) at 37 °C.	48
Figure 3.6: Tryptophan fluorescence of A5, dap-E12-W13, dap-E12-Y13 on liposomes of varying composition at 37 °C.	48
Figure 3.7: Pyrene fluorescence spectrum of A5-pyrene in the presence of 50:50 PC:PG liposomes and increasing Ca^{2+} concentration (mM) at 37 °C.	49
Figure 3.8: Excimer formation comparison of A5-pyrene and dap-E12-Y13-pyrene on liposomes of varying composition at 37 °C.	50
Figure 3.9: Fluorescence spectrum of dap-A7-E12-W13 in the presence of 50:30 PC:PG liposomes and increasing Ca^{2+} concentration (mM) at 37 °C.	51
Figure 3.10: Comparison of dap (<i>left</i>) and A5 (<i>right</i>) on PC/PG liposomes and 1% surfactant. The figures follow	52
Figure 3.11: Comparison of dap-E12-W13 on PC/PG liposomes and 1% surfactant.	53
Figure 4.1: Kynurenine fluorescence of dap on liposomes of varying composition at 37 °C; the exception is the 55% PC, 30% PG, 15% LPG membrane under ambient conditions (~25 °C).	59
Figure 4.2: Tryptophan fluorescence of A5 on liposomes of varying composition at 37 °C; the exception is the 55% PC, 30% PG, 15% LPG membrane under ambient conditions (~25 °C).....	60

Figure 4.3: Excimer formation comparison of A5-pyrene on liposomes of varying composition at 37 °C; the exception is the 55% PC, 30% PG, 15% LPG membrane under ambient conditions (~25 °C).	61
Figure 4.4: Fluorescence spectrum of A5-acrylodan in the presence of 70:30 PC:PG liposomes and increasing Ca ²⁺ concentration (mM) at 37 °C.....	62
Figure 4.5: Acrylodan fluorescence of A5-acrylodan on liposomes of varying composition at 37 °C; the exception is the 55% PC, 30% PG, 15% LPG membrane under ambient conditions (~25 °C).....	63
Figure 4.6: Liposome permeabilization tests using 0.5 uM of multiple lipopeptide analogs in the presence of pyranine-loading liposomes, 5 (or 100) mM Ca ²⁺ and 5 nM CCCP at 25 °C.....	64
Figure 5.1: Structure of dimyristoyl phosphatidylserine.....	67
Figure 5.2: Kynurenine fluorescence of dap on liposomes of varying composition at 37 °C.	69
Figure 5.3: Comparison of NBD-dap (<i>left</i>) and dap-perylene (<i>right</i>) on a 70:30 PC:PS membrane at 37 °C.	69
Figure 5.4: : Tryptophan fluorescence of A5 on liposomes of varying composition at 37 °C.....	70
Figure 5.5: Comparison of A5-acrylodan (<i>left</i>) and A5-pyrene (<i>right</i>) on liposomes of varying composition at 37 °C.....	71
Figure 6.1: Schematic of peptidoglycan synthesis, and the antibiotics which inhibit it at different stages of production.....	74
Figure 6.2: (A) One colony of PDC 134 N-forms grown in LB broth supplemented with 0.5% xylose, and 20 µg/mL chloramphenicol. (B) PDC 134 N-forms subcultured in MSM LB broth (C) PDC 134 N- and L-forms subcultured into MSM LB broth supplemented with 75 µg/mL ampicillin, giving a pure L-form culture.....	77
Figure 6.3: Fluorescence spectrum of dap in the presence of 50:50 PC:PG liposomes and increasing Ca ²⁺ concentration (mM) at 37 °C.	98
Figure 6.4: Fluorescence spectrum of dap in the presence of 70:30 PC:PG liposomes and increasing Ca ²⁺ concentration (mM) at 37 °C.	98
Figure 6.5: Fluorescence spectrum of solid-phase synthesis dap in the presence of 50:50 PC:PG liposomes and increasing Ca ²⁺ concentration (mM) at 37 °C.....	99
Figure 6.6: Fluorescence spectrum of dap dimer in the presence of 70:30 PC:PG liposomes and increasing Ca ²⁺ concentration (mM) at 37 °C.....	99
Figure 6.7: Fluorescence spectrum of dap-E12-Y13 in the presence of 50:50 PC:PG liposomes and increasing Ca ²⁺ concentration (mM) at 37 °C.....	100

Figure 6.8: Fluorescence spectrum of dap-E12-Y13-pyrene in the presence of 50:50 PC:PG liposomes and increasing Ca^{2+} concentration (mM) at 37 °C.....	100
Figure 6.9: Fluorescence spectrum of dap-perylene in the presence of 70:30 PC:PG liposomes and increasing Ca^{2+} concentration (mM) at 37 °C.	101
Figure 6.10: Fluorescence spectrum of A5 in the presence of 50:50 PC:PG liposomes and increasing Ca^{2+} concentration (mM) at 37 °C.....	101
Figure 6.11: Fluorescence spectrum of A5-acrylodan in the presence of 50:50 PC:PG liposomes and increasing Ca^{2+} concentration (mM) at 37 °C.	102
Figure 6.12: Fluorescence spectrum of A5-pyrene in the presence of 70:30 PC:PG liposomes and increasing Ca^{2+} concentration (mM) at 37 °C.	102
Figure 6.13: Fluorescence spectrum of dap in the presence of 55:30:15 PC:PG:LPG liposomes and increasing Ca^{2+} concentration (mM) under ambient conditions (~25 °C).....	103
Figure 6.14: Fluorescence spectrum of A5 in the presence of 55:30:15 PC:PG:LPG liposomes and increasing Ca^{2+} concentration (mM) under ambient conditions (~25 °C).....	103
Figure 6.15: Fluorescence spectrum of A5-acrylodan in the presence of 55:30:15 PC:PG:LPG liposomes and increasing Ca^{2+} concentration (mM) under ambient conditions (~25 °C).....	104
Figure 6.16: Fluorescence spectrum of A5-pyrene in the presence of 55:30:15 PC:PG:LPG liposomes and increasing Ca^{2+} concentration (mM) under ambient conditions (~25 °C).	104
Figure 6.17: Fluorescence spectrum of dap in the presence of 70:30 PC:LPG liposomes and increasing Ca^{2+} concentration (mM) at 37 °C.....	105
Figure 6.18: Fluorescence spectrum of A5 in the presence of 70:30 PC:LPG liposomes and increasing Ca^{2+} concentration (mM) at 37 °C.....	105
Figure 6.19: Fluorescence spectrum of A5-acrylodan in the presence of 70:30 PC:LPG liposomes and increasing Ca^{2+} concentration (mM) at 37 °C.	106
Figure 6.20: Fluorescence spectrum of A5-pyrene in the presence of 70:30 PC:LPG liposomes and increasing Ca^{2+} concentration (mM) at 37 °C.	106
Figure 6.21: Fluorescence spectrum of dap in the presence of 70:30 PC:PS liposomes and increasing Ca^{2+} concentration (mM) at 37 °C.....	107
Figure 6.22: Fluorescence spectrum of NBD-dap in the presence of 70:30 PC:PS liposomes and increasing Ca^{2+} concentration (mM) at 37 °C.	107
Figure 6.23: Fluorescence spectrum of dap-perylene in the presence of 70:30 PC:PS liposomes and increasing Ca^{2+} concentration (mM) at 37 °C.	108

Figure 6.24: Fluorescence spectrum of A5 in the presence of 70:30 PC:PS liposomes and increasing Ca ²⁺ concentration (mM) at 37 °C.	108
Figure 6.25: Fluorescence spectrum of A5-acrylodan in the presence of 70:30 PC:PS liposomes and increasing Ca ²⁺ concentration (mM) at 37 °C.	109
Figure 6.26: Fluorescence spectrum of A5-pyrene in the presence of 70:30 PC:PS liposomes and increasing Ca ²⁺ concentration (mM) at 37 °C.	109
Figure 6.27: Fluorescence spectrum of dap in the presence of 100% PC liposomes and increasing Ca ²⁺ concentration (mM) at 37 °C.	110
Figure 6.28: Fluorescence spectrum of dap-E12-W13 in the presence of 100% PC liposomes and increasing Ca ²⁺ concentration (mM) at 37 °C.	110
Figure 6.29: Fluorescence spectrum of dap-E12-Y13 in the presence of 100% PC liposomes and increasing Ca ²⁺ concentration (mM) at 37 °C.	111
Figure 6.30: Fluorescence spectrum of A5 in the presence of 100% PC liposomes and increasing Ca ²⁺ concentration (mM) at 37 °C.	111
Figure 6.31: Fluorescence spectrum of A5-acrylodan in the presence of 100% PC liposomes and increasing Ca ²⁺ concentration (mM) at 37 °C.	112
Figure 6.32: Fluorescence spectrum of dap in the presence <i>B. subtilis</i> PDC 134 L-forms (OD ₆₀₀ = 0.8) and increasing Ca ²⁺ concentration (mM) at 30 °C.	112
Figure 6.33: Fluorescence spectrum of dap dimer in the presence <i>B. subtilis</i> PDC 134 L-forms (OD ₆₀₀ = 0.8) and increasing Ca ²⁺ concentration (mM) at 30 °C.	113
Figure 6.34: Fluorescence spectrum of NBD-dap in the presence <i>B. subtilis</i> PDC 134 L-forms (OD ₆₀₀ = 0.8) and increasing Ca ²⁺ concentration (mM) at 30 °C.	113
Figure 6.35: Fluorescence spectrum of dap-perylene in the presence <i>B. subtilis</i> PDC 134 L-forms (OD ₆₀₀ = 0.8) and increasing Ca ²⁺ concentration (mM) at 30 °C.	114
Figure 6.36: Fluorescence spectrum of dap in the presence <i>B. subtilis</i> PDC 134 N-forms (OD ₆₀₀ = 0.4) and increasing Ca ²⁺ concentration (mM) at 30 °C.	114
Figure 6.37: Fluorescence spectrum of A5 in the presence 1% BLES and increasing Ca ²⁺ concentration (mM) at 30 °C.	115
Figure 6.38: Fluorescence spectrum of dap in the presence of 1% BLES and increasing Ca ²⁺ concentration (mM) at 30 °C.	115
Figure 6.39: Fluorescence spectrum of dap-E12-W13 in the presence of 1% BLES and increasing Ca ²⁺ concentration (mM) at 30 °C.	116

Figure 6.40: Liposome permeabilization test controls for the multiple lipopeptide analogs at 25 °C.
..... 116

Figure 6.41: Liposome permeabilization test using dap in the presence of 5 mM Ca²⁺ and 5 nM CCCP at 25 °C..... 117

Figure 6.42 Liposome permeabilization test using dap-E12-W13 in the presence of 5 mM Ca²⁺ and 5 nM CCCP at 25 °C. 117

Figure 6.43 Liposome permeabilization test using dap-E12-Y13 in the presence of 5 (or 100) mM Ca²⁺ and 5 nM CCCP at 25 °C. 118

Figure 6.44 Liposome permeabilization test using A5 in the presence of 5 mM Ca²⁺ and 5 nM CCCP at 25 °C..... 118

Figure 6.45 Liposome permeabilization test using A5-Pyrene in the presence of 5 mM Ca²⁺ and 5 nM CCCP at 25 °C..... 119

List of Tables

Table 1.1: Mechanism of action of select antibiotics.....	11
Table 1.2: Mechanism of resistance of selected antibiotics.....	13
Table 2.1: Fluorophore, excitation wavelength, and emission range of relevant lipopeptide analogs.	36
Table 2.2: MIC ($\mu\text{g}/\text{mL}$) of dap and dap dimer on <i>B. subtilis</i> strains.....	38
Table 2.3: MIC ($\mu\text{g}/\text{mL}$) assay results using dap and the dap dimer at 5 and 100 mM Ca^{2+} on <i>B. subtilis</i> ATCC 1046.....	39
Table 3.1: Fluorophore, excitation wavelength, and emission range of relevant lipopeptide analogs.	44
Table 3.2: MIC ($\mu\text{g}/\text{mL}$) assay results of various lipopeptide analogs at 5 and 100 mM Ca^{2+} on <i>B. subtilis</i> ATCC 1046.	45
Table 3.3: MIC ($\mu\text{g}/\text{mL}$) of lipopeptides in the absence and presence of lung surfactant on <i>B. subtilis</i> ATCC 1046.....	52
Table 3.4: Antibacterial activities of select dap analogs produced by different groups. Only relevant amino acid positions are listed. MIC ratio refers to the MIC of the analog divided by the MIC of native dap.....	55
Table 4.1: Fluorophore, excitation wavelength, and emission range of relevant lipopeptide analogs.	57
Table 5.1: Fluorophore, excitation wavelength, and emission range of relevant lipopeptide analogs.	68
Table 6.1: Antibiotics and their effect on peptidoglycan presurcors and dap activity. Dap activity changes assume it binds to the affected peptidoglycan precursor. UC indicates unchanged.....	75
Table 6.2: MIC ($\mu\text{g}/\text{mL}$) of <i>B. subtilis</i> strains ATCC 1046 and PDC 134. PDC 134 includes both N- and L-form.	76
Table 6.3: MIC ($\mu\text{g}/\text{mL}$) of various antibiotics on <i>B. subtilis</i> ATCC 1046 and PDC 134 L-forms and N-forms.....	79
Table 6.4: MIC ($\mu\text{g}/\text{mL}$) of dap in the prescence of peptidoglycan precursor modulating antibiotics and 5 mM calcium, on <i>B. subtilis</i> PDC 134 L-forms.	80
Table 6.5: MIC ($\mu\text{g}/\text{mL}$) of dap on <i>B. subtilis</i> PDC 134 L-forms, in the prescence of media with differing composition, but always supplemented with 5 mM Ca^{2+}	80
Table 6.6: MIC ($\mu\text{g}/\text{mL}$) of nisin on <i>B. subtilis</i> PDC 134 L-forms, in the prescence of media with differing composition.....	82

List of Abbreviations

A site	Aminoacyl site
A-domain	Adenylation domain
A5	A54145 (Factor D)
ATP	Adenosine triphosphate
Abu	2-aminobutyric acid
Acrylodan	6-acryloyl-2-dimethylaminonaphthalene
Ala	Alanine
Asn	Asparagine
Asp	Aspartic acid
BLES	Bovine lung extract surfactant
<i>B. subtilis</i>	<i>Bacillus subtilis</i>
C-domain	Condensation domain
CAMP	Cationic antimicrobial peptide
CDA	Calcium-dependent antibiotic
CD	Circular dichroism
CL	Cardiolipin
Cat	Chloramphenicol resistance gene
CoA	Coenzyme A
DXDG	Aspartic acid – X – Aspartic acid – Glycine
Dap	Daptomycin
Dha	Didehydroalanine
Dhb	Didehydroaminobutyric acid
<i>E. coli</i>	<i>Escherichia coli</i>
<i>E. faecalis</i>	<i>Enterococcus faecalis</i>
E site	Exit site
E-domain	Epimerization domain
FA	Fatty acid
FDA	Food and Drug Administration
FRET	Fluorescence resonance energy transfer

GlmT	Glutamate 3-methyltransferase
Glu	Glutamate
Gly	Glycine
Gram+	Gram-positive
Gram-	Gram-negative
HBS	HEPES-buffered saline
HDP	Host defense peptide
HEPES	2-[4-(2-hydroxyethyl)piperazin-1-yl]ethanesulfonic acid
HO-Asn	3-hydroxyasparagine
HPLC	High-performance liquid chromatography
ITC	Isothermal titration calorimetry
Ile	Isoleucine
K ⁺	Potassium
Lac	Lactate
Kyn	Kynurenine
LB	Luria-Bertani
LPG	lysyl-phosphatidylglycerol 1,2-dioleoyl- <i>sn</i> -glycero-3-[phospho- <i>rac</i> -(3-lysyl(1-glycerol))]
LPS	Lipopolysaccharide
LUV	Large unilamellar vesicles
Lan; Ala-S-Ala	Lanthionine
Lys	Lysine
MeGlu	(2 <i>S</i> ,3 <i>R</i>)-3-methylglutamate
MeLan; Abu-S-Ala	Methyl-lanthionine
MeOAsp	3-methoxyaspartic acid
MIC	Minimum inhibitory concentration
MprF	Multiple peptide resistance factor
mraY	Phosphor-MurNAc-pentapeptide translocase
mRNA	Messenger RNA
MRSA	Methicillin-resistant <i>Staphylococcus aureus</i>
MSM	Maleic acid, sucrose, magnesium chloride
MurA	UDP-N-acetylglucosamine-3-O-enolpyruvyl transferase

MurNAc	N-acetylmuramic acid
NBD	Nitrobenzoxadiazole
NRPS	Non-ribosomal peptide synthetase
OD	Optical density
Orn	Ornithine
P site	Peptidyl site
PBPs	Penicillin-binding proteins
PC	Phosphatidylcholine 1,2-dimyristoyl- <i>sn</i> -glycero-3-phosphocholine
PE	Phosphatidylethanolamine
PEP	Phosphoenolpyruvate
PG	Phosphatidylglycerol 1,2-dimyristoyl- <i>sn</i> -glycero-3-phospho-(1'- <i>rac</i> -glycerol)
PS	phosphatidylserine 1,2-dimyristoyl- <i>sn</i> -glycero-3-phospho-L-serine
P _{xyI}	Xylose promoter
Pyranine	trisodium 8-hydroxypyrene-1,3,6-trisulfonate
RNA	Ribonucleic acid
Sar	Sarcosine
SAR	Structure-activity relationship
<i>S. aureus</i>	<i>Staphylococcus aureus</i>
Ser	Serine
<i>S. fradiae</i>	<i>Streptomyces fradiae</i>
<i>S. pneumoniae</i>	<i>Streptococcus pneumoniae</i>
SPPS	Solid phase peptide synthesis
<i>S. roseosporus</i>	<i>Streptomyces roseosporus</i>
Sulfa	Sulfonamide
TE-domain	Thioesterase domain
T-domain	Thiolation domain
Thr	Threonine
Tricine	N-(2-Hydroxy-1,1-bis(hydroxymethyl)ethyl)glycine
Triton X-100	Polyethylene glycol p-(1,1,3,3-tetramethylbutyl)-phenyl ether

tRNA	Transfer RNA
Trp	Tryptophan
Tyr	Tyrosine
UDP	Uridine diphosphate
Val	Valine
WHO	World Health Organization
XylR	Xylose repressor

Chapter 1

Introduction: antibiotics, daptomycin and L-forms

Since 1977, the World Health Organization (WHO) has maintained the Model List of Essential Medicines.¹⁻³ Essential medicines were first defined as “of utmost importance, basic, indispensable, and necessary for the health and needs of the population.”¹⁻³ A year later at the Alma Ata conference, the provision of essential medicines was declared one of the eight elements of primary health care.^{2,3} The list has been updated on average every 2 years; the most recently released is, as of now, the 19th edition in April of 2015. The medicines are selected by criteria of disease relevance, evidence of efficacy and safety, and cost-effectiveness.²⁻⁴ Since its inception, the list has included a multitude of antibiotics, which are our main defense against bacterial infections. Nonetheless, the problem of antibacterial resistance has been increasing.

The list of essential medicines now contains antibiotics of last resort for “the treatment of life-threatening hospital-based infection due to suspected or proven multidrug-resistant infection.”⁴ These include medicines such as vancomycin and imipenem. Clinical bacterial isolates resistant to vancomycin, and imipenem, have already long been discovered.^{5,6} In May 2015, the World Health Assembly endorsed the WHO’s global action plan on antimicrobial resistance⁷. The WHO calls to “strengthen knowledge through surveillance and research” and to “optimize the use of antimicrobial agents.”⁷

In 2003, the FDA approved daptomycin (dap; section 1.2), the most recent antibiotic belonging to a new class of antibacterials. Dap soon became a powerful antibiotic against the multi-drug resistant “superbug” methicillin-resistant *Staphylococcus aureus* (MRSA). Unfortunately, resistance has already been seen in clinical bacterial isolates subjected to dap.^{8,9} With few medicines being developed to replace them, research on these antibiotics of last resort is imperative. This thesis will investigate various aspects of dap, this includes: the means by which lysyl-phosphatidylglycerol (LPG) disrupts its action mode, whether phosphatidylserine (PS) is related to dap-induced toxicity in humans, the characterization of synthetic dap analogs to further the structure-activity relationship (SAR) of dap residues, and its reliance on peptidoglycan precursors in its mode of action.

1.1 The history of antibiotics

Antibiotics were first developed in the early 20th century. Paul Ehrlich had been devoted to early anti-trypanosome (eukaryotic human parasite) chemicals, but had begun work with bacteria by 1907.^{10,11}

Ehrlich asserted substances may act as a “magic bullet” and eliminate pathogenic bacteria through a selective affinity for their cells.^{10,11} By 1909, his group had discovered Salvarsan (arsphenamine), an anti-syphilis drug, through large-scale drug screening.¹¹ Salvarsan and its modifications remained the standard treatment for syphilis until the first sulfonamide (sulfa) drug, Prontosil rubrum, was developed in the mid-1930s.^{10,11} Sulfa drugs dominated the market until the work of Alexander Fleming, which was underway in the late 1920s, came to fruition in the 1940s with the release of penicillin G.^{11,12} Penicillin G (benzylpenicillin) was the first antibiotic in the penicillin class, which is itself a class within the broader family of β -lactam antibiotics.

The discovery of these initial drugs, and the pressures of the Second World War, led to an antibiotic era now called the “Golden Age”.^{13,14} The discoveries of this era are summarized by Silver¹³ in a timeline spanning over a hundred years (Figure 1.1). The most abundant discoveries were made in the 1940s through to the 1960s; the years following 1987 are characterized by a “discovery void”.

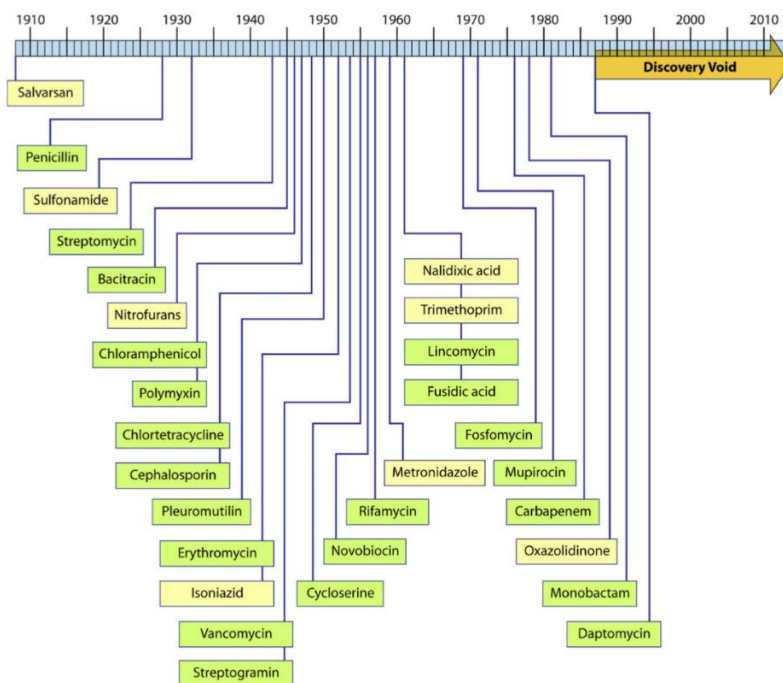


Figure 1.1: The progress of antibacterial development. Each antibiotic represents a new drug class at the date of their initial discoveries.¹³

During the discovery void, new antibiotics have come to market. However, in all cases this has been due to class modifications rather than novel discoveries; the general antibiotic class of these drugs had already been discovered.¹³ This includes dap, which came to market in 2003, but whose class was first

reported in 1987 and resides at the edge of the discovery void.^{13,15} The decline in novel discoveries results from a decrease in research from large pharmaceutical companies, highly profitable improvements from class modification, and higher screening costs.¹³ In regards to screening costs, Baltz¹⁶ recounts the difficulties encountered by GlaxoSmithKline researchers in screening chemical libraries against multiple potential Gram-positive (Gram+) or broad spectrum targets.

Over 300 genes were evaluated, and 160 were found to be essential for viability. They screened against 67 target proteins covering a wide range of cellular metabolic activities, and 16 yielded hits, but only 5 yielded leads... Of these, peptide deformylase, FabH, and FabI are proven targets for antibiotics produced by actinomycetes or fungi, leaving only two (3%) as potentially new targets. The authors noted that: 'The level of success was unsustainably low in relation to the large effort invested'

In spite of the lack of new antibiotic classes during the discovery void, the widespread use of antibacterials has continued to decrease morbidity and mortality from infectious diseases.¹⁷ Some have predicted that this trend will reverse as resistance to antibiotics increases, eventually giving rise to a "post-antibiotic era".¹⁷ Ehrlich saw early evidence of resistance in his work with trypanosomes: the red dye fuchsin lost trypanocidal activity after prolonged application.¹⁰ Salvarsan, his first antibacterial drug, did not initially encounter the same difficulties. However, Prontosil and the other sulfa drugs have since seen widespread resistance.¹¹ Penicillin G suffered the same outcome; within a few years of its introduction, fifty percent of *Staphylococcus aureus* bacteria were no longer susceptible.¹⁷ As the development of antibiotics has progressed, so has resistance. Across the world multidrug-resistant bacteria, or "super bugs", have been found in clinical isolates. It is now acknowledged that it is simply a matter of time before bacterial resistance threatens new antibiotics.

1.1.1 Action modes of select antibiotics

Antibiotics have a wide variety of action modes. However, they usually fall within four broad classes, three of which consist in the inhibition of enzymes involved in: (1) peptidoglycan synthesis (2) protein synthesis and (3) nucleic acid synthesis, regulation, or repair. Common enzyme targets include transpeptidases, transglycosylases, topoisomerases, RNA polymerase and peptidyl transferases. The fourth mechanism involves disruption of the bacterial cell membrane. Below, antibiotics in three of the four classes will be discussed. The examples are limited, but relevant, to the research discussed throughout this thesis. For an overview, refer to Table 1.1.

Inhibitors of peptidoglycan synthesis

The contents of Gram+ bacteria are enclosed by a system composed of a cell membrane and cell wall (Figure 1.2). Gram-negative (Gram-) bacteria have developed a more complex system, which includes an additional outer membrane. In both, the cell membrane(s) consists of lipids, and the cell wall is made of peptidoglycan.

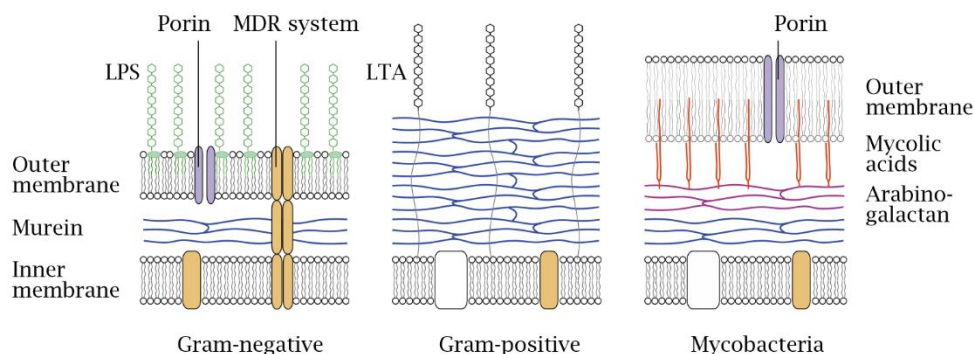


Figure 1.2: Cell wall and membrane structure of Gram+ and Gram- bacteria, and mycobacteria. LPS: lipopolysaccharide, LTA: lipoteichoic acid, MDR: multi-drug resistance (efflux) system.¹⁸

Peptidoglycan, also called murein, is a highly organized and peptide cross-linked carbohydrate polymer. Its synthesis occurs through several successive enzyme-catalyzed steps (Figure 1.3). The backbone is composed of alternating β -1,4-linked N-acetylglucosamine (GlcNAc) and N-acetylmuramic acid (MurNAc) carbohydrate units. The peptide cross-links contain varying L- or D-amino acids; alanine (Ala), lysine (Lys) and glycine (Gly) are often present.

The biosynthetic enzymes of peptidoglycan provide high specific activity against bacteria within mammalian tissues, as they are absent from eukaryotic cells. However, in these environments the rigid peptidoglycan layer is required to prevent osmotic lysis; the bacterial cytosol is of higher osmotic activity than mammalian tissues, resulting in the influx of water and high osmotic pressure.¹⁹ Consequently, the loss or weakening of the integrity of the peptidoglycan layer within mammalian tissue by the action modes of antibiotics can cause osmotic lysis of the bacterial cells.

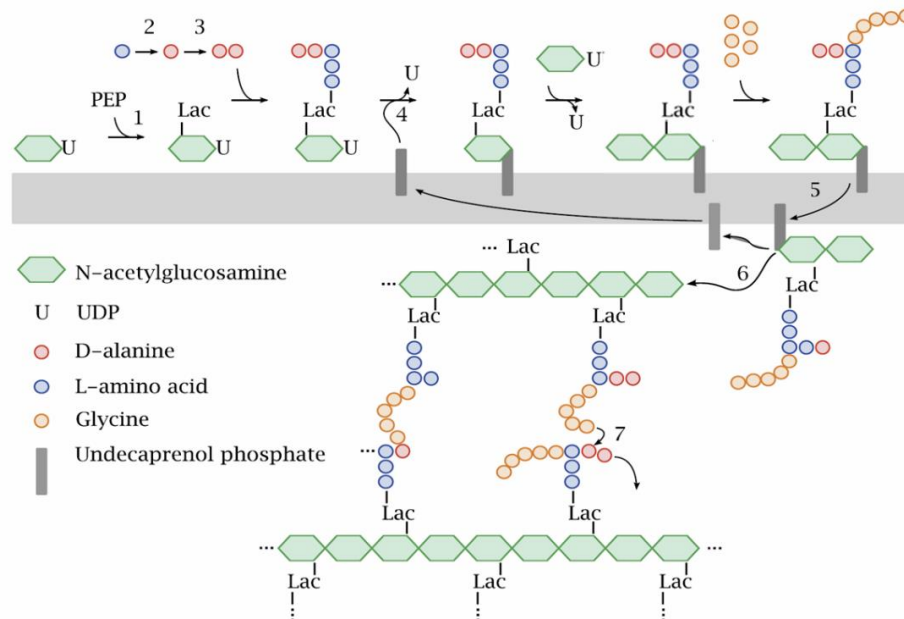


Figure 1.3: Simplified biosynthesis of peptidoglycan: (I) Phosphoenolpyruvate (PEP) supplies a lactate residue (Lac) to GlcNAc, yielding MurNac [UDP-GlcNAc-enolpyruvyltransferase; murA (1)]. (II) A pentapeptide containing a terminal D-Ala dipeptide is built onto MurNac [L-Ala racemase (2) and Ala ligase (3)]. (III) The building block is transferred to undecaprenol phosphate, yielding lipid I [phosphor-MurNac-pentapeptide translocase; mraY (4)]. (IV) The building block is extended with GlcNAc and glycine, yielding lipid II, and flipped across the membrane [lipid II flippase (5)]. (V) Lipid II is transferred to a growing strand with a transglycosylase (6). (VI) The final transpeptidase reaction (7) crosslinks the strands. Light gray: cell membrane, UDP: uridine diphosphate.¹⁸

Fosfomycin. The first step of peptidoglycan synthesis (Figure 1.3 I) involves PEP providing lactate to form MurNac from GlcNAc; murA catalyzes the reaction²⁰⁻²². The antibiotic fosfomycin, is an antimetabolite of murA (Figure 1.4). Uptake of the antibiotic is mediated by the glycerophosphate transporter. Fosfomycin inactivates murA through a reaction between its epoxide ring and an active site cysteine residue in the enzyme, which produces a stable thioether.²¹ Inactivation of murA leads to a depletion in a main substrate required for peptidoglycan synthesis. The result is a loss of the peptidoglycan layer. Fosfomycin is used clinically for treatment of urinary tract infections.²³

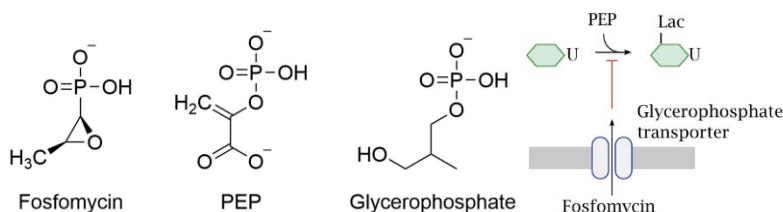


Figure 1.4: Fosfomycin, PEP, and glycerophosphate structures. Uptake of fosfomycin and PEP are mediated by the glycerophosphate transporter. Fosfomycin inactivates the active site murA, the enzyme required for addition of Lac to GlnNAc, preventing MurNAc synthesis and thus peptidoglycan synthesis.

Cycloserine. Following production of the MurNAc substrate, a pentapeptide is synthesized to form UDP-MurNAc-pentapeptide (Figure 1.3 II). The pentapeptide is important for peptidoglycan strand cross-linking. The C-terminus of the mature peptide is formed by two D-Ala residues. The D-Ala monomers are produced and linked by two enzymes: alanine racemase and alanine ligase, respectively. Alanine racemase converts L-Ala to D-Ala; D-alanine ligase is an ATP-dependent enzyme which catalyzes the formation of the peptide bond between the two residues. The dipeptide is then attached as a unit.²⁴ The antibiotic cycloserine, a structural analogue of Ala, is an antimetabolite of both enzymes (Figure 1.5). Cycloserine uptake is mediated by the same transport system as D-Ala, L-Ala, and Gly in *B. subtilis*.²⁵ Inhibition of the enzymes is said to occur through competitive inhibition.^{24,26} However, evidence has shown that inhibition of D-alanine ligase may occur in a different manner.²⁷ Inhibition of the enzymes leads to a decrease in the intracellular production of lipid I and lipid II. The result is the loss of the peptidoglycan layer. Cycloserine is used clinically for treatment of tuberculosis and is on the WHO's list of essential medicines.⁴

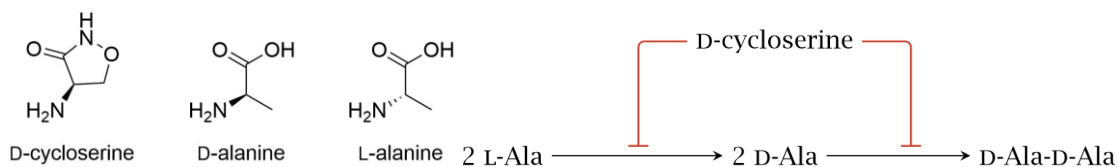


Figure 1.5: Cycloserine inhibits the two enzymes which successively produce the D-alanyl-D-alanine dipeptide used in the production of the precursors to lipid I. The first enzyme is alanine racemase, and the second is D-alanine ligase. Cycloserine works as it is a structural analogue of Ala (structures shown).

Laspartomycin. The initial synthesis of peptidoglycan occurs on the inner face of the cytoplasmic membrane with the production of UDP-MurNAc-pentapeptide, as described above. This precursor is then transferred to the carrier lipid undecaprenol phosphate, yielding lipid I (Figure 1.3 III). Addition of GlcNAc to lipid I yields lipid II, which is subsequently flipped across the membrane. Laspartomycin,

and some other lipopeptides like amphomycin, sequester the bare undecaprenol phosphate in the membrane.^{28,29} This interaction blocks the production of membrane-bound peptidoglycan precursors, and results in the loss of the peptidoglycan layer. Lapartomycin is an interesting antibiotic as it has structural similarity to dap and belongs to the same acidic lipopeptide antibiotic class, but they have different modes of action (see section 1.2.2). Laspartomycin is not used clinically.

Ampicillin. Peptidoglycan synthesis concludes with the cross-linking of the peptidoglycan strands on the extracellular side of the cell membrane (Figure 1.3 VI). This is essential for the mechanical strength of the cell wall. Cross-linking occurs through muramyl-transpeptidase activity performed by the penicillin-binding proteins (PBPs). The β -lactam antibiotics inhibit the transpeptidase reaction through an irreversible covalent bond with the catalytic serine residue in the muramyl-transpeptidase active site (Figure 1.6).¹⁸ Ampicillin belongs to the β -lactam class. The mechanism of action, and name of the class, arises from a shared β -lactam ring which resembles the peptide bond of the D-alanyl-D-alanine dipeptide in the pentapeptide. Irreversible inhibition of the enzymes leads to a decrease in peptidoglycan cross-linking. The result is the loss of the peptidoglycan structural integrity. Ampicillin is used clinically as a broad-spectrum antibiotic, and is on the WHO's list of essential medicines.⁴

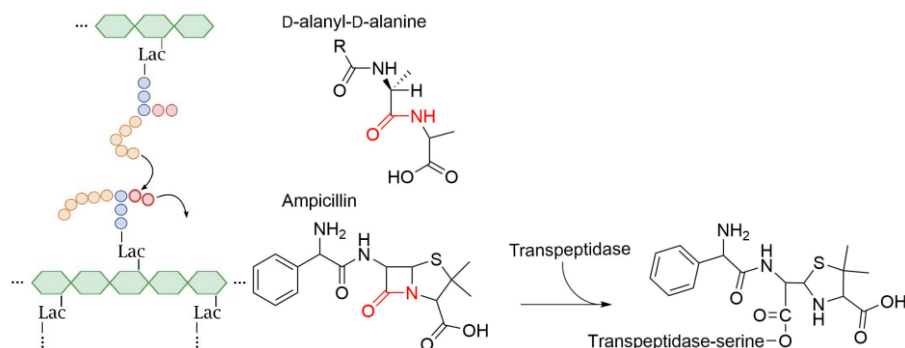


Figure 1.6: Deactivation of peptidoglycan transpeptidases by ampicillin occurs through covalent bond formation with the active site serine residue. Bond formation occurs due to the resemblance of the ultimate lipid II dipeptide to the β -lactam group within ampicillin.

Vancomycin. The concluding step of peptidoglycan synthesis is also inhibited by vancomycin; however, contrary to the β -lactam antibiotics, the antibiotic interacts with the substrate of the transpeptidase reaction, rather than the enzyme itself. Vancomycin sequesters the D-alanyl-D-alanine dipeptide by interacting through five essential hydrogen bonds (Figure 1.7).³⁰ Sequestration of the substrate blocks the active site serine from interacting with the pentapeptide. As with ampicillin, vancomycin leads to a decrease in peptidoglycan cross-linking. The result is the loss of the

peptidoglycan structural integrity. Vancomycin is used clinically against a range of infections, including MRSA, and is on the WHO's list of essential medicines.^{4,31}

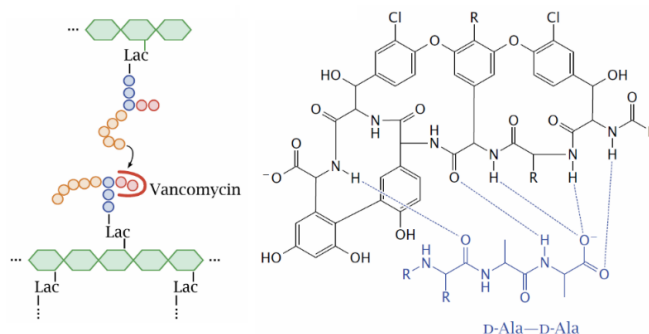


Figure 1.7: Sequestration of D-alanyl-D-alanine dipeptide by vancomycin. Sequestration occurs through five essential hydrogen bonds and blocks the cross-linking of peptidoglycan by PBPs. Black: vancomycin, blue: terminal D-alanyl-D-alanine dipeptide of lipid II.

Inhibitors of ribosomal protein synthesis

Protein synthesis is a vital process performed within every bacterial species. The ribosome, together with transfer RNAs (tRNA) and messenger RNA (mRNA), is the functional unit of protein production through a process called translation. tRNAs are the molecules which ‘translate’ the mRNA into an amino acid sequence by matching codons and anti-codons from the mRNA and tRNA, respectively. The bacterial ribosome is constructed of a combination of multiple ribosomal RNAs (rRNA) and ribosomal proteins, which are divided into two subunits (50S and 30S). The large ribosome subunit (50S) is constructed of 23S rRNA, 5S rRNA and 32 ribosomal proteins.³² The 23S rRNA forms the highly structured pocket which houses the aminoacyl (A), peptidyl (P), and exit (E) sites.³³ The P and A sites position the growing amino acid chain and the aminoacyl-tRNA to allow for peptidyl transfer through peptide bond formation. Prokaryotic ribosomes are smaller than those of eukaryotes, and they are sufficiently distinct in structure to allow for selective inhibition by some antibiotics. However, ribosomes within the mitochondria resemble those of bacteria, which may give rise to toxicity.^{18,32}

Chloramphenicol. The antibiotic chloramphenicol binds directly to RNA within the peptidyl transferase site of the ribosome, and inhibits peptide bond formation (Figure 1.8).^{18,34,35} The result is a loss of protein production, and consequently, the eventual death of the bacterial cell. Unfortunately, chloramphenicol toxicity involves bone marrow suppression in humans due to its interaction with mitochondrial ribosomes.^{18,36} Chloramphenicol is used clinically, although often as a second line of defense due to its adverse effects; nonetheless, it is on the WHO's list of essential medicines.⁴

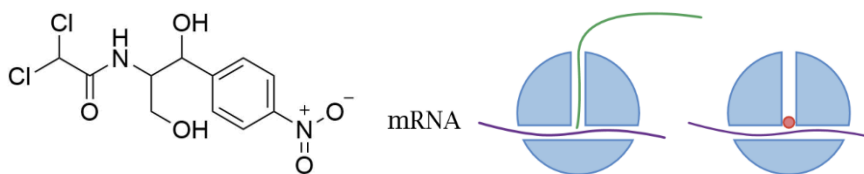


Figure 1.8: Structure of chloramphenicol, and its binding position within the peptidyl transferase site of the ribosome. Red: chloramphenicol, blue: ribosome, green: nascent protein, purple: mRNA.

Disruptors of bacterial cell membranes

The cell membrane is one of the essential structures of a bacterial cell (Figure 1.2). The membrane encloses the cellular contents and acts as a passive barrier to molecules in the environment. It is composed of a wide variety of lipid and protein molecules, which depend heavily upon the bacterial species. In the case of lipids, phospholipids are highly abundant. Two in particular are phosphatidylethanolamine (PE) and PG. All phospholipids contain a hydrophilic phosphate head group and hydrophobic fatty acyl tail; in an aqueous environment, this allows the spontaneous generation of a lipid bilayer due to the hydrophobic effect. A phospholipid bilayer corresponds to a significant fraction of the cell membrane and is characterized by a hydrophobic membrane core and hydrophilic surface. The organization of this structure is the basis for much of the restriction of passive diffusion of molecules. Polar molecules may not partition into the membrane, while hydrophobic molecules readily pass by partitioning into and then out of it again on the other side. Conversely, extremely hydrophobic molecules may become trapped within the hydrophobic membrane core.

At generally half the mass of the membrane, proteins have important and highly regulated functions.³³ Of note, are ion transporters, which actively transfer specific ions across the membrane, and ion channels, which allow free movement of ions down a concentration gradient. These, together with the passive diffusion of ions through the cell membrane, establish a typical membrane potential of -40 to -80 mV, with respect to the outside of the cell.³³ The potential is used as a source of energy for numerous metabolic functions, including bacterial cell division.³⁷

Nisin. The antibiotic nisin binds to the cell membrane through an interaction mediated by lipid II, and successively forms membrane-spanning pores. (Figure 1.9).³⁸ Lipid II is the final monomeric, membrane-bound precursor in the synthesis of peptidoglycan, which is flipped across the membrane and exposed to the extracellular environment (Figure 1.3 IV). Notably, nisin's interaction with lipid II is more complex than it acting as a 'target molecule'. Research has shown that lipid II is a constituent of the nisin pore complex and is essential for stable pore formation.³⁹ In contrast, model membrane

systems have shown the formation of nisin pores in the absence of lipid II; yet, these were formed at nisin concentrations 1,000-fold over the level required for formation of pores on model membranes supplemented with lipid II.³⁹ In the case of bacteria, pore formation by nisin leads to the loss of ions, amino acids and ATP. This results in the eventual death of the cell through dissipation of the membrane potential, and loss of important intracellular molecules. Nisin is not used clinically, though it has potential; as of now it is solely used as a food preservative.⁴⁰

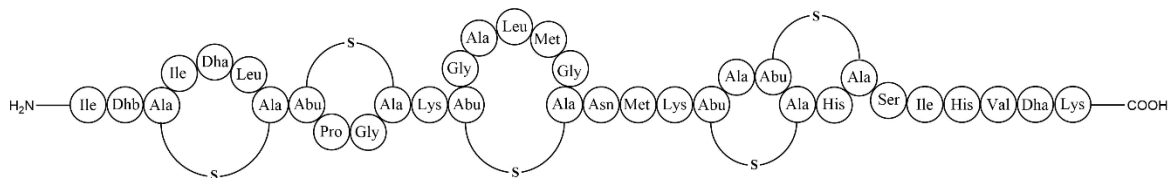


Figure 1.9: Structure of the lantibiotic nisin. The N-terminal portion is required for lipid II binding, while the C-terminal portion is necessary for membrane interaction. Amino acids: 2-aminobutyric acid (Abu), didehydroalanine (Dha), didehydroaminobutyric acid (Dhb), lanthionine (Lan; Ala-S-Ala), methyl-lanthionine (MeLan; Abu-S-Ala). These unusual amino acids are introduced by post-translational modification of the precursor peptide.

Daptomycin. In a comparable manner to nisin, dap has been shown to permeabilize bacterial cell membranes; although, whether this is the sole mechanism of action is still unclear (Figure 1.10). Pore formation, in this case, is mediated by an interaction with PG and calcium. The background and method of action of dap will be discussed in detail below, see section 1.2.

Table 1.1: Mechanism of action of select antibiotics

Antibiotic	Spectrum	Mechanism of action
Inhibitors of peptidoglycan synthesis		
Fosfomicin	Gram+, Gram ⁻	Loss of activity through modification of an active site cysteine residue in enzyme murA
Cycloserine	Gram+, Gram ⁻	An analog of D-alanine which interferes with L-alanine racemase and D-alanine ligase by competitive inhibition
Vancomycin ^(a)	Gram+	Inactivation of cell wall transpeptidases through (a) blocking the substrate (b) irreversible inhibition of the active site
Ampicillin ^(b)	Gram+, Gram ⁻	
Laspartomycin	Gram+	Blocks undecaprenol, inhibiting production of lipid II
Inhibitors of ribosomal protein synthesis		
Chloramphenicol	Gram+, Gram ⁻	Blocks peptide bond formation in the 50S ribosomal subunit
Disruptors of bacterial cell membranes		
Nisin	Gram+	Loss of membrane potential due to pore formation
Dap ^c	Gram+	

^cSee section 1.2.4 for additional information

1.1.2 Mechanisms of resistance

Bacterial resistance is an increasingly serious problem across the globe. Many hospital-acquired infections are now attributable to multidrug-resistant bacteria. Infections of this kind can greatly worsen patient outcome.⁴¹ Antibacterial resistance can arise through three main pathways: natural resistance, genetic mutation, and acquired resistance. The first involves innate morphological and genetic differences between bacteria. The second may be spontaneous or mutagen-induced mutations, which diminish specific action modes. The third may pose the most critical difficulty for future antibiotic use; it involves transferable genetic elements such as plasmids, which allow for horizontal gene transfer between bacteria. This allows the transfer of existing genetic elements of antibacterial resistance

between bacteria, even across species barriers. As with action modes, mechanisms of resistance fall into a handful of broad classes. Below, these classes are briefly noted. For an overview of the mechanism of resistance of select antibiotics, refer to Table 1.2.

Natural resistance. This arises by the absence of an antibacterial target in the organism. An example is the resistance of Gram⁺ bacteria to the polymyxin class of antibiotics. An essential part of the action mode of the polymyxins involves interaction with lipopolysaccharide (LPS).⁴² Gram⁺ bacteria, in contrast to Gram⁻, do not produce LPS.

Target modification. Resistance to antibiotics which target essential cellular pathways are often by target modification.⁴³ This occurs as the loss of target function may prove fatal to a cell. Target modifications can occur from point mutations in one gene, to changes in multiple gene pathways.³⁰ In general, changes to the target reduce affinity for the antibiotic.

Enzymatic degradation/modification. The antibiotic is modified or degraded to a point where it is no longer functional. This has large implications in clinical practice; it is a prevalent mechanism of antibiotic resistance and it dates back to the beginning of the antibiotic era with penicillin. It is also important for bacterial selection throughout scientific fields. Transformation of bacteria with antibiotic resistance plasmids which contain genes coding for antibiotic degradation or modification enzymes allows for the selection of resistant bacteria from those which are antibiotic-sensitive.

Mutation to antibiotic transport. Many antibacterial agents require high intracellular concentrations to affect their respective targets. The inability of antibiotics to gain access to the bacterial cell interior, or the ability of bacteria to keep them out, can drastically reduce antibiotic effectiveness.

Compensatory metabolic changes. There remains a broad set of mechanisms of resistance which occur in bacteria outside of those already listed. This set can be covered by the diverse metabolic changes which occur in bacteria. The changes often result in the up-regulation or down-regulation of lipids, enzymes, proteins, etc. This can then affect antibiotics in specific, or indirect, fashion.

Table 1.2: Mechanism of resistance of selected antibiotics

Antibiotic	Target	Mechanism of resistance
Inhibitors of cell wall synthesis		
Fosfomycin	murA	Mutation in transport pathways, ring opening by epoxide hydrolases ⁴⁴⁻⁴⁶
Cycloserine	L-alanine racemase and D-alanine ligase	Mutation in the target enzymes, target overexpression
Vancomycin	D-Ala-D-Ala of lipid II pentapeptide	Mutation of amino acid sequence from D-Ala-D-Ala to D-Ala-D-Lac ^{30,43}
Ampicillin	Transpeptidases	Inactivation by β -lactamases ⁴⁴
Inhibitors of ribosomal protein synthesis		
Chloramphenicol	50S ribosomal subunit (23S rRNA)	Mutation of 23S rRNA, chloramphenicol acetyltransferase, reduced membrane permeability ^{35,44,47}
Disruptors of bacterial cell membranes		
Nisin	Lipid II	Modification of lipid II sequence, enzymatic inactivation, cell wall and membrane composition ⁴⁸
Dap ^a	PG in bacterial membranes	Adaptations in phospholipid membrane composition, bacterial esterases and deacylases ⁴⁹⁻⁵²

^aSee section 1.2.6 for additional information

1.2 Daptomycin

Dap is a cyclic lipodepsipeptide antibiotic that belongs to the broader class of acidic lipopeptides.⁵³ Its immediate family is designated A21978C.⁵⁴⁻⁵⁷ These natural antibiotics are produced by the microorganism *Streptomyces roseosporus*, which was discovered by the pharmaceutical company Eli Lilly.⁵⁴ The A21978C family shares the same core macrolactone ring and exocyclic tripeptide (Figure 1.10). The macrocycle contains 10 amino acids, 5 of which are D-amino acids or other non-proteinogenic amino acids. These include ornithine (Orn6), D-Ala8, D-serine (D-Ser11), (2S,3R)-

methylglutamate (MeGlu12), and kynurenine (Kyn13). The cycle is closed by a depside bond between the hydroxy side chain of threonine (Thr4) and the α -carboxylic acid group of Kyn13. The exocyclic tripeptide consists of aspartic acid (Asp3); a third D-amino acid, D-asparagine (D-Asn2); and tryptophan (Trp1). The point of variance for the antibiotic family is the fatty acyl tail attached to the N-terminal α -amino group of Trp1. Dap has an n-decanoyl acyl tail and is typically produced in low quantities by *S. roseosporus*; fortunately, Eli Lilly discovered that fermenting *S. roseosporus* with decanoic acid will produce dap in appreciable quantities.⁵⁵

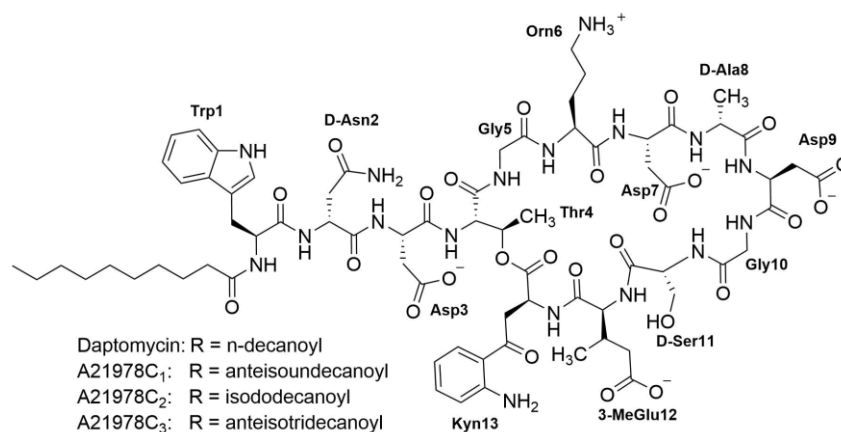


Figure 1.10: The structures of dap and A21978C₁₋₃ at physiological pH. The overall charge of dap is -3 .

1.2.1 Clinical use

Clinical studies for intravenous dap were first carried out by Eli Lilly.⁵⁴ In phase 1 trials that used a twice-daily dosage regimen, volunteers tolerated the antibiotic. In phase 2 clinical trials, the dose was increased to levels more effective against *S. aureus* bacteremia; volunteers began to develop adverse musculoskeletal effects and the trials were aborted. Later, Cubist Pharmaceuticals displayed interest and entered into licensing negotiations with Eli Lilly. Negotiations were finalized in 1997, and Cubist began their independent clinical trials.⁵⁴ It was discovered that a low once-daily dosage regimen avoided the adverse effects and retained antibacterial effectiveness.⁵⁸

Dap treatment of complicated bacteremia and right-sided endocarditis caused by *S. aureus* and MRSA met non-inferiority criteria against the standard therapy.⁵⁹ However, dap performed poorly and did not meet the non-inferiority criteria against pneumonia.⁶⁰ The low efficacy against pneumonia likely results from an interaction with pulmonary surfactant, which sequesters the drug.⁶⁰ In 2003, dap was

approved by the Food and Drug Administration (FDA) under the name Cubicin for intravenous therapy, making it the only clinically used acidic lipopeptide. In 2014, Merck acquired Cubist Pharmaceuticals.

1.2.2 The acidic lipopeptides

The acidic lipopeptides are a new class of antibiotic, mostly produced by species of *Streptomyces*.⁵³ The class can be separated into two large families: the lipodepsipeptides, and the lipopeptides. The two families share many structural elements, such as the macrocyclic core and fatty acyl tail; however, the former, have a ring-closing depsi (ester) bond, while the latter, have a ring-closing amide bond. The lipodepsipeptides include dap, A54145 (A5), and calcium-dependent antibiotic (CDA).⁵³ The lipopeptides include amphomycin, tsushimycin, and laspartomycin.⁵³ Both families depend upon calcium for their antibacterial activity; however, as of now, the lipopeptides are known to act by a different mechanism of action than the lipodepsipeptides.^{28,29,61} A structural DXDG motif, which in dap comprises residues 7–10, is conserved between the families; it is presumed to be a calcium binding site.^{55,62} Disruption of either aspartic acid within the motif in dap completely abolishes activity.⁶² Conservation of several D-amino acid sites also occurs.

Other than dap, A5 is the most relevant lipodepsipeptides to this thesis. A5 encompasses a family of antibiotics, the natural host of which is the microorganism *Streptomyces fradiae*.^{53,63} As with A21978C, the A5 family shares the same core shape: a macrolactone ring to which is attached an exocyclic tripeptide bearing a fatty acyl tail. However, in addition to a variable tail, residues 12 and 13 can be substituted with MeGlu or glutamate (Glu); and valine (Val) or isoleucine (Ile), respectively.⁶³ The macrocycle contains 10 amino acids, 5 of which are D-amino acids or other non-proteinogenic amino acids. These include sarcosine (Sar5), D-Lys8, 3-methoxyaspartic acid (MeOAsp9), D-Asn11, and sometimes MeGlu12. The cycle is closed by a depsi bond between the hydroxy side chain of threonine (Thr4) and the α -carboxylic acid group of Val or Ile. The exocyclic tripeptide consists of tryptophan (Trp1) and the non-proteinogenic amino acids D-glutamate (D-Glu2) and 3-hydroxyasparagine (HO-Asn3). As with *S. roseosporus*, the quantity of a certain lipopeptide can be increased by supplementing *S. fradiae* with the amino acid precursors required for that variant.⁶⁴ A5 is as potent as dap, however, it is clinically non-practical due to its increased toxic effects; substitutions to the amino acid sequence or acyl chain may allow for improved pharmacological properties.^{56,63} The variant used in our laboratory is “Factor D”, which has an anteisoundecanoyl acyl tail, Glu12, and Ile13 (Figure 1.11).

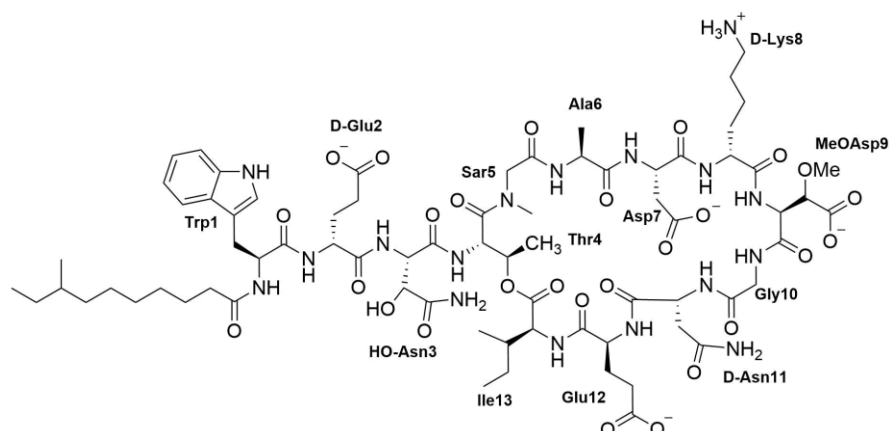


Figure 1.11: The structure of A5 Factor D at physiological pH.

1.2.3 Biosynthesis

Dap, like other the lipopeptides, is synthesized by its host organism non-ribosomally. *S. roseosporus* contains the DptE and DptF enzymes for initiation of synthesis, as well as three non-ribosomal peptide synthetases (NRPS) and other trans acting enzymes for elongation and cyclization. The three NRPSs, DptA, DptBC, and DptD are individually comprised of linear modules that in turn contain several distinct functional domains – the modules are responsible for incorporating five, six, and two amino acids, respectively.⁶² Each module contains a minimum of an adenylation (A-) domain, a condensation (C-) domain and a thiolation (T-) domain. The A-domains are responsible for the specific recognition and activation of an amino acid through adenylation with ATP to give AMP-amino acids. The AMP-amino acids are transferred to the T-domains, with release of AMP, and formation of a thioester. The C-domains catalyze the ligation of amino acids on preceding and subsequent T-domains. Modules may also include epimerization (E-) domains; E-domains are responsible for switching the stereochemistry of the α -carbon of an amino acid. The modules which contain these E-domains give rise to the non-proteinogenic D-amino acids in dap. After biosynthesis of the peptide it must be cyclized and released. This is accomplished by the unique thioesterase (TE-) domain located on the final module.

To initiate synthesis, DptE and DptF activate the fatty acyl tail (FA, decanoic acid) for condensation to the nascent Trp1 amino acid. DptE, an acyl-CoA ligase homolog, ligates the FA to the acyl carrier protein DptF in an ATP-dependent manner. The first of the NRPSs, DptA, catalyzes the transfer of the FA from DptF to the N-terminal Trp1 with its C-domain. The FA substrate specificity of DptE is low; this is proposed to be responsible for the A21978C family variation.⁶² Amino acid chain elongation proceeds with transfer of the lipopeptide from DptA to DptBC, and finally to DptD. DptA and DptBC

contain the E-domains responsible for the epimerization of Asn, Ala, and Ser. DptD contains the module for the addition of MeGlu12 and the ultimate TE-domain. The MeGlu12 amino acid is synthesized by the GlnT (glutamate 3-methyltransferase) enzyme DptI.⁶² The final TE-domain mediates formation of the depsi bond between the side chain of Thr4 and the α -carboxylic acid group of Kyn13.

Biosynthesis of A5 follows a comparable route to that of dap. Whereas dap contains three NRPS genes, the A5 biosynthetic route contains four: LptA, LptB, LptC and LptD.⁶⁴ The change of units results from DptBC, the largest NRPS from dap, being analogous to a fusion of LptB and LptC.⁶⁴ The NRPS modules are responsible for incorporating five, two, four and two amino acids, respectively, and function with the same catalytic domains as dap, and an additional methylation domain.

1.2.4 Mechanism of action

Several action modes for dap have been proposed; among them, the dissipation of the membrane potential due to the interaction of dap with bacterial phospholipid membranes is best supported by experimental evidence. Potassium (K^+) leakage from *S. aureus* cells interacting with dap and A21978C initially led researchers to explore the cell membrane as a site of action.⁶⁵ Early results indicated that dap did increase the conductivity of planar bilayers in the presence of calcium and magnesium.⁶⁶ Antibacterial activity, unlike the conductivity changes, could not be replicated with magnesium.⁶⁶ Dap is consequently said to be calcium-dependent; potent antibacterial activity requires around 1.25 mM Ca^{2+} .⁵⁶ Serendipitously, this concentration is similar to the normal level of free (as opposed to protein-bound) calcium in human plasma.⁶⁷ Dap activity also correlates to levels of the acidic lipid PG in the membrane (Figure 1.12).⁶⁸ This correlation has been demonstrated on model membranes, as well as in *B. subtilis*.^{69,70}

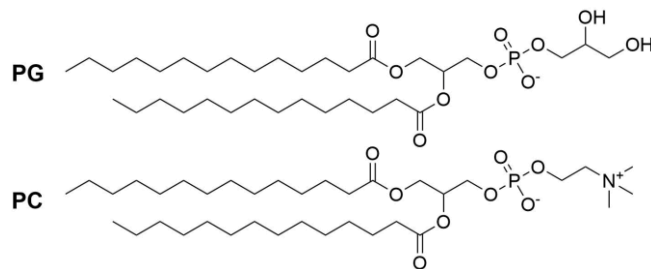


Figure 1.12: Structures of phosphatidylglycerol (PG) and phosphatidylcholine (PC). PG is the major lipid necessary for dap activity. Phosphatidylcholine (PC) is the most abundant phospholipid in eukaryotic membranes, and mostly inert with respect to dap. The lipids are shown with myristoyl tails, but may vary.

The interactions of dap with model membranes have been principally characterized through fluorescence studies. In these, the intrinsic fluorophore Kyn13 has been advantageous. Early research showed that, upon the addition of calcium in the presence of PC membranes, Kyn13 fluorescence blue-shifted and had an increased quantum yield.^{68,71} This indicated a decrease in the polarity of its environment, most likely due to membrane insertion. Addition of PG to these membranes yielded a significantly greater blue-shift and increase in Kyn13 quantum yield, suggesting deeper insertion.⁶⁸ Circular dichroism (CD) spectroscopy corroborated these results.⁶⁸ Dap in the presence of calcium produced only a minor conformational change; dap with PC membranes in the presence of calcium produced another minor change. In contrast, dap with PC/PG membranes in the presence of calcium produced a significant conformational change.

Membrane-permeabilizing proteins or peptides often form oligomeric structures on target membranes. Dap was shown to promote K⁺ leakage from bacterial cells, therefore it was suggested that it forms an oligomeric structure.⁷² Using fluorescence resonance energy transfer (FRET), the Palmer group showed oligomerization of dap on PC/PG liposome model membranes.⁷³ The FRET donor was the intrinsic Kyn13 residue from native dap and the acceptor was an extrinsic nitrobenzoxadiazole (NBD) fluorophore attached to the Orn6 residue of dap (Figure 1.13). For FRET to occur between the two fluorophores, they must be in close proximity to each other within the membrane, which was interpreted as oligomerization. Oligomerization was detected at calcium concentrations relevant for antibacterial activity, suggesting that the oligomers could be the functional membrane defect. Later, quantitative analysis of FRET techniques was used to estimate the subunit stoichiometry of the oligomers; a number of 6 to 7 subunits was found.⁷⁴ However, this study did not address how dap distributes between the two membrane leaflets, and due to limitations of the technique and assumptions made in the calculations, the estimated number of subunits may deviate from the true value. Oligomerization has also been detected with A5; the FRET donor was Trp1 from native A5 and the acceptor was an extrinsic acrylodan fluorophore attached to the Lys8 residue of A5 (Figure 1.13).

Furthermore, the NBD and acrylodan labels are both environmentally sensitive fluorophores capable of concentration-dependent self-quenching; this alone can be used to detect oligomerization. In oligomers of labeled dap or A5, the monomers should assemble in sufficient proximity to begin self-quenching; the production of mixed oligomers, with the introduction of unlabeled peptides, should suppresses the self-quenching behavior by decreasing the mutual interactions of NBD or acrylodan labels.⁷³ Without oligomerization, the extent of self-quenching should be unaffected by the presence of

unlabeled peptide. Comparison of the fluorescence of mixed and unmixed oligomers showed a suppression of self-quenching when unlabeled peptide was included, indicating oligomerization.⁷³

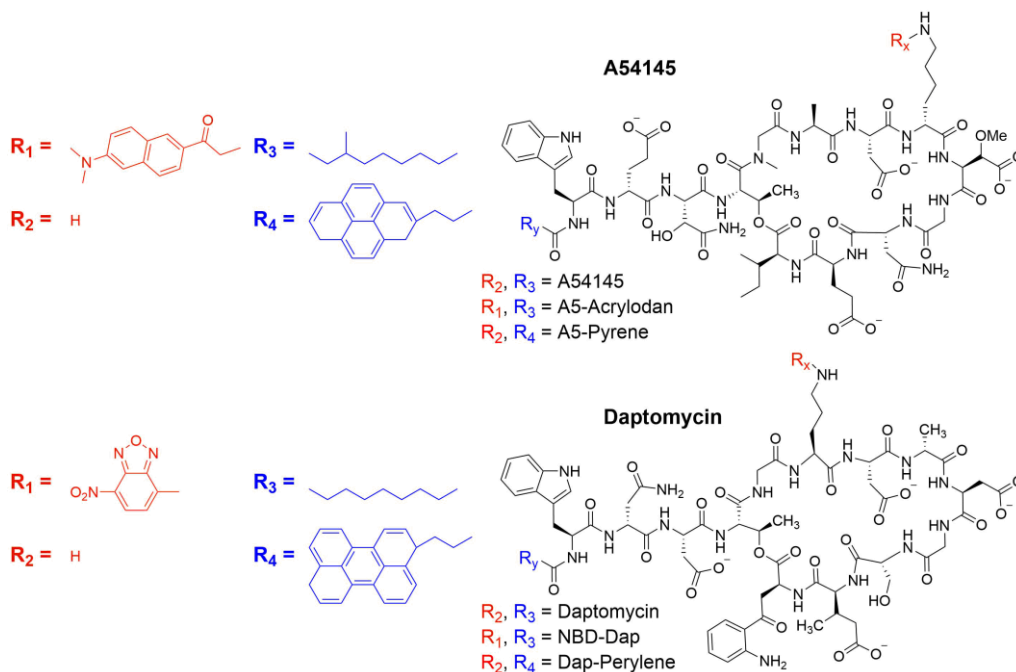


Figure 1.13: The structures of A5 and dap analogs used in the demonstration of oligomer formation on liposome model membranes. A5 analogs (top) include: A5-acrylodan (R₁, R₃) and A5-pyrene (R₂, R₄). Dap analogs (bottom) include: NBD-dap (R₁, R₃) and dap-perylene (R₂, R₄).

The interaction of dap monomers on PC/PG liposome model membranes was further demonstrated by examining the excimer formation of perylene-labelled dap (Figure 1.13).⁷⁵ Excimers, or excited dimers, are formed when an excited perylene monomer is in close proximity to one in the ground state; in fact, the interaction requires a closer approach of fluorophores than FRET.⁷⁵ Pyrene is the most widely used label for studies such as these, however, perylene was used because pyrene has a monomer emission spectrum that overlaps with the absorption spectrum of the intrinsic Kyn13 residue; the overlap vastly reduces pyrene fluorescence due to energy transfer to Kyn13. The perylene label is attached through the N-terminus of the exocyclic Trp1 residue of dap, thereby replacing the native acyl tail. Consequently, the experiments probe the interaction of the acyl tail groups in the membrane. The experiments used conditions which mirrored those of the FRET experiments, thus oligomers were assumed to be forming. The resulting extent of excimer formation emphatically indicated oligomers were forming. Analysis showed dap had an extent of oligomerization of over 90% on equimolar PC:PG liposomes, and only slightly lower on bacterial membranes.⁷⁵ Oligomerization was also found to be

driven by a stoichiometric interaction with PG. An exhaustive study of this phenomenon using A5 has recently been submitted.⁷⁶ A5 avoids the problem of spectral overlap as it lacks a Kyn residue, thus pyrene can be attached to the N-terminal Trp1 residue (Figure 1.13). Furthermore, analysis of the spectrum is aided by the advantages of pyrene: greater excimer intensity and better spectral separation from the monomer signal.

Despite the importance of demonstrating oligomerization, the presence of oligomers does not clearly indicate that they are important for antibacterial activity, or that a pore is being formed. Consequently, both FRET and excimer formation were used to search for the formation of hybrid oligomers of dap and CB-182,462, a semisynthetic derivative of A5, using NBD and perylene labels.⁷⁷ The existence of the functionally impaired oligomers would indicate that oligomer formation is important for antibacterial activity.⁷⁸ Hybrid oligomers were indeed formed, and when tested for antibacterial effectiveness, they showed a significantly reduced activity. This also shows that oligomerization is not sufficient for antibacterial activity; after formation, the oligomers must take an additional step in order to acquire a functional antibacterial effect.⁷⁸

Lastly, the presence of a functional pore was investigated using a liposome permeabilization assay which takes advantage of pyranine (Figure 1.14). Pyranine is a hydrophilic, fluorescence dye which can act as a pH-sensitive probe for the liposome interior.⁷⁹ It is non-fluorescent at low pH, when the molecule is protonated on the phenolic hydroxyl group; deprotonation between pH 6 and 8.5 causes fluorescence emission at 510 nm. The assay consists of the generation of two opposite ion gradients, through the use of differing buffers – one being a proton gradient and the other a different ion, such as K^+ .⁸⁰ The addition of a proton transporter, such as CCCP, will release a small quantity of protons, but dissipation of the proton gradient is prevented by the ensuing diffusion potential – this will not change the internal pH of the liposome as it is moderately buffered.⁸⁰ The addition of dap will dissipate the K^+ gradient only if it allows influx of K^+ through a functional pore. Consequently, only in combination will the transporter and potential pore allow dissipation of the opposing ion gradients. This will overcome the internal liposome buffering capacity and the pH will increase; the pH increase stimulates pyranine fluorescence and indicates the lipopeptide is producing a functional pore. By changing the cation in the exterior buffer, as well as reversing the gradients to detect permeabilization of anions, dap was found to produce cation- and size-selective pores.⁸⁰

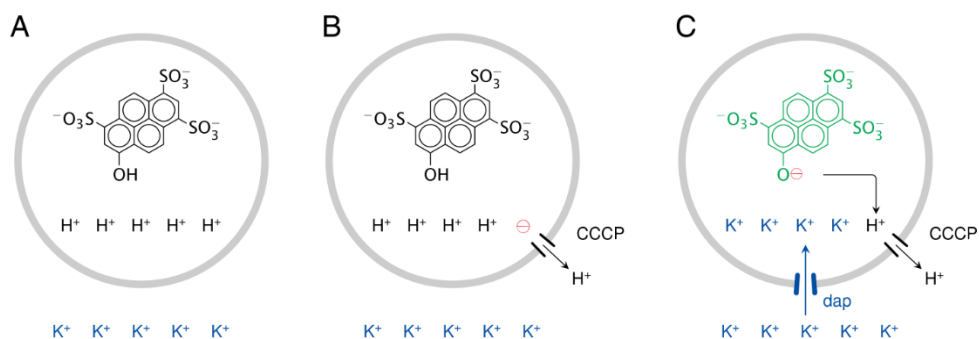


Figure 1.14: Schematic of the pyranine-based liposome permeabilization assay. (A) Encapsulated pyranine with a H⁺ gradient inside and K⁺ gradient outside. (B) Application of the protonophore CCCP alone allows insignificant loss of protons. (C) If dap allows dissipation of the opposing K⁺ gradient, concurrent dissipation of the proton gradient occurs increasing pH and causing pyranine fluorescence.⁸⁰

An experiment-derived model of the structure of the dap pore was proposed by studying the interaction of dap with liposome model membranes containing cardiolipin (CL) in addition to PC and PG (Figure 1.20).⁵² CL has been implicated by genetic studies as a mechanism of resistance to dap by *Enterococci*.⁸¹ Within the model membrane system, incorporation of 10% CL was sufficient to inhibit pore formation, as measured by the pyranine-based permeabilization assay; this encompasses the upper range reported for bacterial membranes, suggesting that this mechanism may be relevant *in vivo*.⁵² Estimation of the oligomer subunit number, by Kyn13 to NBD-dap FRET, on these membranes gives an oligomer of 4 subunits.⁵² The study mentioned above, estimated an oligomer of 6-7 subunits, but did not address how dap distributes between the two membrane leaflets, and may have provided an underestimate due to experimental limitations. The authors proposed that the decrease in oligomer size was due to CL suppressing translocation of dap from the outer leaflets of the membrane, to the inner leaflet. On high CL-containing membranes, dap would then remain as a tetramer on the outer leaflet; on susceptible membranes, translocation of tetramers would occur and the alignment of two tetramers in opposite leaflets would form a functional octameric pore (Figure 1.15).⁵²

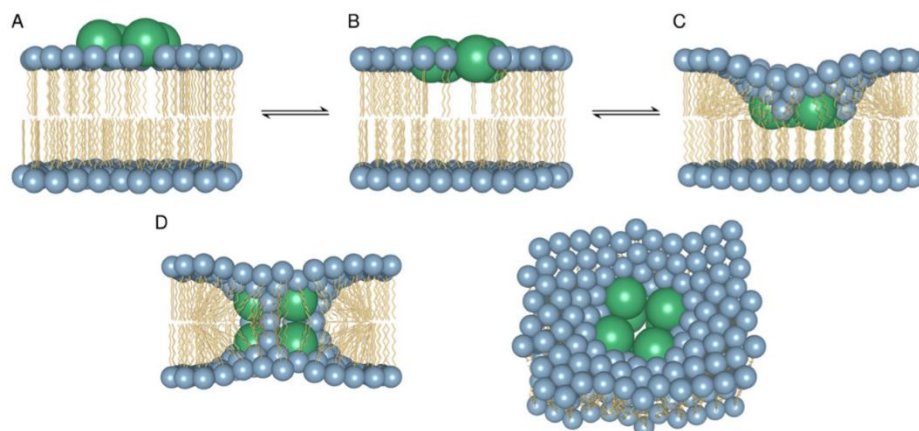


Figure 1.15: Model of dap on liposomes, with and without CL. (A) Formation of a dap tetramer. (B) Insertion into the membrane is limited by distension and creation of voids in the lipid acyl chains layer. This situation may be stabilized by addition of CL. (C) In the absence of CL, the lipid layer may cave in, forming the half-toroidal structure shown in (D). Finally, a tetramer which has flipped to the inner membrane through (D), may combine with a second tetramer in the outer leaflet, and produce an octameric pore.⁵²

To test the hypothesis, an experimental procedure to quench NBD-dap fluorescence was used.⁵² Quenching occurs through reduction of NBD by dithionite. If NBD-dap is distributed as tetramers along both leaflets, any NBD-dap on the inner-leaflet would not be quenched, and half of the fluorescence would remain. However, as dap creates pores, and membranes are rather permeable to dithionite, a control was conducted using NBD-PE to show dithionite is excluded from the membrane interior (Figure 1.16A). Approximately half of the fluorescence was quenched; this indicates only the NBD-PE on the outer leaflet was reduced, even in the presence of dap's pores. PC/PG membranes with NBD-dap exhibited results similar to NBD-PE, showing only quenching of NBD-dap on the outer leaflet; therefore, half of the dap is translocating to the membrane interior. PC/PG membranes including 10–20% CL had most of the NBD-dap fluorescence quench as dithionite was added (Figure 1.16B). This indicates dap is indeed confined to the outer leaflet by CL. In both, the remainder of fluorescence was slowly reduced, likely due to subsequent translocation from the inner leaflet to the outer leaflet.

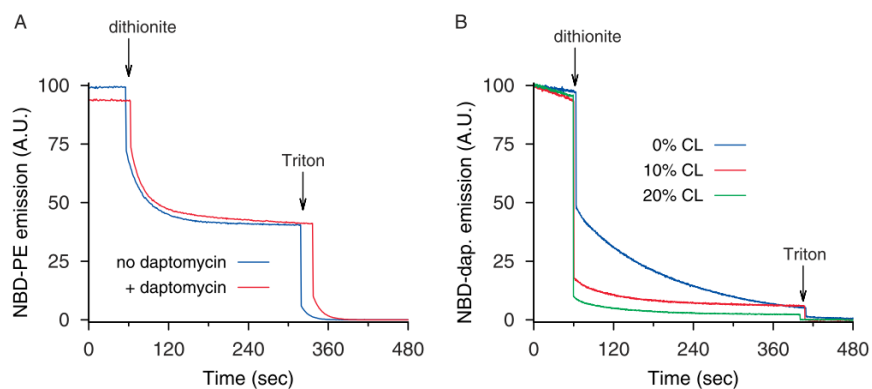


Figure 1.16: NBD-dap fluorescence quenching assay, using dithionite. (A) A control showing dithionite is excluded from the liposome interior in the presence of dap pores. (B) In PC/PG membranes including 10-20% CL most of the NBD-dap fluorescence has been reduced by dithionite instantly. This indicates it is confined to the outer leaflets.⁵²

More recently, the interaction of dap and A5 with calcium has been established in more detail. The requirement of calcium for the activity of dap has long been recognized, but the molecular details and stoichiometric ratio of calcium to dap were not well characterized. To date, as described above, CD experiments described two possible calcium-dependent conformational changes in dap: one with calcium and dap in solution, and the other in the presence of PG-containing membranes. Also, NMR studies of dap in solution have indicated that calcium binds to dap in solution with a 1:1 stoichiometry.^{68,82,83} Isothermal titration calorimetry (ITC) studies have now shown that dap binds two calcium ions per lipopeptide molecule and that the two ions are bound successively and with different affinity.⁸⁴ Furthermore, fluorescence studies have shown that the two successive calcium-dependent transitions mediate the membrane binding and oligomerization of dap and A5.⁸⁴

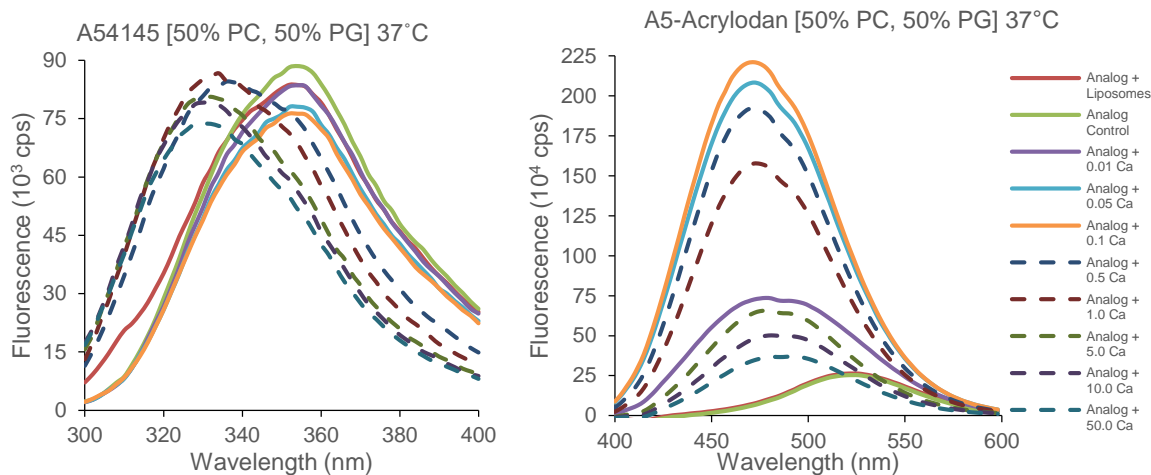


Figure 1.17: Fluorescence spectra of tryptophan from A5 (left) and acrylodan from A5-acrylodan (right) in the presence of 70:30 PC:PG liposomes and increasing Ca^{2+} concentration (mM) at 37 °C. Trp and acrylodan excitation wavelengths are 280 nm and 360 nm, respectively.

The fluorescence studies used separately incubated dap and dap-acrylodan, and A5 and A5-acrylodan. Above, the fluorescence spectra of A5 and A5-acrylodan are shown and will be used as an example; the fluorescence was observed as calcium was added incrementally from 0 to 50 mM. The intrinsic Trp1 fluorophore of A5 shows no response up to 0.1 mM but then rapidly blue-shifts (left: Figure 1.17). In contrast, the fluorescence of A5-acrylodan rapidly peaks at 0.1 mM Ca^{2+} but then decreases at higher concentrations (right: Figure 1.17).

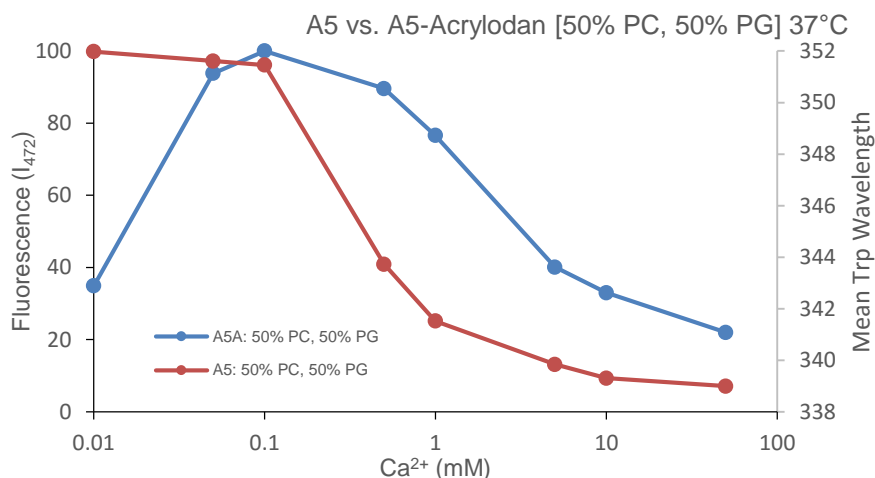


Figure 1.18: Mean tryptophan wavelength emission of A5 compared to maximum fluorescence intensity of A5-acrylodan emission (I_{472}), each as a function of Ca^{2+} concentration. Liposome composition is 50:50 PC:PG. Legend: A5A refers to A5-acrylodan.

Directly comparing the mean tryptophan wavelength emission of A5 and the maximum fluorescence intensity of A5-acrylodan emission as a function of calcium concentration, clarifies the different responses (Figure 1.18). As calcium is increased, the Lys8 residue bearing the acrylodan label binds to the membrane and its fluorescence both increases and blue-shifts; at 0.1 mM Ca²⁺ the residue is fully inserted. Further increasing calcium causes Trp1 to bind the membrane and blue-shift; concomitantly, the acrylodan labels begin to self-quench. As mentioned above, the self-quenching of acrylodan is interpreted as oligomerization.⁷³

A second study using A5-pyrene found some complementary findings.⁷⁶ Two successive calcium-dependent transitions were observed at similar calcium concentrations seen above. The first transition displayed interaction of the fluorophore-labeled acyl tail of monomers through excimer formation, indicating oligomerization; the second transition displayed increased excimer intensity, indicating a tighter interaction of the acyl residues or a larger number of subunits.^{76,84} Together, the studies suggest a mechanism of dap membrane binding and oligomerization wherein the first calcium ion causes lipopeptide monomers to bind to the membrane and to form a loosely associated structure, in which the acyl tail interact but not portions of the lipopeptide head group; increased calcium concentration induces the binding of a second calcium ion and the initial structure transitions to a tightly associated and functional oligomer.^{76,84} From here, the oligomers could translocate and form the pore required for leakage of cellular ions.

The latest preliminary work using A5-acrylodan has shown that the self-quenching action may report more directly on the translocation/pore formation of dap or A5, rather than the oligomerization. This would change the interaction of the acrylodan labels from between subunits within an oligomer on a specific membrane leaflet, to an interaction of acrylodan labels between separate oligomers on opposing membrane leaflets. This proposal arises from the suppression of A5-acrylodan self-quenching on CL-containing membranes. CL at concentrations of 10% or higher has been shown to confine dap to the outer membrane leaflet and abolish pore-dependent membrane permeabilization.⁵² The two calcium-dependent transition described above may then indicate initial oligomerization and subsequent oligomer translocation and cross-leaflet alignment.

1.2.5 Daptomycin analogs

Dap analogs are a valuable tool to establish the structure-activity relationship (SAR) of dap. Altering the structure of the antibiotic allows for characterization of the specific role of different amino acids in the overall activity. Substitutions to specific amino acids may also improve pharmacological properties

such as antibacterial activity, spectrum, toxicity. Generation of analogs resistant to sequestration in surfactant is also possible. Four approaches to producing different analogs are genetically engineered biosynthesis, chemoenzymatic synthesis, semi-synthesis, and total synthesis.

Genetically engineered biosynthesis, or combinatorial biosynthesis, manipulates the NRPS modules to substitute single or multiple amino acid sites. In one study, *S. roseosporus* was altered to have deletions in NRPS modules. Plasmids were transferred through conjugation with *Escherichia coli* to functionally complement the missing modules.⁶² This was used to generate analogs with Ile13 or Trp13 instead of Kyn13. Combinatorial methods have also been used to produce hybrids of A5 and dap. The antibacterial activity of A5 (Factor E) is inhibited 32-fold in 1% surfactant, whereas that of dap is inhibited 128-fold; dap analogs including portions of the amino acid sequence of A5 may then prove an easy method to increase activity against *Streptococcus pneumoniae in vivo*.⁸⁵ Many analogs were generated; several were less inhibited by surfactant but also comparatively less active against *S. aureus* than dap.

Semi-synthesis is the process of altering the chemical structure of molecules through organic chemistry. An early experiment used semi-synthesis to investigate the significance of Asn2 stereochemistry.⁸⁶ The fatty acyl tail attached to Trp1 was first enzymatically removed to allow access to the N-terminus of an Orn6-protected dap. Edman degradation was used to remove Trp1 and Asn2, and the resulting undecapeptide was reacted with N-decanoylated L-Trp-D-Asn and L-Trp-L-Asn dipeptides. The L-Asn isomer showed a 10-fold increase in MIC, indicating the stereochemistry at this position is important. Using similar chemistry, the Trp1 residue was also replaced or modified in an attempt to increase the activity of dap in lung surfactant. Attachment of electron-withdrawing groups to the aromatic portions of Trp1 tended to improve or preserve activity, but also to increase the negative effect of surfactant; electron-donating groups generally had the opposite effect, and groups with hydrogen-bond donor sites were mostly inactive.⁸⁷ Synthetic methods to attach fluorophores to the Orn6 and fatty acyl tail have also been advantageous in studies of the mechanism of action of dap.^{52,73,75,78}

Chemoenzymatic synthesis uses bacterial enzymes such as peptide cyclases (NRPS TE domains) and organic, or biological, synthesis to produce analogs. Advances in the sequence information for dap and A5 allowed the cloning and expression of their native TE enzymes.⁶² Multiple amino acids were substituted, including MeGlu12, Kyn13, Asp3, and the acidic amino acids in the DXDG motif that comprises residues 7–10 in dap. Exchange of Asp7 or Asp9 with Asn eliminated all antibacterial activity, however, the substitution of Asp3 with Asn only slightly decreased activity.⁶² This

corroborates the theory that the acidic members of the DXDG motif are involved in calcium binding. Nguyen *et al.*⁸⁸ conducted many substitutions: (1) MeGlu12 with Glu increased MIC 16-fold. (2) Kyn13 with Trp, Ile, or Val increased MIC 2-, 4-, and 8-fold. (3) D-Ser11 with D-Ala or D-Asn increased MIC 2-fold. (4) D-Ala8 with D-Ser or D-Asn increased MIC 2- and 16-fold. That some substitutions did not highly affect the MIC against the bacteria is advantageous as amino acids in these positions may be able to be changed to give rise to beneficial pharmacodynamics or pharmacokinetic effects.

Total synthesis is the newest method to generate dap analogs and has begun to develop into a powerful tool. The total synthesis of dap is difficult due to the characteristics of the lipodepsipeptide, which includes non-proteinogenic amino acids, cyclic structure, and the fatty acyl tail; racemization of amino acids and hydrolysis of the depsi bond are also concerns. However, these obstacles have mostly been overcome. This allows total synthesis to have wide selection of targets for substitution, which will allow for a more comprehensive look at the SAR of dap. Three full dap syntheses have been published. Two include a patent by Cubist and an article by Lam *et al.*⁷⁷ The latter used a combination of solution and solid-phase techniques and has begun producing new analogs. The last synthesis is the first full solid-phase peptide synthesis (SPPS) of dap, developed by the Taylor group.⁸⁹ SPPS techniques are conducive to the generation of combinatorial dap analog libraries, which would improve the speed of discovery of significant analogs. New analogs have been produced, most notably, dap-E12-W13, which does not contain Kyn13 or the synthetically challenging MeGlu, but retains an MIC similar to dap.⁸⁹

1.2.6 Mechanisms of resistance

Dap resistance was observed early in its clinical application but remains relatively rare. Reports from clinical trials conducted by Eli Lilly and Cubist detailed three resistant strains.^{9,90,91} The reports from Cubist involved immunocompromised patients with bacteremia. The first case involved a vancomycin-resistant *Enterococcus faecium* with an original dap MIC of 2 $\mu\text{g mL}^{-1}$, which increased to 6 $\mu\text{g mL}^{-1}$ when isolated 17 days later.⁹¹ The second case involved a methicillin-resistant *S. aureus* with an MIC of $\leq 1 \mu\text{g mL}^{-1}$, which increased to 2 $\mu\text{g mL}^{-1}$ when isolated 27 days later.⁹ While resistant clinical isolates are readily available, selecting for resistant bacteria in the laboratory is tedious. Eleven strains with dap resistance were recovered after using methyl-nitrosoguanidine mutagenesis and serial passage with increasing concentrations of dap for 21 days.⁹² In either case, clinical and laboratory-manufactured non-susceptible bacteria are useful subjects for study into antibiotic mechanisms of resistance.

One group, using *S. aureus* with induced resistance, was able to discover several genetic changes that correlate to increased resistance to dap.⁵¹ The non-susceptible strains used were recovered via a

method similar to that detailed above. To determine the genetic basis of the resistance, the authors used full genomic comparisons of the resistant bacteria and their susceptible parent. Two different proteins, with amino acid substitutions due to single point mutations, were correlated to resistance: YycG and MprF. Furthermore, these proteins were also shown to be relevant to non-susceptible bacteria from clinical isolates.⁵¹

YycG is a member of the two-component system YycFG (now termed WalRK) from the *yyc* operon first discovered in *B. subtilis*.⁹³ The system is conserved throughout many low-GC Gram+ bacteria, including *S. aureus*. YycG is a membrane-spanning sensor/histidine kinase, and YycF is a response regulator.^{55,93} Autophosphorylation of YycG and phosphotransfer to YycF, indicate these proteins are part of a bacterial signal transduction cascade.⁹³ In *B. subtilis*, YycG localizes to the cell division septum and is involved in cell division and cell wall restructuring.⁹⁴ DNA analysis of the components in *S. aureus* reveal similarities to those in *B. subtilis*, showing regulation of target genes that control cell wall metabolism, membrane-bound transport systems, and virulence.⁹³ Using a recombinant *yyc* operon with an inducible promoter, the *S. aureus* operon was also found to be essential for growth at 37 °C. Depletion of the YycFG system through inhibition of transcription causes cell death without lysis.

The fashion in which YycFG in susceptible and non-susceptible bacteria potentially interact with dap is not known. It could be possible that in susceptible bacteria dap binds to YycG and inhibits signal transduction to the response regulator. This would cause cell death in the same fashion as depletion of the protein. Dap-resistant strains would have mutant YycG proteins with lessened binding affinity for the antibiotic. There is no direct evidence of dap binding to YycG; however, Gram- bacteria lack the two-component system and dap is not active against them. The outer membrane (OM) formed by Gram- bacteria is often demonstrated as the reason for the increased resistance, but not in the case of dap.⁹⁵ Nisin – a cell membrane-active antibiotic – has an MIC of 2 µg/mL on *S. aureus*. On *E. coli* the MIC increases to >64 µg/mL; removal of the *E. coli* OM decreases the MIC to 8 µg/mL. Dap on *S. aureus* gives an MIC of 2 µg/mL. On *E. coli* the MIC increases to >256 µg/mL; in the absence of the OM, the MIC does not change. Nevertheless, this does not preclude other factors which may cause dap to have ineffective activity on Gram- bacteria, such as efflux transporters and a much lower PG content.⁹⁵

MprF, or multiple peptide resistance factor, has been characterized as an LPG synthetase. LPG is synthesized through the transfer of L-lysine from lysyl-tRNA to PG; this reverses the -1 charge of PG to +1.⁹⁶ MprF gain-of-function mutants have been associated with increased resistance to many cationic

antimicrobial peptides (CAMPs), such as host defense antimicrobial peptides (HDPs).⁹⁷ As with dap, many HDPs initially interact with the bacterial cell membrane, but their subsequent mechanisms of action can be different.⁹⁸ MprF was first characterized in *S. aureus* through gene deletion, complementation and recombinant trans-expression in *E. coli*.⁹⁹ Two separate functions have been assigned to the C- and N-terminus.⁹⁶ The hydrophilic C-terminal domain contains the synthetic machinery, while the hydrophobic N-terminal domain contains a lipid flippase. Incorporation of the MprF N-terminus alone did not confer CAMP resistance; in addition, incorporation of the MprF C-terminal alone did not lead to effective CAMP resistance.⁹⁶ Only when overexpressed together as one protein, or two, did the MprF C- and N-terminals successfully mediate full-level CAMP resistance. This indicates that CAMP resistance is dependent upon both increased LPG synthesis and its concomitant exposure to the outer surface of the membrane.⁹⁶

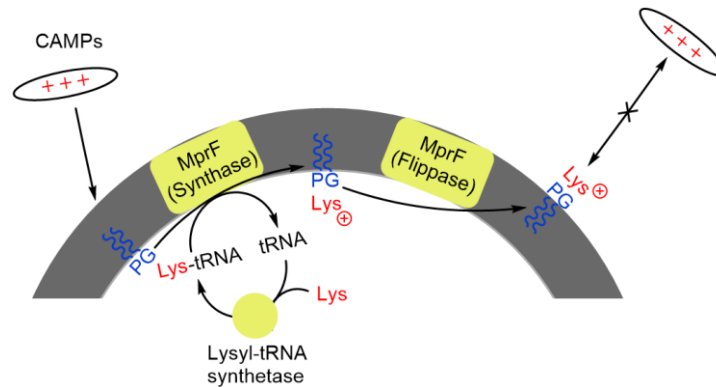


Figure 1.19: Model for the mode of MprF-mediated bacterial CAMP resistance.⁹⁶

The proposed mechanism through which MprF gain-of-function mutants decrease susceptibility to CAMPs is decreased membrane association. The reduced interaction is presumed to occur through electrostatic repulsion between the increased relative positive charge of the bacterial membrane and the cationic antibiotics (Figure 1.19).⁹⁶ In relation to dap resistance, the mechanism has yet to be characterized, but can potentially act in a similar manner; dap, in conjunction with calcium, would supposedly act in a CAMP-like manner and the upregulation of LPG renders the mutant bacteria less susceptible by repelling the lipopeptide.

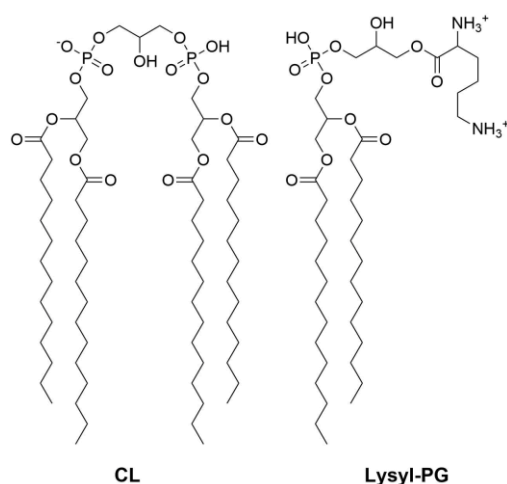


Figure 1.20: Structures of cardiolipin (CL) and lysyl-phosphatidylglycerol (LPG). CL and LPG are correlated to dap resistance.

Two other cell membrane composition changes have been implicated in dap resistance. The first is the down-regulation of PG. In both *S. aureus* and *B. subtilis*, this occurs through a mutation in the *pgsA* gene, whose product is an enzyme within the PG synthesis pathway.^{70,100} As dap is reliant on PG for its mechanism of action, a reduction in the cell membrane concentrations reduces dap's effectiveness. The second is an up-regulation of cardiolipin. It was discovered by Palmer *et al.*,⁸¹ who used serial passage over two weeks to induce resistance to dap in *Enterococcus faecalis*. Whole-genome sequencing was then used to compare the resistant bacteria and their susceptible parent. Mutations were studied for their putative effects, and also compared to *E. faecalis* clinical isolates. One mutation, EF0631, was found to reside within a cardiolipin synthase; when compared a similar mutation was also found within a dap-resistant *E. faecalis* clinical isolate. Cardiolipin is proposed to confer resistance through the prevention of dap oligomer translocation from the outer membrane leaflet to the inner membrane leaflet.⁵² This results in a loss of bacterial permeabilization, and consequently no change in membrane potential.

Degradation processes have also shown to increase resistance to dap. A group of 60 environmental actinomycete strains were showing high dap resistance ($\geq 256 \mu\text{g/mL}$). D'Costa *et al.*⁴⁹ demonstrated the bacteria were degrading dap through multiple hydrolytic mechanisms. HPLC and mass spectrometry results on the soil isolate library concluded there was ester hydrolysis, deacylation and secondary degradation by the bacteria. Ester hydrolysis refers to the cleavage of the depsi bond between Kyn13 and the side-chain of Thr4 and was the predominant method of deactivation. Deacylation was the second most prevalent and refers to the removal of the n-decanoyl acyl tail. Both of these

mechanisms have been shown previously to eliminate all antibacterial activity.¹⁵ Secondary degradation was most often due to cleavage between Trp1 and D-Asn2, and Kyn13 and MeGlu12.

1.3 Discovery of bacterial L-forms

In 1935, Emmy Klieneberger discovered a new form of bacteria; they were entitled “L” forms, after the Lister Institute in which she worked.^{101,102} L-forms are capable of growth and division without a cell wall.¹⁰³ Many L-forms have the ability to revert to the parental cell-walled state (N-form). L-forms able to revert are called *unstable*, while those who cannot are *stable*. Unstable L-forms are considered genetically identical to the parent N-form; stable L-forms are genetic mutants, which show some differing characteristics compared to their parent N-form.¹⁰⁴

The originally discovered L-forms were naturally derived. Researchers soon discovered that L-forms can be induced through chemical means. In all cases, the inducer affects the stability of the cell wall which allows for the transition to L-form, where propagation in this form can begin. In the case of both induced and naturally-derived L-forms, growth must occur on a suitable medium; the cell wall, in addition to providing shape and rigidity, protects bacteria from osmotic lysis in the presence of hypotonic solutions. In general, this means the wall-less bacteria need an osmotically enriched medium. Sodium chloride (1–5%) and sucrose (5–20%) are commonly used as osmoprotectants.¹⁰⁵ Divalent cations such as magnesium can also be used to stabilize the cytoplasmic membrane.^{105,106}

1.3.1 Creation of *B. subtilis* PDC 134, an efficient producer of L-forms

Conventional methods for the production and propagation of stable L-forms are tedious. This makes obvious the importance of a bacterial strain which can stably convert from the N-form to the L-form in a quick and efficient manner. Domínguez-Cuevas *et al.*¹⁰⁷, with initial research by Leaver *et al.*¹⁰⁸, developed and isolated such a strain. The bacteria they produced was a transformed and mutated *B. subtilis* 168 strain called PDC 134. *B. subtilis* PDC 134 contains a xylose promoter (P_{xyl}) fused to the beginning of its chromosomal *murE* operon; the *murE* operon is important for peptidoglycan synthesis as it contains the enzymes required for multiple steps in the synthetic pathway.¹⁰⁹ In the presence of the inducer, xylose, the xylose repressor (*xyIR*) is removed from P_{xyl} and the growth rate and shape of the cells is normal (N-form). In the absence of the inducer, *xyIR* remains and peptidoglycan synthesis is repressed; this causes the cells to transition to L-form. To reduce background expression from the promoter and reduce spontaneous reversion through mutations in the *xyIR* gene, an additional copy was added.^{107,110}

The other mutations in PDC 134 were characterized by sequencing the genome and comparing to the ‘wild-type’ *B. subtilis* 168 genome and relevant laboratory strains. Of the polymorphisms, two were found to be significant towards the formation of L-forms: *sepF*^{T11M} and *walR*^{R204C}.¹⁰⁷ The *sepF* gene codes for a cell division protein that binds to the FtsZ protein, and is essential for proper cell division; the mutants, such as *sepF*^{T11M}, are viable but division septa have abnormal morphology.^{111,112} The *walR* gene codes for the WalR protein, which is the response regulator in the WalRK (formerly YycFG) two-component system that regulates cell wall metabolism by controlling expression of autolysins.⁹⁴ In dividing cells, WalRK upregulates autolysin to break down peptidoglycan and allow for growth; in non-dividing cells autolysin activity is down regulated.⁹⁴ The *walR*^{R204C} mutation of the PDC 134 strain leads to partially constitutive WalR activity, which allows for sustained autolysin activity. These mutations aid in the efficient and high frequency of L-form transition in the PDC 134 strain; this likely occurs due to their aberrant peptidoglycan layer facilitating breach points which allow for the emergence of the protoplast.¹⁰⁷

Chapter 2

Characterizing an acyl-linked dimer of daptomycin

2.1 Introduction

Membrane-permeabilizing proteins or peptides often form oligomeric structures on target membranes. Since dap causes K^+ leakage from cells, it was suggested that it forms an oligomeric structure.⁷² Later, oligomerization was unequivocally detected and found at calcium concentrations relevant for antibacterial activity.⁷³ It is now known that oligomer formation is a necessary but not sufficient condition for pore formation, the end result required for antibacterial activity.^{52,78} Due to the necessity of oligomerization for antibacterial action, studying the effects of alterations to its progression is important.

One method of altering the process of oligomerization is to change its entropy cost. This might be accomplished by producing partially ‘pre-oligomerized’ dap molecules. By reducing the entropy cost of oligomer formation, the activity of the analog might increase. No high-resolution structure of dap oligomers or pores have been generated; thus, the question of how to synthesize a pre-oligomerized dap analog remains uncertain. Fortunately, a working model derived through fluorescence experiments has been proposed by the Palmer group.⁵² Dap was suggested to assemble into tetramers; on susceptible membranes, translocation of tetramers would occur and the alignment of two tetramers in opposite leaflets would form a functional octameric pore.⁵² Within oligomers, the acyl tails of monomers have been shown to directly interact. This was characterized by the production of excimers in a perylene-labeled dap analog.⁷⁵ Consequently, an acyl-linked dap dimer has the potential to remain active, as its point of dimerization ought not introduce extensive steric constraints (Figure 2.1).

Characterization of the acyl-linked dimer of dap is possible through assays which indicate membrane binding, pore formation, and antibacterial activity. Membrane binding is detected in the presence of liposomes or bacteria by calcium-dependent increases to the quantum yield of dap’s intrinsic Kyn13 fluorophore. Pore formation is detected with a liposome permeabilization assay which displays pore-dependent increases in the fluorescence of liposomes loaded with a pH-sensitive dye. Antibacterial activity is measured through minimum inhibitory concentration (MIC) assays on susceptible bacteria.

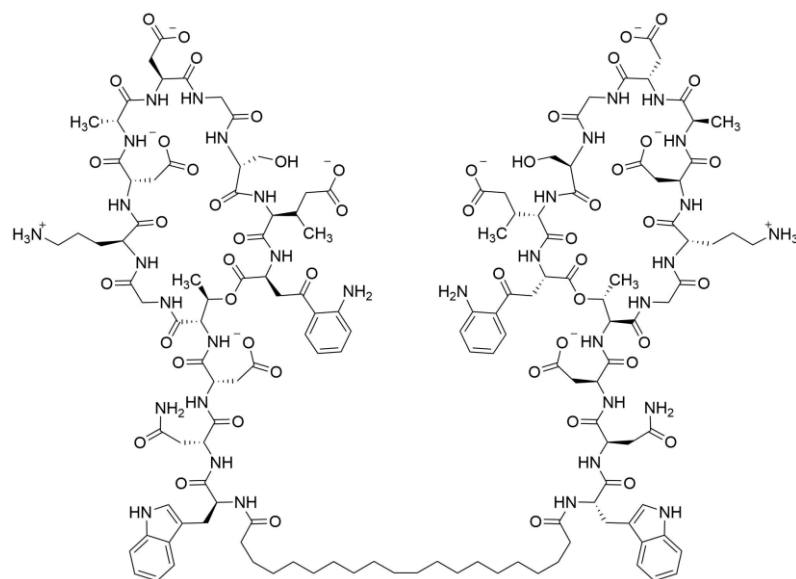


Figure 2.1: Structure of the acyl-linked dap dimer.

2.2 Materials and Methods

Lipids used in the preparation of liposomes were purchased from Avanti Polar Lipids, Inc. (Alabaster, AL, USA). *Bacillus subtilis* PDC 134 was generously provided by the Centre for Bacterial Cell Biology, Institute for Cell and Molecular Biosciences (Newcastle upon Tyne, UK). Daptomycin was provided by Jared Silverman (Cubist Pharmaceuticals, Inc; Lexington, MA, USA). Fluorescence studies are done on a QuantaMaster 4 spectrofluorimeter (Photon Technology International, London, ON). Calcium is used as CaCl_2 . The acyl-linked daptomycin dimer was produced semi-synthetically by Dr. Scott Taylor (University of Waterloo; Waterloo, ON.); high purity was assessed by HPLC and mass spectroscopy.

2.2.1 Preparation of liposomes

The lipids (PG, PC, LPG, PS) are weighed to the corresponding molar ratios and transferred to a clean round bottom flask. The lipids are of the saturated dimyristoyl variety, with the exception of LPG, which is an unsaturated dioleoyl lipid. The lipids are dissolved in chloroform and methanol (3:1) and then dried under a stream of purified nitrogen gas to form a thin lipid film. Further drying is performed for 3 or more hours under vacuum. The lipid films are used immediately, or stored until hydration at $-20\text{ }^\circ\text{C}$. Before use, the lipids are left to warm to ambient temperature and then hydrated by addition of 3 mL of buffered solution and mixing until homogeneous, for a final concentration of 5 mM. Liposomes (large unilamellar vesicles, LUVs) of a defined and homogeneous size are produced by

repeatedly extruding the mixture through a 100 nm polycarbonate membrane with pressurized nitrogen. The average diameter of the liposomes approximates the pore diameter of the polycarbonate membrane.¹¹³ The liposomes are stored in glass vials at 4 °C until use. Liposomes containing LPG need to be used immediately due to instability.

2.2.2 Preparation of *B. subtilis* PDC 134 L-forms for fluorescence studies

B. subtilis strains are grown in their respective medium from frozen stocks (−80 °C); 5-100 µL of culture is used to inoculate 5 mL of medium in a 50 mL flask (1:10 allows for proper air flow). *B. subtilis* ATCC 1046 is grown in Luria-Bertani (LB) broth. *B. subtilis* PDC 134 N-form is grown in LB supplemented with 0.5% xylose. *B. subtilis* PDC 134 L-form is grown in osmoprotectant LB supplemented with Mg²⁺ (20 mM), maleic acid (20 mM), and sucrose (500 mM; MSM LB). ATCC 1046 and PDC 134 N-forms are grown overnight, while PDC 134 L-forms require 3 to 4 days. L-forms are incubated at 30 °C, while the others can be grown at either 30 °C or 37 °C. After growth, the cells are washed twice with HEPES-buffered saline (HBS; supplemented with 500 mM sucrose for L-forms) with use of a centrifuge (1500×g for 20 min, for L-forms). The final pellet is re-suspended in the standard, or osmoprotectant, HBS buffer and the optical density at 600 nm (OD₆₀₀) is determined. The cells can also be microscopically visualized to ensure proper morphology. For the isolation of PDC 134 N-forms and L-forms see sections 6.2.1 and 6.2.2.

2.2.3 Fluorescence studies

Liposomes of a given molar ratio are prepared, as described previously. The hydration buffer is HEPES-buffered saline (HEPES, 20 mM; NaCl, 150 mM; pH 7.4). For optimum signal, the samples contain a total lipid concentration of 250 µM, and a final lipopeptide analog concentration of 3 µM. Calcium is added step-wise titration as indicated in the results; upon addition of calcium the samples are mixed and then incubated for three minutes. If bacterial cells are used, a variable volume of cell suspension is added to reach an OD₆₀₀ of 0.4. Cell samples are prepared as described previously. If surfactant is being used in place of liposomes, it is added to a concentration of 1 percent. Excitation wavelength is chosen depending on the appropriate lipopeptide fluorophore (Table 2.1). Controls include measurements of the liposomes alone and the lipopeptide alone.

Table 2.1: Fluorophore, excitation wavelength, and emission range of relevant lipopeptide analogs.

Lipopeptide	Fluorophore	Excitation (nm)	Emission (nm)
Dap	Kyn13	365	400–600
Dap dimer	Kyn13	365	400–600

2.2.4 Determining the antibacterial activity of antibiotics

The antibiotics were tested for their specific antibacterial activity by broth dilution in a 96-well plate. The antibiotics were added at varying concentrations until the MIC was found; each concentration is tested 9 times. Osmotically stable bacterial strains (ATCC 1046, PDC 134 N-forms) used LB broth, while osmotically sensitive bacterial strains (PDC 134 L-forms) used MSM LB broth (Mg²⁺, 20 mM; maleic acid, 20 mM; sucrose, 500 mM). The media was additionally supplemented with 5 mM calcium for calcium-dependent antibiotics. Each well was inoculated with the appropriate bacterial strain (ATCC 1046, PDC 134 N-forms, PDC 134 L-forms) and incubated at 30 °C overnight (N-forms) or for 3 days (L-forms). Bacterial growth in each well was evaluated visually by turbidity.

2.3 Results

Initial antibacterial activity tests indicated that the dap dimer did not have increased activity compared to the native antibiotic; rather to the opposite, the MIC of the dimer increased from 0.75 µg/mL for the native monomer to over 100 µg/mL (Table 2.2). It was possible that dimerization inhibited a necessary step for antibacterial activity, such as membrane binding, oligomerization, or pore formation; therefore, determination of membrane binding was examined using the standard membrane binding assay on a liposome model membrane. The chosen membrane composition was 70:30 PC:PG, representing a simple dap-sensitive membrane; PG is required for the action mode of dap, while PC is mostly inert lipid with respect to dap at low calcium concentrations.

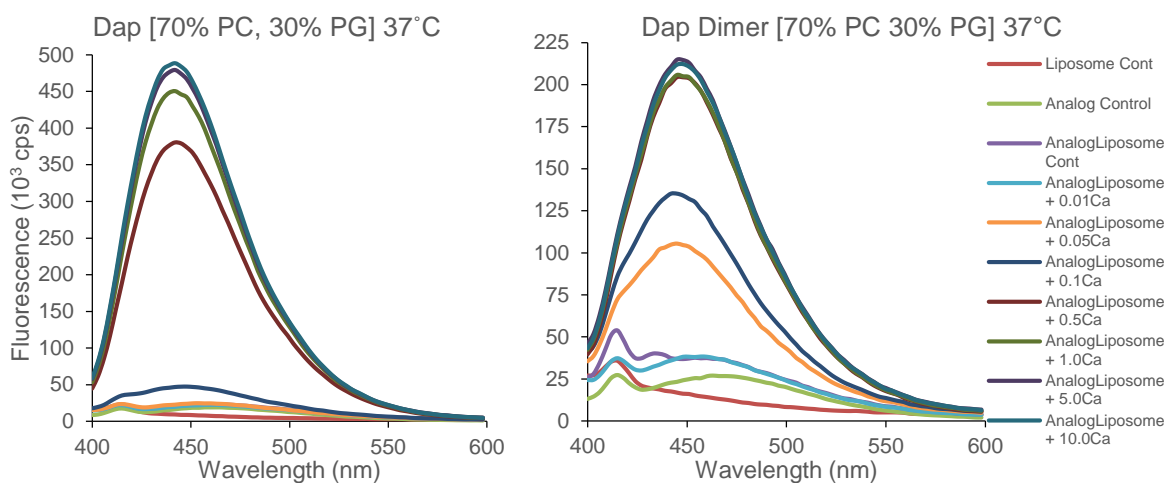


Figure 2.2: Kynurenine fluorescence spectra of dap and the dap dimer in the presence of 70:30 PC:PG liposomes and increasing Ca^{2+} concentration (mM) at 37 °C.

The fluorescence spectra show that as calcium is added incrementally, the quantum yield of Kyn increases, indicating membrane binding (Figure 2.2). The loss of antibacterial activity by the dap dimer is thus not due to inhibited interaction with the membrane. In fact, the fluorescence intensity response of the dap dimer is comparatively higher at low calcium concentrations than dap. Visualization of the difference in response can be improved by plotting maximum Kyn fluorescence as a function of calcium (Figure 2.3).

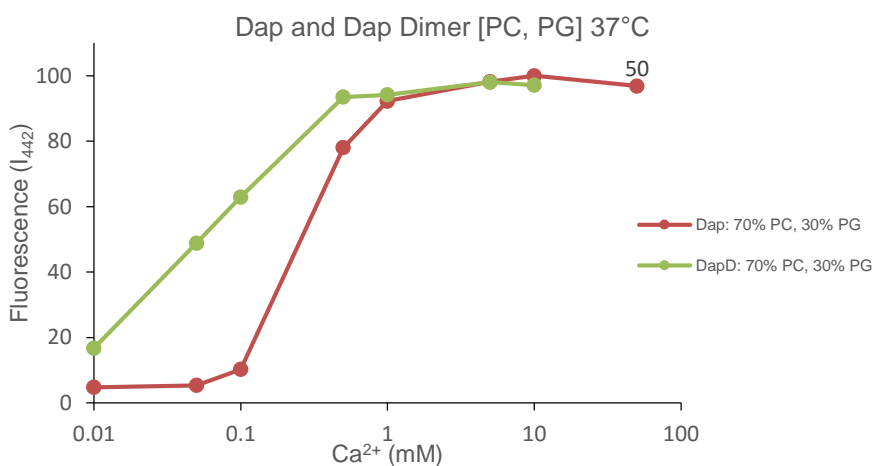


Figure 2.3: Kynurenine fluorescence of dap and dap dimer on liposomes of varying composition at 37 °C. The figure follows maximum normalized analog fluorescence (I_{442}) as a function of Ca^{2+} concentration.

The data displays a clear shift in the dimer’s fluorescence intensity response at low calcium concentrations. Only by 1 mM Ca²⁺ is the difference in relative fluorescence minimal, and at this concentration both dap and the dimer display nearly saturated fluorescence. The fluorescence shift may be a product of the assumed reduction in oligomerization entropy cost; in the assay the fluorescence of membrane binding is not differentiated from that of oligomerization. However, despite the antibiotic responding at lower calcium concentrations, it did not correspond to increased antibacterial activity.

Subsequently, the dap dimer was examined for the production of a functional pore. This was tested using a fluorescence-based liposome permeabilization assay. Preliminary data shows that the dimer forms functional pores (data not shown). Since the dimer appeared to be active on model membranes but not bacterial cells, it was considered that the peptidoglycan layer might be responsible for the loss of activity against cells. This was plausible as native dap has been seen to bind to bacterial cell walls which lack any cell membrane in the presence of calcium.¹¹⁴ In order to test this hypothesis, the activity of the dimer was examined on *B. subtilis* PDC 134 L-forms; the L-form bacteria are able to propagate without a cell wall, making them perfect test organisms (Table 2.2).

Table 2.2: MIC (µg/mL) of dap and dap dimer on *B. subtilis* strains.

Antibiotic	<i>B. subtilis</i> strain		
	ATCC 1046	PDC 134 (N-form)	PDC 134 (L-form)
Dap ^a	0.75	0.5–0.75	0.075
Dap dimer ^a	>100	30	0.2–0.25

^a5 mM Ca²⁺

Dap and the dap dimer presented with and MIC of 0.075 µg/mL and 0.20 µg/mL, respectively, on the cell wall deficient L-forms. Thus, removal of the cell wall restores most of the activity to the dimer, suggesting the peptidoglycan layer may sequester the dimer or otherwise restrict its access to the cell membrane. Removal of the cell wall is also greatly beneficial to the activity of native dap. Dap and the dap dimer presented with and MIC of 0.75 µg/mL and 30 µg/mL, respectively, on the cell walled N-form of *B. subtilis* PDC 134. The difference in activity between *B. subtilis* ATCC 1046 and PDC 134 N-forms may arise from the mutations in PDC 134 that affect cell wall integrity; for example, increased autolysin activity and aberrant division septa.¹⁰⁷ These mutations are essential to the strains efficient transition to the L-form; the protoplast must escape the peptidoglycan layer to propagate in its cell wall deficient form. The decrease in cell wall integrity allows for breach points within the peptidoglycan.

Table 2.3: MIC ($\mu\text{g/mL}$) assay results using dap and the dap dimer at 5 and 100 mM Ca^{2+} on *B. subtilis* ATCC 1046.

Lipopeptide	Ca^{2+} Concentration	
	5 mM	100 mM
Dap	0.75	0.50
Dap dimer	>100	5.0

Interestingly, high calcium concentrations are able to restore reasonably high antibacterial activity to the dap dimer (Table 2.3). The physical constraints of dimerization likely do not affect the calcium affinity of the lipopeptide, as the charged head group is unaffected. Other factors must then account for the activity change, one might be a reduction in electrostatic repulsion. In Gram+ bacteria, the teichoic acids throughout the cell membrane and cell wall are the primary carriers of negative charge. The lipo- and wall teichoic acids are known to bind calcium.¹¹⁵ NMR studies of dap in solution have indicated that Ca^{2+} binds to dap in solution with a 1:1 stoichiometry; this would leave dap in solution as a singly-charged anion.^{82,83} Theoretically, the dimer would bind calcium in solution in a 2:1 stoichiometry, one calcium for each head group, leaving it as a doubly charged anion. Calcium masking the charges of the teichoic acids may allow for increased passage through the cell wall. More research is needed to conclusively answer how calcium affects the interaction of the dimer with the cell wall.

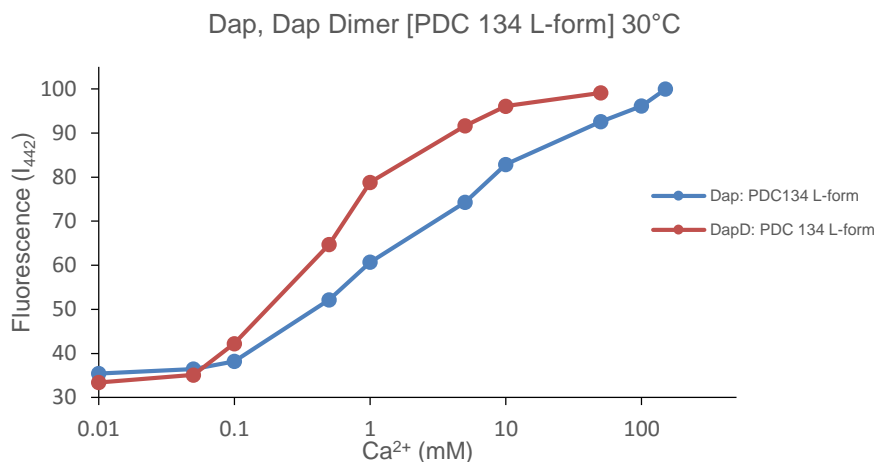


Figure 2.4: Kynurenine fluorescence of dap and dap dimer on PDC 134 L-forms at 30 °C. The figure follows maximum normalized analog fluorescence (I_{442}) as a function of Ca^{2+} concentration.

Last of all, the membrane binding assay can be used with live bacterial cells in place of model membranes. Dap and the dap dimer indicate binding to the L-form membrane, as expected from the

antibacterial activities. As with these analogs on the 70:30 PC:PG membrane, the dimer displays a comparatively higher fluorescence intensity response; though, on the bacterial cells the shift in response is not as extensive until higher calcium concentrations. As with the result on model membranes, the fluorescence shift may be a product of the assumed reduction in oligomerization entropy cost; once again, it does not correspond to the MIC of dap and the dap dimer on the L-forms. Perhaps the physical constraints of dimerization affect the final functionality of the pore.

2.4 Discussion

Characterization of the acyl-linked dimer of dap shows it is not an effective analog for the treatment of bacteria within dap's known antibacterial spectrum. Dimerization altered the physical properties of dap sufficiently to cause sequestration within the cell wall matrix of *B. subtilis* to a point where activity was greatly diminished. Increased calcium concentration can partially rescue the analog's activity, however, this is unlikely to be able to be exploited in a clinical setting as dap *in vivo* relies on the physiological calcium concentration of its host.

The underlying principle behind the synthesis of the analog may have worked in part. The fluorescence intensity response of the Kyn13 fluorophore in the pre-oligomerized analog is shifted to comparatively lower calcium concentrations in the presence of PC/PG membranes than dap. This could indicate deeper membrane binding or some change in the process of oligomerization; the difference cannot be distinguished as the fluorescence of binding is coupled with that of oligomerization in this assay. To solely study oligomerization, the addition of an extrinsic fluorophore to the analog would be required. If a change to oligomerization did occur, this could be due to the expected reduction in the entropy cost of oligomer formation. Nevertheless, the change in Kyn13 response did not correspond to an increase in the antibacterial activity of the dimer. Even when used with wall-deficient susceptible bacteria, the activity was comparatively decreased to dap. The physical constraints of the dimer may have changed the structure of the ultimate membrane-spanning pore, by altering the conformation of its oligomeric components.

The importance of the cell wall as a barrier to native dap activity was also shown. The activity of dap increased 10-fold on the cell-wall deficient L-form bacteria, compared to their walled N-form state. This clarifies why increased cell wall thickness is correlated to dap resistance – it is likely it increases the quantity of antibiotic sequestered.¹¹⁶ The presence of this significant barrier also calls into question the dap action mode proposed by some researchers. The action mode suggests the production of

micellar dap as the first step.^{117,118} The micelle then diffuses to the bacterial membrane and once in close proximity, it dissociates and dap monomers insert into the bilayer; oligomerization or conformational changes then occur and the cells are ultimately killed by membrane perforation. The formation of the micelle is supported by NMR studies which indicate a 14–16mer of dap with the addition of 1 molar equivalent of calcium.^{117,118} However, if the direct dimerization of dap causes the antibiotic to lose function in the presence of peptidoglycan, it is likely that the multimer described would not penetrate the cell wall and deliver dap to the bacterial cell membrane.

Chapter 3

Characterizing synthetic analogs of daptomycin

3.1 Introduction

Dap analogs are a valuable tool to establish the structure-activity relationship (SAR) of dap. Altering the structure of the antibiotic allows for characterization of the specific role of different amino acids in the overall activity. Substitutions to specific amino acids may also improve properties such as antibacterial activity, spectrum, toxicity, and susceptibility to surfactant sequestration. There are multiple approaches to the synthesis of these analogs, however, only dap analogs produced through the solid-phase peptide synthesis (SPPS) method developed by the Taylor group will be discussed here.¹¹⁹ The use of SPPS to synthesize dap is highly beneficial as the technique is conducive to the generation of combinatorial analog libraries. This would drastically improve the speed of discovery of significant analogs. However, the structure of dap poses some difficulties in the production of a library; two are the presence of MeGlu and Kyn residues in position 12 and 13, respectively. MeGlu of the correct stereochemistry is synthetically challenging and tedious to prepare in large quantities. The α -carboxylic acid group of kynurenine is a component in the ring-closing depside bond of dap; kynurenine in this position imparts low cyclization yields during synthesis. Consequently, replacing the residues with amino acids which resolve the synthetic difficulties and preserve antibacterial activity would be advantageous. The resulting peptide could then be used as the base scaffold for library generation.

MeGlu12 and Kyn13 have been substituted previously by other groups, both alone and in combination with additional changes; however, the acyl tail of the analogs was anteisoundecanoyl, rather than the decanoyl tail of dap.⁸⁵ The substitution of the native MeGlu residue in position 12 with Glu (E) decreased the activity; the MIC increased nearly 16-fold.⁸⁵ The substitution of the native Kyn residue in position 13 with Trp (W), Ile, or Val decreased the activity; the MICs increased by 2-, 4- and 8-fold, respectively.⁸⁵ The Taylor group chose to initially synthesize the double mutants dap-E12-W13 and dap-E12-Y13 (Figure 3.1). Dap-E12-Y13 has Glu at position 12 and tyrosine (Tyr; Y) at position 13. Subsequently, dap-A7-E12-W13 and dap-E12-Y13-pyrene were synthesized. Dap-A7-E12-W13 is a triple mutant with alanine (Ala, A) at position 7, in addition to E12 and W13; it was synthesized to help resolve differences in analog activities at high calcium. Dap-E12-Y13-pyrene attaches a pyrene fluorophore to the acyl tail of the aforementioned dap-E12-Y13 analog; this allows for the characterization of oligomerization.

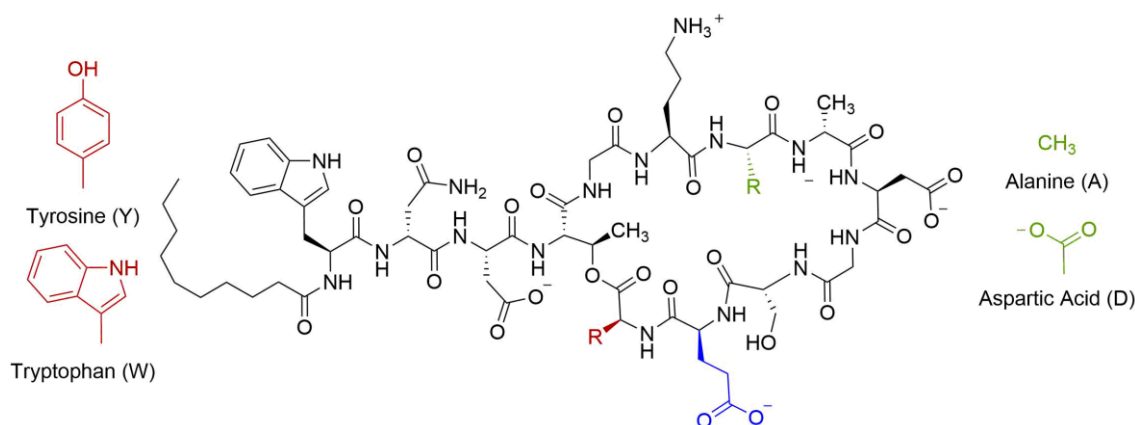


Figure 3.1: Initial dap analogs synthesized through SPSS: dap-E12-W13, dap-E12-Y13, and dap-A7-E12-W13. Dap-E12-W13, dap-E12-Y13 contain the native Asp (D) at position 7; dap-A7-E12-W13 contains Ala (green). All analogs contain Glu (E) at position 13 (blue). Dap-E12-W13 and dap-A7-E13-W13 contain Trp (W), and Dap-E12-Y13 contains Tyr (Y), at position 13 (red).

Characterization of the synthesized analogs is possible through assays which indicate membrane binding, oligomerization, pore formation, and antibacterial activity. Membrane binding is detected in the presence of liposomes by calcium-dependent increases to the quantum yield of dap's intrinsic Kyn13 fluorophore, or the blue-shift of A5's intrinsic Trp1 fluorophore. The formation of oligomers is detected in the presence of liposomes through the calcium-dependent formations of excimers within pyrene-labeled dap. Pore formation is detected with a liposome permeabilization assay which displays pore-dependent increases in the fluorescence of liposomes loaded with a pH-sensitive dye. Antibacterial activity is measured through MIC assays on susceptible bacteria.

Some of the tests can also be performed on, or in the presence of, artificial lung surfactant to test the analogs' susceptibility to surfactant sequestration. These tests are important as dap performed poorly against pneumonia *in vivo* in Phase 3 clinical trials, despite high *in vitro* activity against *S. pneumoniae*.^{60,120} The low efficacy in the clinical trials likely results from an interaction with pulmonary surfactant, which sequesters the drug.⁶⁰ If the experiments show that the dap analogs are less susceptible to surfactant inactivation, it could be important in devising an analog with *in vivo* activity against pneumonia. The commercial lung surfactant used here is bovine lipid extract surfactant (BLES). It contains 27 mg/mL of phospholipids, 176-500 µg/mL of surfactant-associated proteins B and C, and sodium and calcium chloride salts. The phospholipids likely contain a high percentage of PC, a low percentage of PG, and multiple other trace lipids as these are the lipids within characterized lung surfactant.¹²¹ The proteins are essential to the *in vivo* usage of lung surfactant.¹²¹

3.2 Material and Methods

A54145 Factor D was provided by Jared Silverman (Cubist Pharmaceuticals, Inc; Lexington, MA, USA). The daptomycin analogs were produced through SPPS by the Taylor research group (University of Waterloo; Waterloo, ON.); high purity was assessed by HPLC and mass spectroscopy.

3.2.1 Preparation of liposomes

The procedure for the preparation of the liposomes (LUVs) has been described in a preceding chapter (see section 2.2.1).

3.2.2 Fluorescence studies

The procedure for performing the fluorescence studies has been described in a preceding chapter (see section 2.2.3).

Table 3.1: Fluorophore, excitation wavelength, and emission range of relevant lipopeptide analogs.

Lipopeptide	Fluorophore	Excitation (nm)	Emission (nm)
Dap	Kyn13	365	400–600
Dap-E12-W13	Trp1 / Trp13	280	300–400
Dap-E12-Y13	Trp1	280	300–400
Dap-E12-Y13-pyrene	Pyrene	340	360–600
Dap-A7-E12-Y13	Trp1	280	300–400
A5	Trp1	280	300–400
A5-pyrene	Pyrene	340	360–600

3.2.3 Determining the antibacterial activity of antibiotics

The procedure for determining the minimum inhibitory concentration of the antibiotics has been described in a preceding chapter (see section 2.2.4).

3.3 Results

The synthetic procedure developed by Dr. Chuda Lohani from the Taylor group was first used to produce unsubstituted dap.⁸⁹ The synthetic dap is generated through SPPS and thus designated dap-SPPS. Part of validating the synthetic procedure was to compare the antibacterial activity and membrane binding characteristics of authentic dap to the synthetic dap.

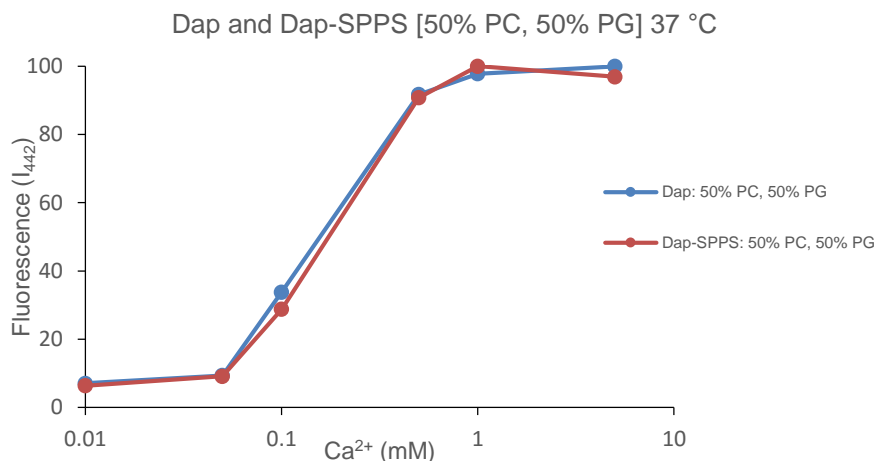


Figure 3.2: Kynurenine fluorescence of Dap and Dap-SPPS on liposomes of varying composition at 37 °C. The figure follows maximum normalized analog fluorescence (I_{442}) as a function of Ca^{2+} concentration.

The antibacterial activity results at 5 mM Ca^{2+} are identical at an MIC of 0.75 $\mu\text{g}/\text{mL}$ (Table 3.2); the authentic dap and dap-SPPS also show equivalent responses in fluorescence intensity on a 50:50 PC:PG membrane, as calcium is added incrementally (Figure 3.2). These tests, in addition to HPLC chromatograms, mass spectroscopy and NMR, verify that the synthetic dap is equivalent to the authentic dap. This confirms the synthetic procedure is able to generate authentic dap and thus can reliably generate synthetic derivatives of dap, such as dap-E12-W13 and dap-E12-Y13.

Table 3.2: MIC ($\mu\text{g}/\text{mL}$) assay results of various lipopeptide analogs at 5 and 100 mM Ca^{2+} on *B. subtilis* ATCC 1046.

Lipopeptide	Ca^{2+} Concentration	
	5 mM	100 mM
Dap	0.75	0.50
Dap-SPPS	0.75	N/D
Dap-E12-W13	1.5	1.5
Dap-E12-Y13	35	1.3
Dap-E12-Y13-pyrene	>50	1.5–3.0
A5	0.75	0.75
A5-pyrene	0.75–1.0	N/D

N/D = no data

The antibacterial activities of the dap-E12-W13 and dap-E12-Y13 analogs were tested (Table 3.2). Compared to dap and A5, dap-E12-W13 remained highly active, while dap-E12-Y13 lost considerable

activity; the Trp analog MIC increased 2-fold whereas the Tyr analog MIC increased over 45-fold. The activity of dap-E12-W13 is sufficiently effective for use of the analog as the base scaffold for the synthesis of others.

When the antibacterial activities of the analogs were tested at 100 mM Ca^{2+} , the activity for most decreased, however, unexpectedly, that of dap-E12-Y13 decreased vastly in comparison to the others. The dap-E12-Y13 MICs decreased to just below 2.5-fold over that of dap at 100 mM Ca^{2+} . From this it is assumed that the residues in position 12 and 13 have a role in the calcium affinity of dap.⁸⁹ To investigate the functional differences between the analogs, they were characterized using fluorescence studies which indicate membrane binding and oligomer formation.

3.3.1 Dap-E12-W13 and dap-E12-Y13 membrane binding

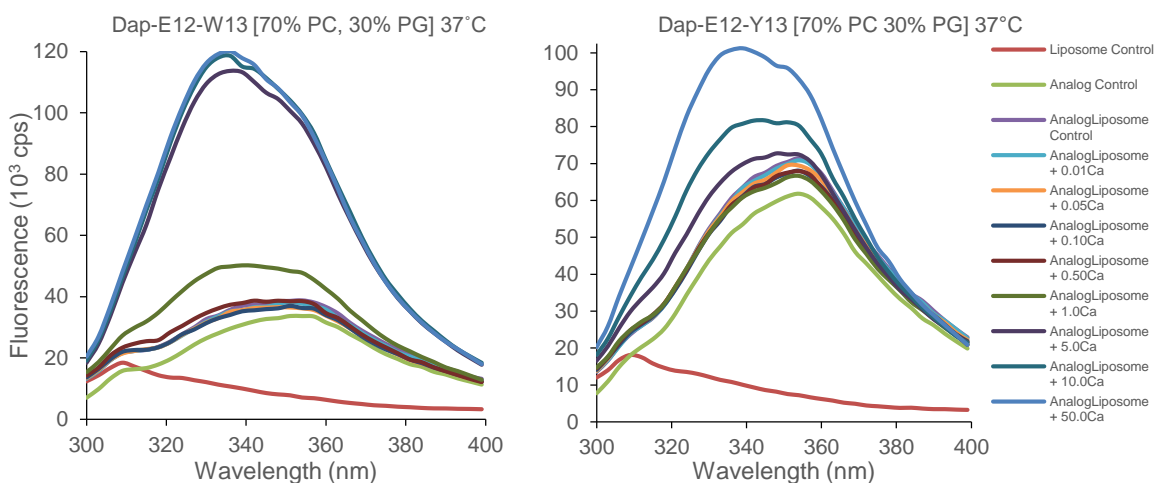


Figure 3.3: Tryptophan fluorescence spectra of dap-E12-W13 and dap-E12-Y13 in the presence of 70:30 PC:PG liposomes and increasing Ca^{2+} concentration (mM) at 37 °C.

The membrane binding assay for dap exploits the intrinsic Kyn fluorophore, as this residue has been substituted in the analogs a different fluorophore must be used. Conveniently, the lipopeptides contain an additional intrinsic fluorophore, the Trp residue in position 1 (and position 13 in dap-E12-W13). The indication of membrane binding using Trp is the distinct blue-shift when it enters a more hydrophobic environment. The analogs both display a blue-shift as calcium is added incrementally, however, it occurs at lower calcium concentrations for dap-E12-W13 (Figure 3.3). To compare to dap a dual plot can be used; dap, as with the other analogs, contains a Trp residue at position 1, however, its Kyn residue vastly reduces its fluorescence through FRET (Figure 3.4). The dual plot follows the

increase in Kyn fluorescence intensity in dap and the fluorescence blue-shift of Trp in the analogs (Figure 3.4).

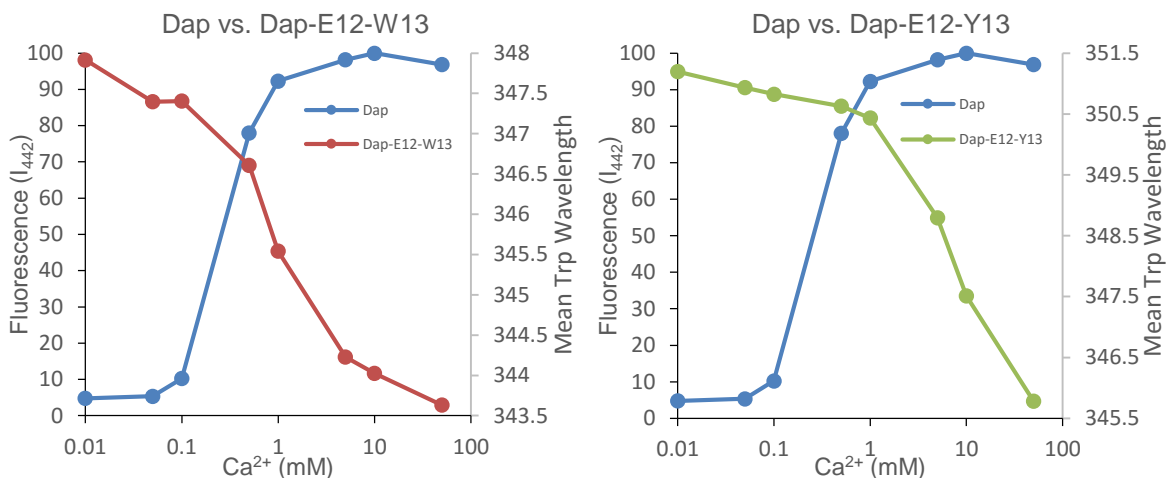


Figure 3.4: Mean tryptophan wavelength emission of dap-E12-W13 (left) and Dap-E12-Y13 (right) compared to maximum fluorescence intensity of dap emission (I_{442}), each as a function of Ca^{2+} concentration. Liposome composition is 70:30 PC:PG.

The native dap fluorescence signal increases significantly after 0.1 mM Ca^{2+} and saturates around 5–10 mM Ca^{2+} ; the midpoint of the transition occurs between 0.1 and 0.5 mM Ca^{2+} . The dap-E12-W13 fluorescence blue-shift progresses slowly as the calcium concentration is increased, with the most significant blue-shifting occurring past 0.5 mM Ca^{2+} ; its transition midpoint occurs around 1 mM Ca^{2+} . Dap-E12-Y13 shows a vastly delayed response, and does not blue-shift prominently until over 1 mM Ca^{2+} ; its transition midpoint occurs just over 5 mM Ca^{2+} . The order of the transition midpoints, from lowest to highest, is dap, dap-E12-W13, then dap-E12-Y13. This corresponds to their respective MICs at 5 mM Ca^{2+} , which are 0.75, 1.5 and 35 μ g/mL.

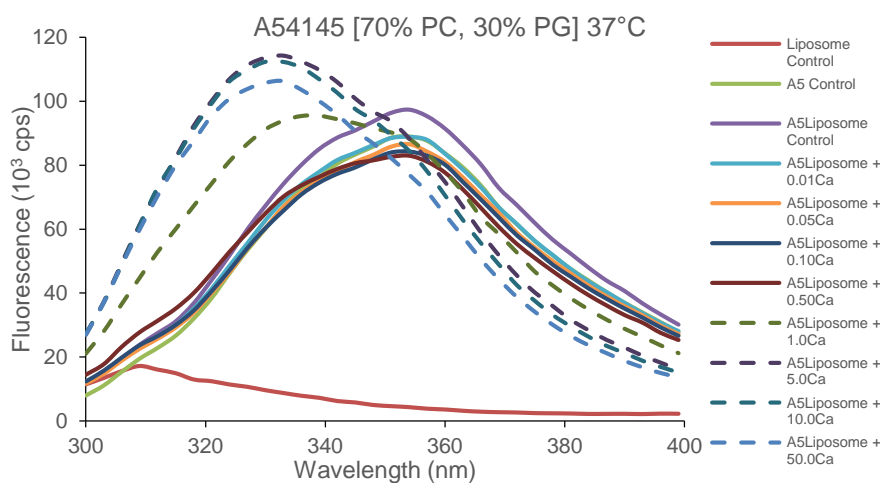


Figure 3.5: Tryptophan fluorescence spectrum of A5 in the presence of 70:30 PC:PG liposomes and increasing Ca^{2+} concentration (mM) at 37 °C.

As an alternative to the dual plots, direct comparison of the analogs to A5, whose Trp residue is free from quenching, is possible (Figure 3.5). The comparison remains informative, as A5 has an identical MIC to dap and it has been shown to be functionally closely related – dap and A5 are able to form partially functional hybrid oligomers.⁷⁸ Following the blue shift of A5 and the dap analogs is possible by plotting the ratio of emission at 333 nm to that at 354 nm as a function of calcium – the ratio will increase as the blue-shift progresses (Figure 3.6).

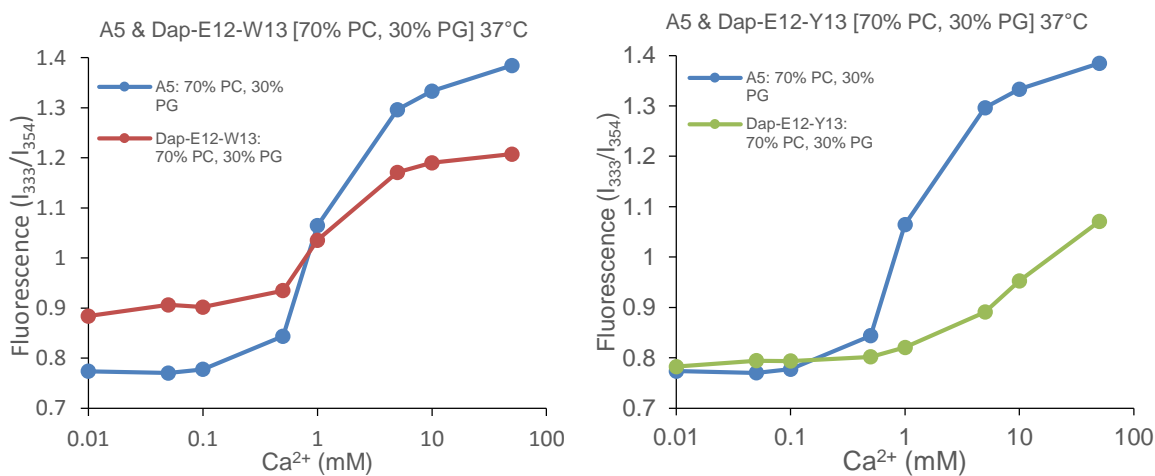


Figure 3.6: Tryptophan fluorescence of A5, dap-E12-W13, dap-E12-Y13 on liposomes of varying composition at 37 °C. The figure follows the fluorescence blue-shift (I_{333}/I_{354}) as a function of Ca^{2+} concentration.

A5 begins its blue-shift at calcium concentrations over 0.5 mM on 70:30 PC:PG; of the analogs, dap-E12-W13, is the most similar. Its blue-shift also begins at calcium concentrations over 0.5 mM, but it is less pronounced. The transition midpoint for both occurs in the region above 1.0 mM, but below 5 mM Ca^{2+} . Dap-E12-Y13 shows a delayed response, and does not blue-shift prominently until over 1 mM Ca^{2+} ; the transition midpoint remains around 5 mM Ca^{2+} . As with dap, these results mostly correspond with the MIC results; the transition midpoints of A5 and dap-E12-W13 are comparable, yet the MIC of the analog is higher – this difference may be reflected in the less pronounced blue-shift.

3.3.2 Dap-E12-Y13 oligomer formation

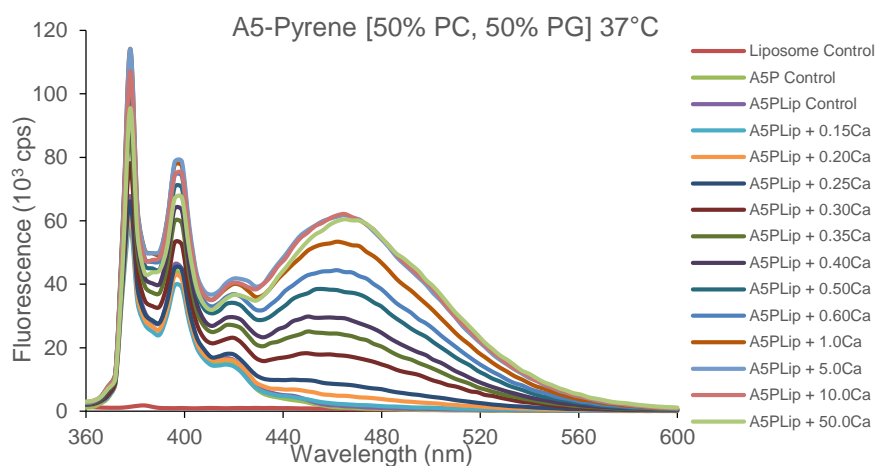


Figure 3.7: Pyrene fluorescence spectrum of A5-pyrene in the presence of 50:50 PC:PG liposomes and increasing Ca^{2+} concentration (mM) at 37 °C. Legend: A5P and A5PLip refer to A5-pyrene alone or in the presence of liposomes, respectively.

Perylene and pyrene fluorophores have been used previously to characterize the oligomerization of dap and A5, respectively (Figure 3.7).⁷⁵ This was accomplished through the detection of excimers at calcium concentrations known to promote oligomer formation. Excimers, or excited dimers, are complexes that form from the direct contact of a fluorophore molecule in the excited state with another in the ground state. The fluorophore is within the acyl tail of the analogs, consequently, excimer fluorescence indicates that the acyl tails of nearby oligomer subunits are in immediate contact with one another.

Oligomerization is known to be a necessary but not sufficient condition for pore formation, the end result required for antibacterial activity.^{52,78} Therefore, if oligomer formation is shifted to higher calcium concentrations, you can assume its antibacterial response is shifted as well. Characterizing the

excimer formation of dap-E12-Y13-pyrene over a wide calcium concentration range will indicate whether oligomerization is shifted, and consequently its requirement of high calcium for antibacterial activity is appropriate. The pyrene spectrum is composed of monomer peaks from 360–440 nm and an excimer peak above 440 nm.¹²² For easy comparison of analogs it is possible to find the ratio of the excimer fluorescence at 471 nm and the monomer fluorescence at 378 nm (extent of excimer formation) as a function of calcium (Figure 3.8).

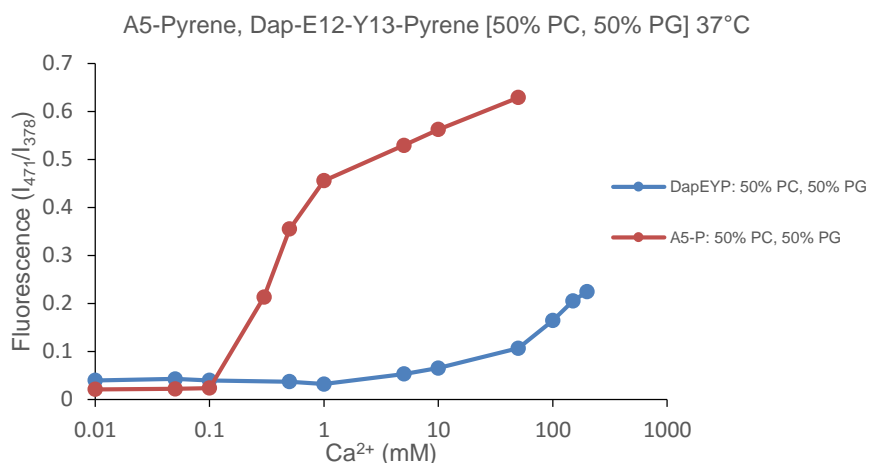


Figure 3.8: Excimer formation comparison of A5-pyrene and dap-E12-Y13-pyrene on liposomes of varying composition at 37 °C. The figure follows the extent of excimer formation (I_{471}/I_{378}) as a function of Ca^{2+} concentration.

The spectrum of dap-E12-Y13-pyrene shows both weak and shifted excimer formation compared to A5-pyrene. A5-pyrene excimers begin forming after 0.1 mM Ca^{2+} on the 50:50 PC:PG membrane; by 5 mM Ca^{2+} the extent of excimer formation is high. This corresponds to its low 0.75 $\mu\text{g}/\text{mL}$ MIC. Dap-E12-Y13-pyrene excimers begin forming after 1 mM Ca^{2+} concentration; by 5 mM Ca^{2+} the extent of excimer formation remains very low. Again, this corresponds to its high $>50 \mu\text{g}/\text{mL}$ MIC. At 100 mM Ca^{2+} , the extent of excimer formation of dap-E12-Y13-pyrene has increased and it shows a correspondingly increased antibacterial effect, with an MIC of 1.5–3.0 $\mu\text{g}/\text{mL}$. The shift of dap-E12-Y13 antibacterial activity to higher calcium concentration of appears to be appropriate considering its comparably shifted excimer fluorescence.

3.3.3 Dap-A7-E12-W13 antibacterial activity and membrane binding

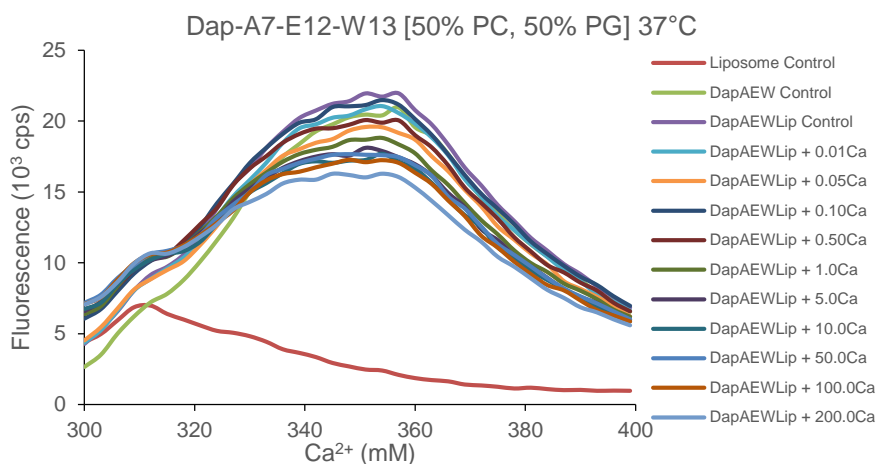


Figure 3.9: Fluorescence spectrum of dap-A7-E12-W13 in the presence of 50:30 PC:PG liposomes and increasing Ca^{2+} concentration (mM) at 37 °C. Legend: DapAEW and DapAEWLip refer to dap-A7-E12-W13 alone or in the presence of liposomes, respectively.

Dap-A7-E12-W13 has a substitution to the conserved lipopeptide aspartic acid residue at position 7. Substitutions to this position have been shown previously to lack antibacterial activity; although that particular analog was a triple mutant, with substitutions to positions 2 and 12 as well.¹²³ This analog was synthesized to show that the bacteria in the antibacterial activity assays were not being adversely affected by high calcium concentration and dying in a fashion non-specific to dap's mechanism of action. Ultimately, the control worked as the MIC for dap-A7-E12-W13 on *B. subtilis* 1046 was over 100 $\mu\text{g}/\text{mL}$ for both 5 and 100 mM Ca^{2+} (Table 3.4).¹¹⁹ The MIC on L-forms was also determined to indicate whether use of this strain increases the activity of all analogs; the MIC remained over 60 $\mu\text{g}/\text{mL}$ at 5 mM Ca^{2+} . The high MICs corresponds to the membrane binding data, which shows no blue-shift up to a calcium concentration of 200 mM (Figure 3.9).

3.3.4 Dap-E12-W13 surfactant sequestration

Lastly, the antibacterial activity of dap-E12-W13 in the presence of the bovine lung extract surfactant (BLES) was determined; comparison is to the results of dap and A5 in identical conditions. Dap-E12-Y13 was excluded due to its low activity. To emulate physiological conditions, 1 mM rather than 5 mM Ca^{2+} was used (Table 3.3).⁶⁷

Table 3.3: MIC ($\mu\text{g/mL}$) of lipopeptides in the absence and presence of lung surfactant on *B. subtilis* ATCC 1046.

Lipopeptide (or antibiotic)	<i>B. subtilis</i> ATCC 1046	
	0% BLES	1% BLES
Dap ^a	2	>40
Dap-E12-W13 ^a	>12	>45
A5 ^a	4	30
Ceftriaxone	0.5	0.5

^a1 mM Ca^{2+}

Dap and A5 have MICs over 2.5- and 5-fold higher than at 5 mM Ca^{2+} ; dap-E12-W13's increased by a minimum of 8-fold. When in the presence of surfactant dap and dap-E12-W13 have MICs over 40 $\mu\text{g/mL}$; A5 has an MIC of 30 $\mu\text{g/mL}$. The antibacterial activity of A5 is therefore more affected by the decrease in calcium concentration than dap, however, its activity in the presence of surfactant is less inhibited. The activity of dap-E12-W13 is most inhibited by the decrease in calcium concentration, and the amino acid substitutions appears not to reduce the sequestration of the antibiotic into surfactant. As a control, ceftriaxone, a β -lactam antibiotic, is used. It confirms that not all antibiotics lose activity in the presence of surfactant.

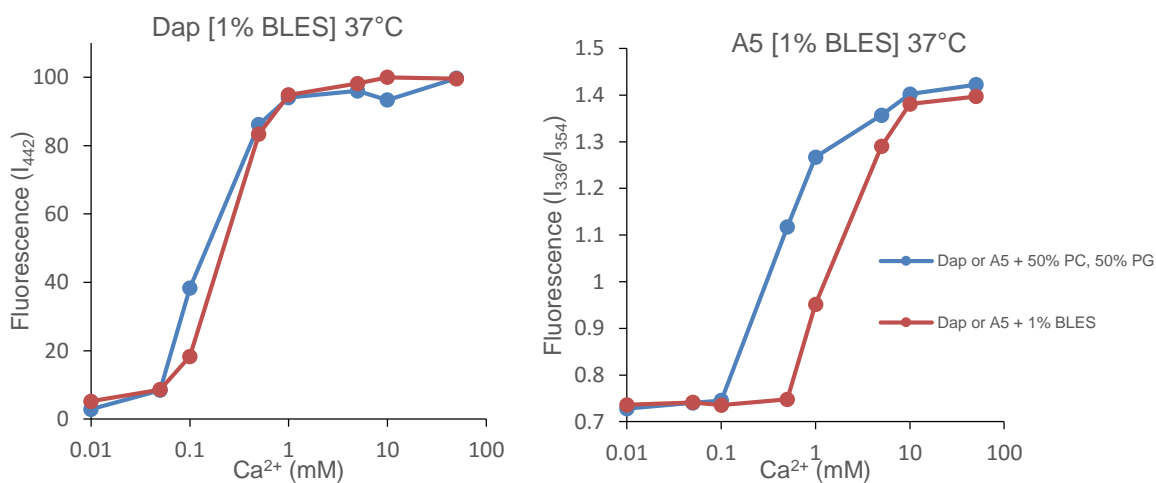


Figure 3.10: Comparison of dap (left) and A5 (right) on PC/PG liposomes and 1% surfactant. The figures follow the fluorescence intensity (left: I_{442}) and the fluorescence blue-shift (right: I_{336}/I_{354}), as a function of Ca^{2+} concentration.

The binding of the lipopeptides to BLES was characterized using the same procedure as membrane binding, however the liposomes were exchanged for surfactant. Dap binds to surfactant in a manner comparable to 50:50 PC:PG liposomes, the fluorescence intensity is nearly identical as calcium is added incrementally (*left*: Figure 3.10). The transition midpoint for both occurs between 0.1 and 0.5 mM Ca^{2+} . A5 binds to surfactant less than to 50:50 PC:PG liposomes, its fluorescence blue-shift requires higher calcium concentrations (*right*: Figure 3.10). The transition midpoint shifts from 0.5 mM to over 1 mM Ca^{2+} . Less binding to surfactant leaves a higher proportion of antibiotic free to interact with bacterial cells, therefore, the binding results agree with the respective antibacterial activity of dap and A5 in the presence of surfactant.

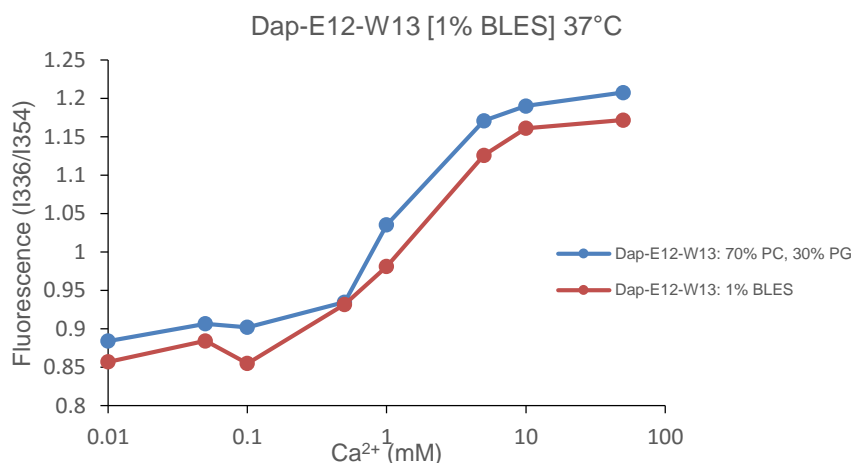


Figure 3.11: Comparison of dap-E12-W13 on PC/PG liposomes and 1% surfactant. Fluorescence intensity (I₃₃₆) is followed as a function of Ca^{2+} concentration.

Dap-E12-W13 on surfactant reflects a binding pattern most similar to that of dap; the midpoint of the transition appears to be shifted very slightly to the right, if at all (Figure 3.11). The amino acid substitutions consequently appear have little or no change to the sequestration of the lipopeptide into surfactant. However, the substitutions do cause the activity of the analog to be significantly decreased at 1 mM Ca^{2+} .

3.4 Discussion

Characterization of the initial synthetic dap analogs produced by the Taylor group reveals dap-E12-W13 as the most notable; its antibacterial activity approaches that of dap and A5, at only double the MIC. The synthesis and partial characterization of these analogs was published by Lohani *et al.*^{89,119} The high antibacterial activity and simplified synthetic procedure of dap-E12-W13 make it a viable

candidate for the role as the base scaffold in the generation of a combinatorial analog library. Nevertheless, the analog does not exhibit significantly increased tolerance to the presence of surfactant, and at physiological calcium concentrations the antibacterial activity is comparatively decreased to dap and A5.

Dap-E12-W13 is amongst the most active dap analogs characterized by research groups in this field.¹²⁴ Table 3.4 displays the antibacterial activities of dap analogs below 10 times that of the native dap, with the exception of the single substitution variants of dap-E12-W13 and dap-E12-Y13. Over twenty additional dap analogs with differing amino acids substitutions have been characterized.¹²⁴ The significant antibacterial activity of dap-E12-W13 is unexpected considering the two amino acid substitution were performed previously and separately yielded an increase in MIC by 2-fold and nearly 16-fold for Trp and Glu, respectively.⁸⁵ Whether the substitutions function better together, or the change to a decanoyl tail altered the analog's activity considerably has not been established; however, A21978C₁, a dap derivative with an anteisoundecanoyl tail, has exhibited lower *in vivo* activity against *S. aureus* and *Streptococcus pyogenes*.⁵⁷

The dap-E12-Y13 analog is on the other end of the spectrum; its antibacterial activity is low. Changing the amino acids at position 12 and 13 may change the geometry of the lipopeptide, making the calcium affinity lower – the defect would be greater with some amino acids, consequently they require higher calcium concentrations to induce calcium binding and the successive membrane association and oligomerization. Dap-A7-E12-W13 is inactive, as expected, and its effect is not rescued by high calcium as the native Asp residue in position 7 likely directly binds to calcium.

Table 3.4: Antibacterial activities of select dap analogs produced by different groups. Only relevant amino acid positions are listed. MIC ratio refers to the MIC of the analog divided by the MIC of native dap.

Lipopeptide	Amino acid position					MIC Ratio
	1	8	11	12	13	
Dap	Trp	D-Ala	D-Ser	MeGlu	Kyn	1
1 ⁸⁵				Glu		16
2 ⁸⁵					Trp	2
3 ⁸⁹				Glu	Trp	2
4 ⁸⁹				Glu	Tyr	47
5 ⁸⁵			D-Ala			2
6 ⁸⁵		D-Lys	D-Asn			2
7 ⁸⁵			D-Asn		Ille	8
8 ⁸⁷	Phe					4
9 ⁸⁵		D-Ser				2

Chapter 4

Characterizing lysyl-phosphatidylglycerol-mediated daptomycin resistance

4.1 Introduction

Resistance, or non-susceptibility, to dap has been correlated in part to changes in the *mprF* gene.^{125,126} *mprF* codes for the multiple peptide resistance factor (MprF) enzyme, which catalyzes the synthesis of LPG from PG; it is also the flippase which moves LPG from the inner membrane leaflet to the outer membrane leaflet.⁹⁶ The relevance of the changes has been corroborated by the detection of similar mutations in clinical isolates of *S. aureus* which have developed treatment-emergent increases to the dap MIC.⁵¹

LPG-mediated dap resistance has yet to be comprehensively studied; due to its clinical significance, it is an important topic of research. Characterization of the mechanism of resistance could yield information which allows for the production of dap analogs with decreased non-susceptibility. A potential mechanism of resistance is available as MprF gain-of-function mutants are also associated to bacterial resistance to cationic antimicrobial peptides (CAMPs).¹²⁷ CAMPs include some host defense peptides (HDPs), which are part of the innate immune response in humans.⁹⁸ In fact, bacteria with treatment-emergent non-susceptibility to dap can develop cross-resistance to HDPs; this provides a distinct survival advantage to the bacteria in bloodstream infections.^{98,128}

The proposed mechanism through which MprF gain-of-function mutants gain resistance to CAMPs is a decrease in the membrane binding of the peptides to the bacterial membrane.⁹⁶ This arises due to electrostatic repulsion between the cationic peptides and the increased positive charge in the membrane; the addition of lysine to PG changes the net charge of the membrane lipid from -1 to $+1$. For this mechanism to occur with dap, it must be presumed that in conjunction with calcium the lipopeptide is acting in a CAMP-like manner and has its membrane association reduced. At physiological pH, dap has a net charge of -3 ; consequently, two calcium ions binding to dap in solution would be required to cause a reversal of charge. NMR studies of dap in solution have indicated that calcium binds to dap in solution with a 1:1 stoichiometry.^{82,83} This would leave dap in solution as a singly-charged anion, bringing question to whether this mechanism is correct. An alternative mechanism has been shown with at least one cationic peptide; rather than reducing association with the membrane, an attenuation of

membrane perturbation decreased peptide-induced membrane permeabilization.⁹⁷ As peptide charge is not a main factor, this mechanism may be more likely for dap.

Characterization of the mechanism of LPG-mediated dap resistance is possible through assays which indicate whether the successive steps of the action mode of dap are occurring.^{52,75,84} The steps include, (1) calcium-mediated binding to PG at the outer leaflet; (2) formation of oligomers; (3) formation of pores through equilibration and alignment of oligomers across both membrane leaflets. Membrane binding can be detected in the presence of liposomes through calcium-dependent increases to the quantum yield of dap's intrinsic Kyn13 fluorophore, or the blue-shift of A5's intrinsic Trp1 fluorophore. The formation of oligomers is detected in the presence of liposomes through the calcium-dependent formations of excimers within pyrene-labeled A5. Translocation can be detected through the self-quenching of acrylodan-labeled A5. Pore formation is detected with a liposome permeabilization assay which displays pore-dependent increases in the fluorescence of liposomes loaded with a pH-sensitive dye.

4.2 Materials and Methods

Gel filtration procedures are done on a Bio-Rad P-6DG column (Bio-Rad, Richmond, CA, USA).

4.2.1 Preparation of liposomes

The procedure for the preparation of the liposomes (LUVs) has been described in a preceding chapter (see section 2.2.1)

4.2.2 Fluorescence Studies

The procedure for performing the fluorescence studies has been described in a preceding chapter (see section 2.2.3)

Table 4.1: Fluorophore, excitation wavelength, and emission range of relevant lipopeptide analogs.

Lipopeptide	Fluorophore	Excitation (nm)	Emission (nm)
Dap	Kyn13	365	400–600
A5	Trp1	280	300–400
A5-acrylodan	Acrylodan	360	400–600
A5-pyrene	Pyrene	340	360–600

4.2.3 Measurement of membrane permeabilization with pyranine-loaded liposomes

Liposomes of a given lipid composition are prepared as described previously. The hydration buffer consists of pyranine (5 mM) in a MES/Tricine (5 mM, pH 6.0), NaCl (5 mM), KCl (5 mM), and sucrose (250 mM) solution. After hydration and membrane extrusion, the mixture is passed through a gel filtration column to remove un-encapsulated pyranine; gel filtration may be repeated as required. The fluorescence assay samples contain a total lipid concentration of 250 μ M, 5 nM CCCP, and a final concentration of 0.5 μ M of lipopeptide analog. The assay buffer is identical to the hydration buffer, except for an increase in pH to 8.0, and a NaCl or KCl concentration of 100 mM. Calcium is added to a concentration of 5 or 100 mM to start the assay. For pyranine, the excitation wavelength is 460 nm, and the emission wavelength is 510 nm. The fluorescence time curve is recorded over 300 seconds, after which Triton X-100 is added to a final concentration of 0.1% to solubilize the liposomes. The spectrum is recorded for an additional 60 seconds to establish the fluorescence intensity equivalent to 100% test solute equilibration. Controls involve measurements of the liposomes alone, and the liposomes in the presence of the lipopeptide, calcium, Triton X-100, and CCCP, separately.

4.3 Results

The chosen base membrane composition was 70:30 PC:PG. It represents a simple dap-sensitive membrane; PG is required for the action mode of dap, while PC is a mostly inert lipid with respect to dap at low calcium concentrations. The initial LPG-containing membranes were 55:30:15 PC:PG:LPG and 70:30 PC:LPG; others were planned, however, LPG research was discontinued due to its prohibitive cost, and initial attempts at its synthesis failed. In the membrane including both PG and LPG, the PG content was kept constant. This was done to distinguish the potential specific inhibitory effect of LPG from that of a diminished amount of PG; in bacterial membranes, the inhibitory role of each is not distinguished – upregulation of LPG synthesis requires increased use of its precursors, which include PG. For simplicity, hereafter, the membrane containing PC, PG, and LPG will be designated the ‘hybrid LPG’ membrane, and the membrane containing PC and LPG will be designated the ‘pure LPG’ membrane.

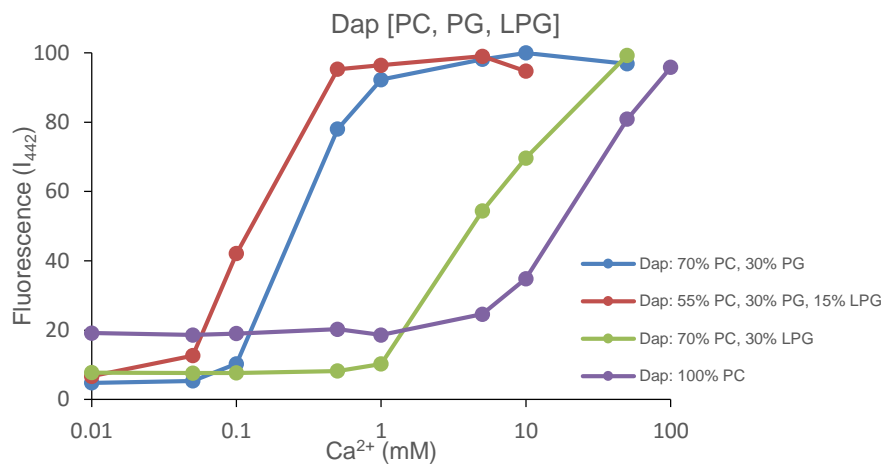


Figure 4.1: Kynurenine fluorescence of dap on liposomes of varying composition at 37 °C; the exception is the 55% PC, 30% PG, 15% LPG membrane under ambient conditions (~25 °C). The figure follows maximum normalized analog fluorescence (I_{442}) as a function of Ca^{2+} concentration.

The results for the dap membrane binding assay using the LPG-containing membranes are intriguing (Figure 4.1). Dap on the hybrid LPG membrane displays a shifted calcium-dependent fluorescence intensity response compared to the 70:30 PC:PG membrane; at lower calcium concentrations the increase in intensity is greater. This could indicate an enhanced interaction with the membrane, such as deeper insertion. If the mechanism of dap resistance is mediated by reduced membrane association, the opposite of this result should occur. Even if 15% LPG in the membrane is not sufficient for high-level dap resistance, the fluorescence intensity response should simply not shift. The cause of the shift has not been established; more membranes with LPG in the presence of PG are needed. Whether the enhanced interaction reverses at higher LPG concentrations, is not known.

Dap on the pure LPG membrane shows the opposite result; compared to the base membrane, increased calcium is required to get dap to bind to the membrane. This is expected as PG is required for dap to bind to membranes at low calcium concentration. However, in comparison to the PC membrane, the fluorescence intensity of dap increases at a lower calcium concentration; consequently, it appears that dap can use LPG in place of PG at high calcium concentrations. Moreover, it shows that electrostatic repulsion is not a factor in dap binding. The membrane is entirely composed of neutral or positively charged lipids, therefore if dap was repulsed it would bind at higher calcium concentrations compared to the PC membrane.

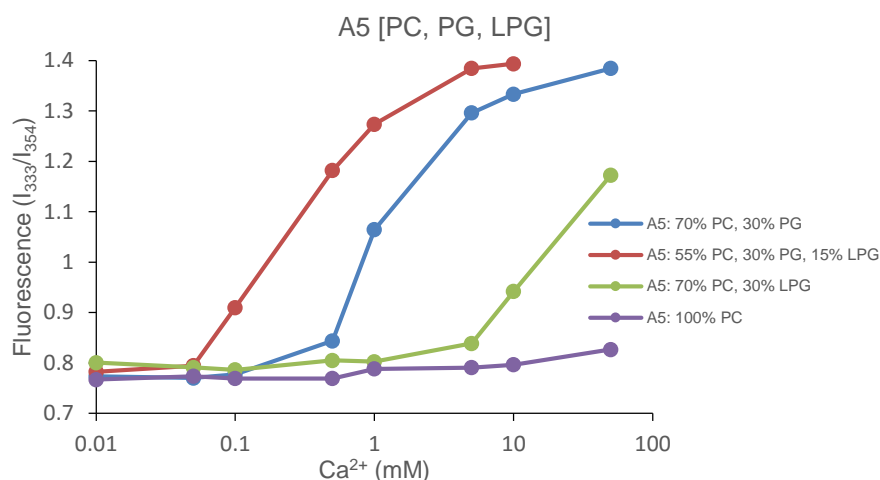


Figure 4.2: Tryptophan fluorescence of A5 on liposomes of varying composition at 37 °C; the exception is the 55% PC, 30% PG, 15% LPG membrane under ambient conditions (~25 °C). The figure follows the fluorescence blue-shift (I_{333}/I_{354}) as a function of Ca^{2+} concentration.

The results for A5 correspond closely to those of dap (Figure 4.2). A5 fluorescence on the hybrid LPG membrane undergoes a blue-shift at a lower calcium concentration. The calcium-binding of A5 in solution has not been studied through NMR, however, it likely binds calcium in the same manner as dap, thus its results are similar (A5 and dap share the same net charge at physiological pH, -3). The pure LPG membrane delays the fluorescence blue-shift until over 5 mM Ca^{2+} has been added, whereas a blue-shift does not occur on the PC membrane. The difference between A5 on the LPG and PC membranes is thus greater than that seen with dap, however the membrane binding begins at over 5 mM Ca^{2+} compared to 1 mM Ca^{2+} for dap. This may be due to the intrinsic differences between the two lipopeptides, or the location of the intrinsic fluorophore (Trp1, exocyclic tripeptide; Kyn13, head group) – in either case, it reaffirms that LPG within the membrane promotes some membrane binding at high calcium concentrations.

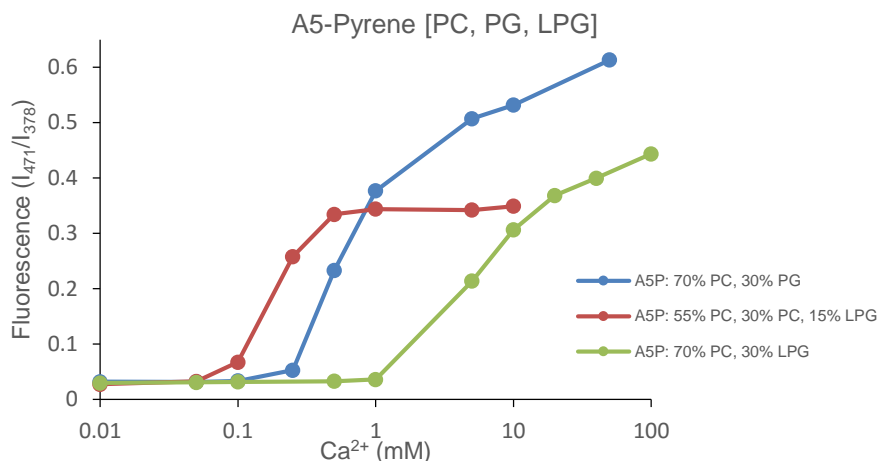


Figure 4.3: Excimer formation comparison of A5-pyrene on liposomes of varying composition at 37 °C; the exception is the 55% PC, 30% PG, 15% LPG membrane under ambient conditions (~25 °C). The figure follows the extent of excimer formation (I_{471}/I_{378}) as a function of Ca^{2+} concentration.

Despite the fact that the dap and A5 are binding to the LPG-containing membranes, the subsequent steps necessary for antibacterial activity, namely oligomerization and pore formation, may not be occurring. To test for the occurrence of oligomerization, A5-pyrene was used (Figure 4.3). Pyrene excimers begin forming around 0.10, 0.25, and 5 mM Ca^{2+} on the hybrid LPG, 70:30 PC:PG, and pure LPG membranes, respectively; the formation continues until saturation at approximately 0.5, 5 and 60 mM Ca^{2+} . The graph displays the extent of excimer formation continuing past the point of saturation on the 70:30 PC:PG membrane and LPG membrane, however, this occurs due to a decrease in monomer fluorescence intensity, with little or no associated excimer fluorescence – detailed fluorescence lifetime studies might resolve the disparity (see appendix: Figure 6.16, Figure 6.20).

The presence of excimers on all the membranes confirms that oligomerization is occurring. The calcium concentrations required to induce excimer formation follow the previously established pattern and resembles those required to induce kynurenine fluorescence on the respective membranes. Most surprising is the formation of oligomers on the pure LPG membrane, as excimers do not form on PC membranes (data not shown). This shows that despite LPG being correlated to resistance it is able to mediate both the binding dap monomers and the formation of dap oligomers in the absence of PG. Nevertheless, oligomerization is necessary but not sufficient for antibacterial activity, and significant formation only begins at calcium concentrations above physiological levels.^{52,78} Whether the addition

of some PG to this membrane could lower the required calcium concentration is not known – but seems likely in light of the hybrid LPG membrane.

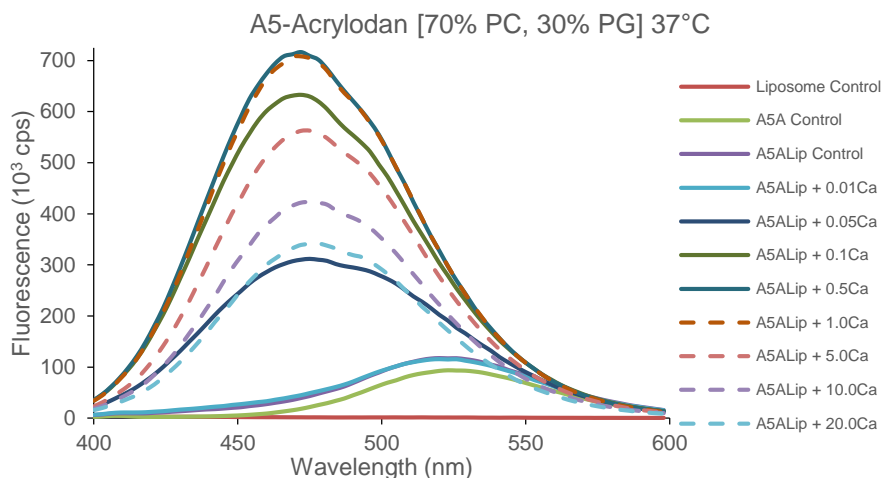


Figure 4.4: Fluorescence spectrum of A5-acrylodan in the presence of 70:30 PC:PG liposomes and increasing Ca^{2+} concentration (mM) at 37 °C. A5A and A5ALip refer to A5-acrylodan alone or in the presence of liposomes.

To support the oligomerization data from A5-pyrene, A5-acrylodan was used. A5-acrylodan is an alternative to NBD-dap, which was used previously by the Palmer group to characterize the oligomerization of dap by fluorescence self-quenching.⁷³ Recently, data from A5-acrylodan interacting on CL-containing liposomes has shown that that the self-quenching occurs due to translocation and alignments of oligomers, rather than oligomer formation. The fluorescence spectrum of A5-acrylodan on 70:30 PC:PG liposomes can be seen in Figure 4.4 (see appendix for other membranes; Figure 6.15, Figure 6.19). The initial rapid blue-shift and increase in acrylodan fluorescence coincides with in the binding of one calcium ion to the analog; the maximum fluorescence occurs at 0.5 mM Ca^{2+} .⁸⁴ Excimer formation is also seen at these calcium concentrations (see above), indicating an oligomer is forming. Increased calcium concentration induces the binding of a second calcium ion and acrylodan fluorescence begins to self-quench, indicating the translocation and alignment of oligomers. A functional pore is likely occurring at this point. To compare between membranes, plotting maximum normalized analog fluorescence as a function of calcium greatly simplifies the spectrum (Figure 4.5).

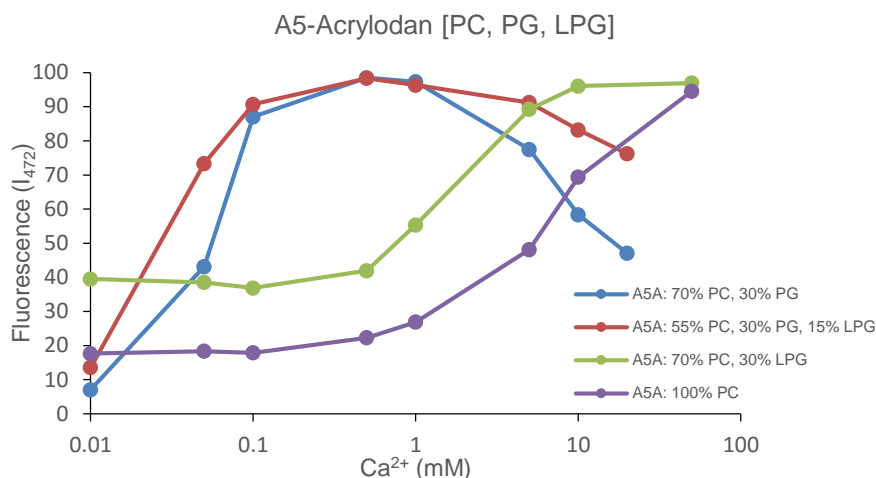


Figure 4.5: Acrylodan fluorescence of A5-acrylodan on liposomes of varying composition at 37 °C; the exception is the 55% PC, 30% PG, 15% LPG membrane under ambient conditions (~25 °C). The figure follows the maximum normalized analog fluorescence (I_{472}) as a function of Ca^{2+} concentration.

The fluorescence spectrum of A5-acrylodan on the hybrid LPG membrane resembles that of the analog on the 70:30 PC:PG membrane; fluorescence increases with calcium at a slightly faster rate but reaches its maximum at the same value, 0.5 mM Ca^{2+} . As calcium continues to increase, self-quenching begins as the oligomers equilibrate and align across the membrane; however, the quenching occurs to a lesser degree. This indicates that the translocation of oligomers may be impaired in some fashion at this LPG concentration – though the majority of oligomers likely still create functional pores.

The pure LPG membrane exhibits different results. The first stage of the A5-acrylodan spectrum, the blue-shift and fluorescence increase, is seen – despite its need for drastically increased calcium. Therefore, the analog is interacting with the membrane; the formations of excimers also demonstrates that oligomerization is occurring at this point. In contrast, A5-acrylodan on the PC membrane shows acrylodan fluorescence increase at high calcium concentrations, but does not exhibit excimer formation. The second stage of the A5-acrylodan spectrum, the self-quenching, is the significant difference. A5-acrylodan on the pure LPG membrane displays a complete loss of self-quenching, even at high calcium concentrations. This indicates that the oligomers forming on the outer membrane leaflet are not undergoing translocation and alignment to form a pore. This is reminiscent of CL-mediated resistance, in which dap can bind and form oligomers on the membrane, but translocation is inhibited and thus pore formation as well.⁵² The pure LPG membrane is of course not the most accurate model due to its lack of PG – nevertheless, the hybrid LPG membrane appears to be presenting the beginning of the

same inhibitory effect. This provides evidence that LPG-mediated resistance does not occur through a reduction of membrane association, rather the translocation of the lipopeptide oligomers may be inhibited.

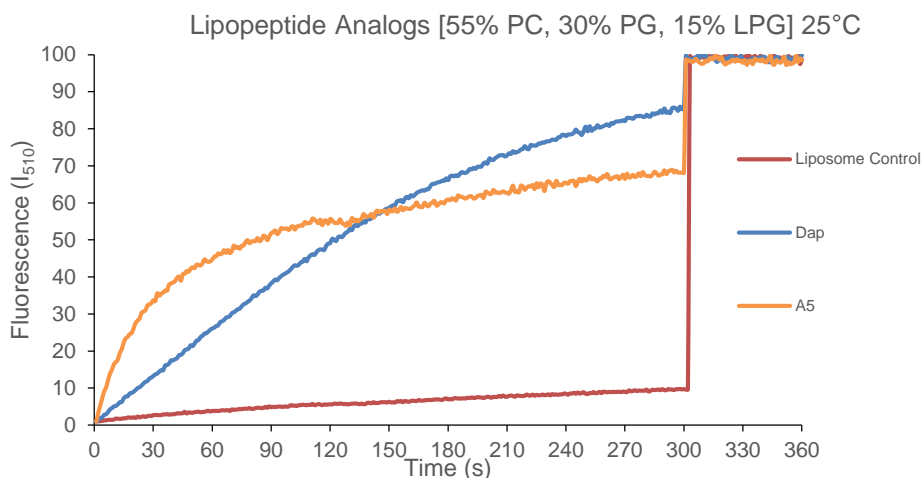


Figure 4.6: Liposome permeabilization tests using 0.5 μ M of multiple lipopeptide analogs in the presence of pyranine-loading liposomes, 5 (or 100) mM Ca^{2+} and 5 nM CCCP at 25 °C. Controls include lipopeptide alone or in the presence of either Ca^{2+} or CCCP (see appendix). Fluorescence (I_{510}) is normalized to the highest signal after Triton-X at 300s.

Lastly, the hybrid LPG membrane was used in the liposome permeabilization assay. Within the assay, the production of a functional pore by an applied analog will cause the liposome interior to increase in pH if a proton carrier such as CCCP is also present. The increase in pH is followed by the pH-sensitive fluorescent dye pyranine loaded into the liposomes. The membrane binding assays and oligomerization assays using dap and A5 analogs on the hybrid LPG membrane showed results similar to those of the analogs on 70:30 PC:PG membrane – the only difference of note is the reduced self-quenching of A5-acrylodan. Pore formation is therefore expected to occur; the results show that dap and A5 are able to permeabilize the membrane (Figure 4.6). Dap caused the highest increase in fluorescence during the experiment time-scale, however, A5 showed the quickest initial rate of fluorescence increase. This might reflect the intrinsic differences between the two lipopeptides.

4.4 Discussion

The preliminary results for dap on the LPG-containing membranes are insufficient for a full characterization of the specific inhibitory effect of LPG. Full characterization would likely require the examination of dap and its analogs on liposome compositions which include upwards of 30–40% LPG in the presence of PG. The LPG range required is high because many dap-susceptible bacteria have been shown to have high percentages of LPG within their membrane. A study on the phospholipid composition of dap-naïve *B. subtilis* showed a total LPG concentration of 22%.¹²⁹ Clinical isolates of *S. aureus* have also been determined to contain up to a total of 30% LPG.⁹⁷

Furthermore, LPG-mediated CAMP and dap resistance have been shown to be dependent upon the exposure of LPG to the outer surface of the bacterial membrane, not only its increased synthesis.⁹⁶ Dap resistance in two non-susceptible *S. aureus* strains showed they did not have significantly increased LPG concentrations compared to the parent strain (23–29%), but LPG translocation to the outer leaflets was 2-fold higher.⁸ Increased outer leaflet exposure of a set concentration of LPG is unable to be reproduced in a model membrane system; LPG used in the preparation of the liposomes partitions equally in the inner and outer leaflets, this essentially halves the concentration of LPG initially interacting with dap.

Once the specific inhibitory effect of LPG has been studied, to finalize the characterization, the effect of the step-wise reduction of PG on a set concentration of LPG can be examined. At commercial cost, the need for such quantities of LPG is cost prohibitive, this is also compounded the instability of LPG within the prepared liposomes. Liposomes containing LPG must be prepared and used immediately. Results obtained over multiple days are not reproducible; as time progresses, the LPG membranes display results similar to those without LPG. This may be due to non-specific hydrolysis of lysine from the PG.

Overall, the results for the two LPG membranes are interesting. Incorporation of 15% LPG within a PC/PG membrane seems to enhance the interaction of dap and A5 with the membrane. Subsequent oligomerization continues to occur, but oligomer translocation may be slightly inhibited. Ultimately, pore formation occurs and permeabilizes the membrane. Incorporation of 30% LPG within a PC membrane vastly reduces the interaction of dap and A5 with the membrane. Surprisingly, subsequent oligomerization occurs – though at non-physiological calcium concentrations. Oligomer translocation is completely inhibited; thus, pore formation is also inhibited. To corroborate the oligomer translocation data another test, such the dithionite quenching assay discussed in section 1.2.4, should be used.

This pattern of inhibition is reminiscent of CL-mediated resistance. CL does not prevent the formation of dap oligomers, but the translocation of oligomers is inhibited by stabilizing the liposome bilayer. A membrane stabilization effect between LPG and PG could account for slightly inhibited oligomer translocation on hybrid LPG membrane; stabilization may also allow for deeper insertion of dap into the membrane, changing its calcium-dependent fluorescence response. While the data shown here is preliminary, it is important to note that Kilelee *et al.*⁹⁷ proposed a membrane stabilization process in LPG-mediated resistance to 6W-RP-1, a structurally unrelated cationic peptide. The group found that 6W-RP-1 surface association with the target membrane varied only slightly with an LPG content between 0–30%. In contrast, the inclusion of increasing amounts of LPG inhibited the permeabilization of liposomes: 20% decreased both the extent and rate of fluorescent dye leakage, and 30% essentially eliminated leakage. Notably, the PG content was not kept constant within their experiments – LPG was directly substituted for PG.

In contrast, a stabilization effect is not possible between LPG and PG on the pure LPG membrane. The self-quenching must then be inhibited in some other manner. The most straightforward is the lack of un-derivatized PG, which has long been known to be needed for the action mode of dap; however, the two preceding steps of the action mode have been shown to occur here. As an alternative, LPG may replace a calcium ion, or block the binding of a calcium ion to the peptide in some other way – this is conceivable as the self-quenching of A5-acrylodan has been shown to coincide with the binding of a second calcium ion to the peptide.⁸⁴

Chapter 5

Investigating the role of phosphatidylserine in daptomycin-induced toxicity

5.1 Introduction

Dap-induced toxicity is characterized foremost by myopathy.¹³⁰ Myopathy manifests itself as muscle aching or muscle weakness in conjunction with increases in creatine phosphokinase (CPK) values in the blood.¹³⁰ CPK is an abundant soluble enzyme found within heart and skeletal muscle cells; high CPK values indicate damage to the muscle tissue and cellular leakage of the muscle constituents.¹³¹ Additional adverse reactions include pneumonia, diarrhea, headache, dizziness, rash, low blood pressure, shortness of breath, and abnormal liver function tests.¹³⁰

The mechanism through which dap induces muscle toxicity has not been established. Interaction with eukaryotic cells is possible, however, dap is known to require PG to efficiently perform its mechanism of action at physiological calcium concentrations (1–1.5 mM Ca^{2+}); PG is only present in eukaryotic cells at around 1% of the total lipid composition, and this is mostly in the mitochondrial membranes.^{67,132} Binding of dap to mitochondrial membranes is possible, however, in bacteria dap has been shown not to extensively infiltrate the cytoplasm of cells.¹¹⁴ Therefore, if dap does to bind eukaryotic cells a different lipid or membrane protein must mediate the interaction.

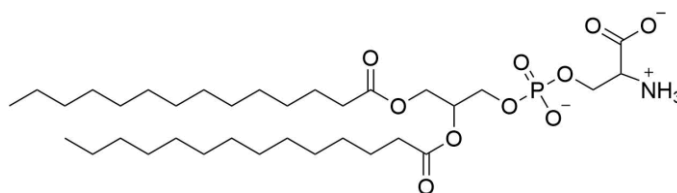


Figure 5.1: Structure of dimyristoyl phosphatidylserine. Phosphatidylserine is a major anionic phospholipid in eukaryotic cells.

This research is to study whether phosphatidylserine (PS) is such a component. PS is an anionic phospholipid and would mediate the binding of dap to mammalian cell membranes by emulating bacterial PG. PS is an essential phospholipid in mammalian cells and composes 3–10% of the total phospholipids.¹³³ However, most is confined to the inner cell membrane leaflet as displaying PS on the surface cellular membranes can trigger cell destruction by macrophages.¹³⁴ Consequently, a substantial interaction between PS-containing membranes and dap would be required at physiological calcium

concentrations to have implications in dap-induced toxicity in humans. The potential interaction can be examined via the same fluorescence assays as dap with LPG-containing membranes, as described above. In this case, the success or failure of the assays on PS membranes gives insight into the extent of dap's interaction with the membrane. Whether full permeabilization of the membranes would be needed for toxicity or simple membrane binding would suffice is not known.

5.2 Materials and Methods

The daptomycin analogs were produced semi-synthetically by the Taylor research group (University of Waterloo; Waterloo, ON.); high purity was assessed by HPLC and mass spectroscopy.

5.2.1 Preparation of liposomes

The procedure for the preparation of the liposomes (LUVs) has been described in a preceding chapter (see section 2.2.1)

5.2.2 Fluorescence studies

The procedure for performing the fluorescence studies has been described in a preceding chapter (see section 2.2.3)

Table 5.1: Fluorophore, excitation wavelength, and emission range of relevant lipopeptide analogs.

Lipopeptide	Fluorophore	Excitation (nm)	Emission (nm)
Dap	Kyn13	365	400–600
NBD-dap	NBD	475	500–600
Dap-perylene	Perylene	430	440–530
A5	Trp1	280	300–400
A5-acrylodan	Acrylodan	360	400–600
A5-pyrene	Pyrene	340	360–600

5.3 Results

As with the LPG studies, the chosen base membrane composition was 70:30 PC:PG. It represents a simple dap-sensitive membrane; PG is required for the action mode of dap, while PC – despite being a major lipid in eukaryotic membranes – is mostly inert with respect to dap at low calcium concentrations. The initial PS-containing membrane was 70:30 PC:PS. For simplicity, the 70:30 PC:PS will be called the 'PS' membrane.

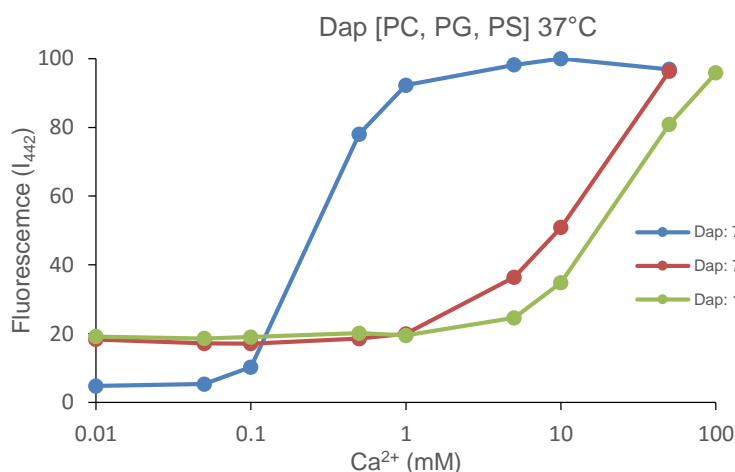


Figure 5.2: Kynurenine fluorescence of dap on liposomes of varying composition at 37 °C. The figure follows maximum normalized analog fluorescence (I_{442}) as a function of Ca^{2+} concentration.

Dap on the PS membrane displays a shifted calcium-dependent fluorescence intensity response compared to the 70:30 PC:PG membrane; higher calcium concentrations are required to increase intensity (Figure 5.2). In fact, the necessary calcium concentrations are only slightly below those of dap on the PC membrane, which is known to be relatively inert. Kyn fluorescence indicates the beginning of PS- and PC-mediated membrane association starts at calcium concentrations over 1 mM; therefore, any significant dap insertion does not coincide with physiological calcium concentrations. Consequently, it is unlikely that PS is involved in mediating dap-induced toxicity *in vivo*.

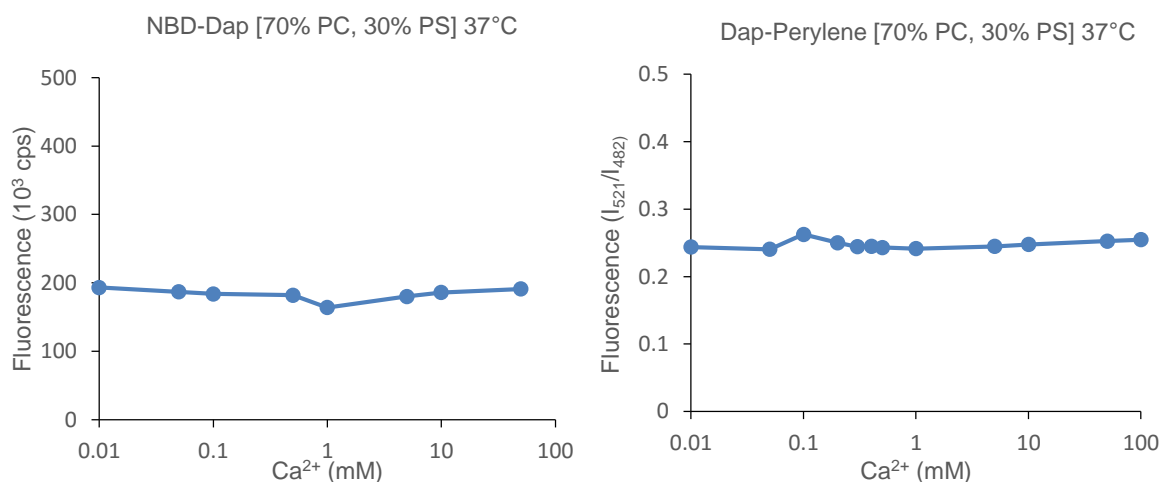


Figure 5.3: Comparison of NBD-dap (left) and dap-erylene (right) on a 70:30 PC:PS membrane at 37 °C. The figures follows the maximum normalized fluorescence (left: I_{536}) and the extent of excimer formation (right: I_{521}/I_{482}), as a function of Ca^{2+} concentration.

NBD-dap and dap-erylene were used to investigate any further interaction of dap residues with the PS membrane. NBD-dap displays no major difference in fluorescence across the calcium concentrations, consequently, the labeled Orn6 residue is not inserting into the membrane (*left*: Figure 5.3). Dap-erylene exhibits no excimer formation, therefore, no oligomerization is occurring (*right*: Figure 5.3). In the absence of excimer formation, the Kyn fluorescence observed at calcium concentrations over 1 mM is likely due to the association of dap monomers with the membrane. On susceptible membranes, the environmentally sensitive fluorophore attached to Orn6 typically responds prior to Kyn if membrane binding is present – in this case, NBD exhibited no fluorescence.⁸⁴ Overall, the results corroborate that dap has no significant association with PS membranes at physiological calcium concentrations, and PS is therefore unrelated to dap-induced toxicity *in vivo*.

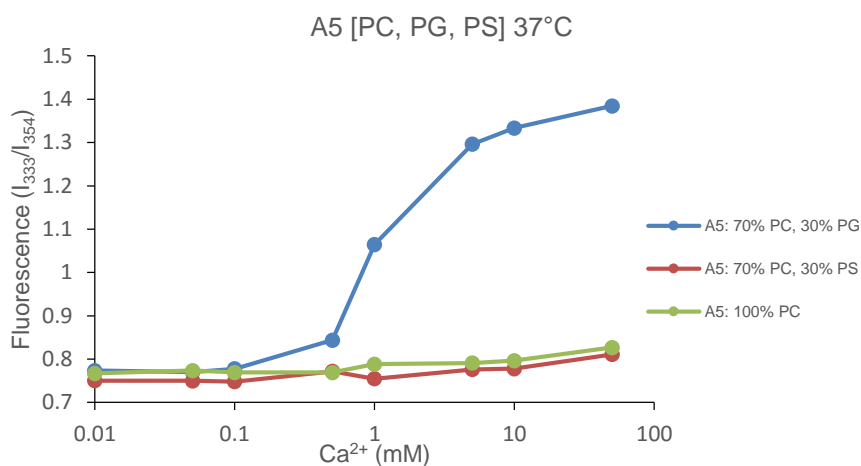


Figure 5.4: : Tryptophan fluorescence of A5 on liposomes of varying composition at 37 °C. The figure follows the fluorescence blue-shift (I_{333}/I_{354}) as a function of Ca^{2+} concentration.

A5 does not display any fluorescence blue-shift on PC or PS membranes; consequently, the Trp residue of A5 does not associate with the membrane (Figure 5.4). A5 is more toxic in mouse models of toxicity than dap; therefore, if PS was a deciding factor in toxicity, an increased interaction of A5 with PS-containing membranes would be expected.⁶⁴ This is not demonstrated in the Trp results, however other A5 residues may interact with the membrane.

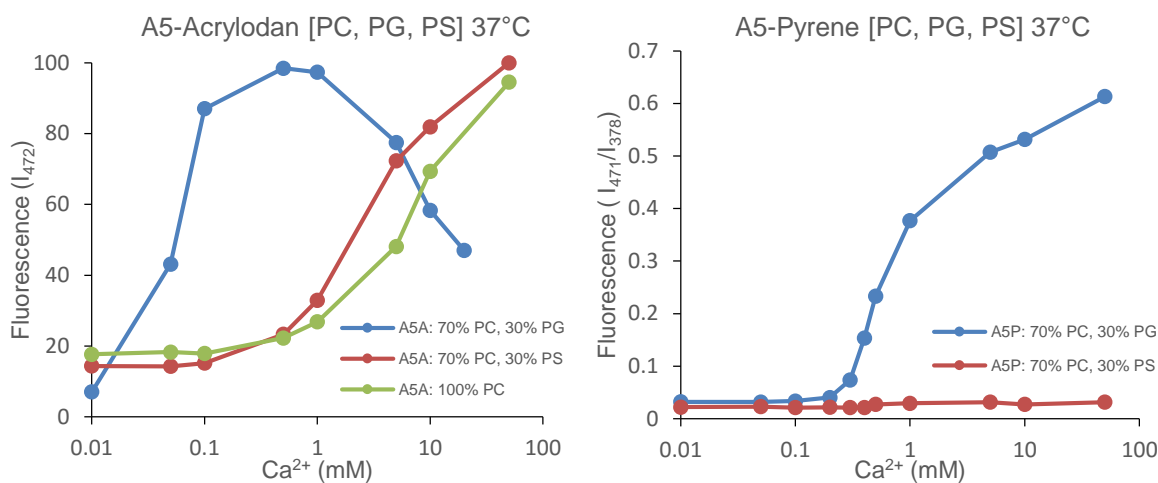


Figure 5.5: Comparison of A5-acrylodan (left) and A5-pyrene (right) on liposomes of varying composition at 37 °C. The figures follows the maximum normalized fluorescence (left: I_{472}) and the extent of excimer formation (right: I_{471}/I_{378}), as a function of Ca^{2+} concentration.

On the PS membrane, the fluorescence of A5-acrylodan increases when calcium is added incrementally above concentrations of 0.1 mM (left: Figure 5.5). By 1 mM Ca^{2+} the fluorescence has blue-shifted and increased to a modest extent (appendix: Figure 6.25). In contrast, no excimer formation is exhibited by A5-pyrene. Consequently, the labeled-Lys8 residue is inserting into the PS membrane, however, no oligomers form. These results are potentially significant in A5-induced toxicity; the Lys8 residue of A5 is inserting into the PS membrane at calcium concentrations which are physiologically relevant. However, the concentration of PS within the model membrane far exceeds that exposed to the outer membrane leaflet *in vivo*. When the PS concentration is decreased, the calcium required to promote binding will increase – as is seen with PG (appendix: Figure 6.3, Figure 6.4). Testing of A5 and its analogs with membranes which better approximate the complex lipid composition of human tissue would be required to establish whether the interaction remains; that it does is unlikely.

A5-acrylodan on the PC membrane exhibits similar results, however, the fluorescence increases to a lesser degree – consequently, the lipopeptide does not bind the PC membrane as avidly. On 100% PC membranes, the formation of excimer with A5-pyrene does not occur, therefore, the lipopeptide is again binding in a monomeric form (data not shown). In contrast to PS, PC is a major phospholipid within eukaryotic membranes, and it is not highly confined to the inner leaflet; therefore, the association of the peptide with PC may be more relevant to toxicity, despite its decreased interaction. However, this would not explain the targeted muscle toxicity seen with these lipopeptides in humans.

5.4 Discussion

Considering the recent findings of Taylor *et al.*⁸⁴, it is unexpected that Kyn fluorescence increased at high calcium concentration on the PS membrane in the absence of NBD-dap fluorescence. The fluorophore on the Orn6 residue typically tracks the first of the two successive calcium-dependent transitions: on PG model membranes, below 0.1 mM Ca²⁺ the labeled-Orn6 fluorescence increases, and above 0.1 mM Ca²⁺ the Kyn residue begins to respond. As a PS membrane is used rather than a PG membrane, it could be expected that the calcium concentrations required to initiate the two transitions is shifted to a higher calcium concentration – instead, the Kyn residue alone is seen to insert. Consequently, with the lack of excimer formation, dap is binding as a monomer. Since the binding is relegated to calcium concentrations above physiological levels, it is unrelated to dap-induced toxicity.

The most straightforward answer as to why the typical calcium-dependent transitions are not observed is that PS cannot emulate PG for dap. Although the lipids share a net charge, the structure of the head group and distribution of the charges is different. The net -1 charge of PS is composed of a positive and negative charge on the serine amino and carboxylic acid groups, respectively, and a second negative charge on the phosphate group. The net -1 charge of PG is derived from a single negative charge on the phosphate group.

On the other hand, A5 and its analogs exhibit a pattern of fluorescence which better reflect the initiation of the typical calcium-dependent transitions. At calcium concentrations above 0.1 mM Ca²⁺ the acrylodan-labeled Lys8 fluorescence begins to increase; this is representative of the first transition, which coincides with the binding of the first calcium ion. The calcium required is higher than usual, however, this is expected due to the lack of PG. The second transition, which coincides with another calcium ion, is not observed; Trp fluorescence does not blue-shift, and acrylodan fluorescence does not self-quench. Consequently, with the lack of excimer formation, A5 is also observed to insert as a monomer. Therefore, PS cannot truly emulate PG for A5 either; however, since the expected order of binding is observed at lower calcium concentration, the interaction may be increased in comparison to dap. Overall, it is unlikely that PS mediates either dap- or A5-induced toxicity in humans.

Chapter 6

Characterizing the reliance of daptomycin on peptidoglycan precursors

6.1 Introduction

Several action modes for dap have been proposed; among them, the dissipation of the membrane potential due to the interaction of dap with bacterial phospholipid membranes is best supported by experimental evidence. The successive steps required to accomplish this mechanism have been demonstrated using various fluorescence-based assays on model membranes.^{52,73,80,124} The steps include the calcium-dependent binding of dap to the membrane, the formation and translocation of oligomers, and the ultimate alignment of cross-leaflet oligomers to form the cation- and size-selective pore. The only molecule in the target membrane proven to be specifically required is PG.⁵⁵

The objective of this work is to investigate whether interactions between peptidoglycan precursors and dap are of importance in its action mode. Related calcium-dependent lipopeptide antibiotics, such as laspartomycin and amphomycin, have an analogous structure – a macrocycle and exocyclic peptide to which is attached a fatty acyl tail – and are known to inhibit peptidoglycan synthesis by sequestration of the peptidoglycan precursor undecaprenol.^{28,29,61} Other antibiotics are also known to require peptidoglycan precursor ‘targeting molecules’, which mediate association with bacterial membranes. This includes the structurally unrelated lantibiotic nisin.³⁸ Nisin is a pore-forming antibiotic which requires lipid II for efficient membrane association and permeabilization. Uncovering the requirement of a targeting molecule for dap, other than the PG, would be a large deviation from its known mechanism of action.

The investigation into the importance of peptidoglycan precursors in dap’s antibacterial activity was carried out using MIC tests on *B. subtilis* L-forms. The MIC tests incorporated two antibiotics: one being dap, and the other to up- or down-regulate the abundance of a specific peptidoglycan precursor. If dap requires a specific precursor, its activity should increase or decrease accordingly. L-forms are essential as the test organism because they are capable of growth in the absence of a fully functional peptidoglycan layer; this allows them to survive the antibiotics which interact with peptidoglycan synthesis. Understanding the reliance of dap on cellular binding sites, may result in lipopeptides with improved activity on dap-resistant bacteria and modifications to the established mechanism of action.

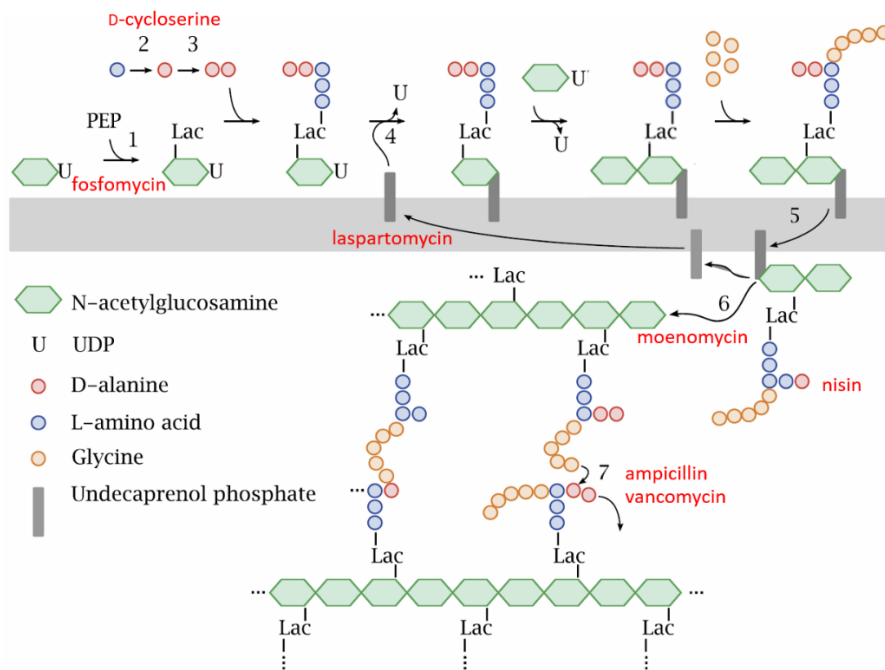


Figure 6.1: Schematic of peptidoglycan synthesis, and the antibiotics which inhibit it at different stages of production. By inhibiting different stages, the abundance of precursors will increase or decrease; this can then be tested for its effect on dap activity.

To up- or down-regulate the abundance of the peptidoglycan precursors, a variety of antibiotics can be used. Selection was made by choosing those which inhibit peptidoglycan synthesis at different stages (Figure 6.1). The list of chosen antibiotics, and the reasoning in regards to its effect on dap is below, for an overview see Table 6.1.

1. Fosfomycin and cycloserine inhibit steps in the synthesis of the intracellular sugar and peptide precursors of peptidoglycan.^{21,24,26} These precursors are directly used for the production of lipid I and II, therefore their concentration will be reduced. Both lipid I and II in turn use the lipid carrier undecaprenol. Inhibited production of these precursors will leave undecaprenol phosphate free in the membrane, possibly at increased levels. If dap binds to undecaprenol, no change or even an increase in activity should be seen. On the other hand, if dap binds to lipid I or lipid II, a decrease in activity should be seen
2. Vancomycin sequesters the D-alanyl-D-alanine dipeptide on lipid II.³⁰ This should block any direct binding to lipid II; if dap binds to lipid II, a decrease in activity should be seen.

3. Moenomycin will block the transfer of lipid II to a growing strand of peptidoglycan.¹³⁵ This will increase the amount of free lipid II. If dap binds to lipid II, the activity could increase.
4. Laspartomycin sequesters undecaprenol.²⁹ This blocks direct binding to undecaprenol, and reduces all upstream peptidoglycan precursors. If dap binds to undecaprenol, a decrease in activity should be seen.

To validate the double antibiotic MIC assay, nisin can be used as a control. Nisin is a known lipid II binder, therefore its activity should be able up- or down-regulated when the abundance of lipid II is changed. In fact, the presence of vancomycin, another lipid II binder, has already been observed to partially block its activity.³⁸ This test was carried out in the bacteria *Micrococcus flavus*, however the effect is expected to carry over to cell wall deficient *B. subtilis* L-form.

Table 6.1: Antibiotics and their effect on peptidoglycan presurcors and dap activity. Dap activity changes assume it binds to the affected peptidoglycan precursor. UC indicates unchanged.

Antibiotic	Precursor abundance or availability			Dap Activity
	Lipid I	Lipid II	Undecaprenol	
Cycloserine	↓	↓	UC (or ↑)	↓ (or ↑)
Fosfomycin	↓	↓	UC (or ↑)	↓ (or ↑)
Vancomycin	UC	↓	UC	↓
Moenomycin	UC	↑	UC	↑
Laspartomycin	UC	UC	↓	↓

6.2 Materials and Methods

B. subtilis strain PDC 134 was generously provided by Centre for Bacterial Cell Biology, Institute for Cell and Molecular Biosciences (Newcastle upon Tyne, UK). Cycloserine, fosfomycin, laspartomycin, and ampicillin were purchased from BioShop Canada, Inc. (Burlington, ON, CAN). Vancomycin and nisin were purchased from Sigma-Aldrich (St. Louis, MO, USA).

6.2.1 Isolation of *B. subtilis* PDC 134 N-forms

The *B. subtilis* PDC 134 strain was initially received as N-form cells within solid agar. A small piece of the original agar was isolated and streaked over an LB agar plate supplemented with 0.5% xylose. Two colonies were obtained after incubation overnight at 30 °C. A portion of one colony was subcultured into LB broth supplemented with both 0.5% xylose and 10 µg/mL of chloramphenicol

(Table 6.2). Chloramphenicol selection was used to isolate PDC 134 from any possible contamination; this antibiotic can be used due to the inserted chloramphenicol resistance gene (*cat*) prior to the xylose-dependent *murE* operon ($\Omega_{spoVD}::cat$ P_{xyl} -*murE*; *spoVD* is a gene necessary for spore formation). Bacterial growth from the LB broth was then streaked across xylose supplemented LB agar. A single colony was isolated and subcultured back into broth. Growth will be genetically homogenous *B. subtilis* PDC 134 N-forms, and can be portioned into individual 150–200 μ L stocks. Stocks contain 15–20% glycerol, and are kept at -80 °C.

Table 6.2: MIC (μ g/mL) of *B. subtilis* strains ATCC 1046 and PDC 134. PDC 134 includes both N- and L-form.

Antibiotic	<i>B. subtilis</i> strain		
	ATCC 1046	PDC 134 (N-form)	PDC 134 (L-form)
Chloramphenicol	1–1.5	>20	>30

6.2.2 Isolation of *B. subtilis* PDC 134 L-forms

A xylose-free medium supplemented with MSM (Mg^{2+} , 20 mM; maleic acid, 20 mM; sucrose, 500 mM) at pH 7 was inoculated with the growth from an N-form stock grown beforehand in the presence of xylose and chloramphenicol (Figure 6.2A). The culture was incubated at 30 °C overnight. Upon microscopic investigation of the growth, rod-shaped cells were interspersed among small, spherical cells assumed to be L-forms (Figure 6.2B). The rod-shaped cells indicated either the transition to L-form was not quantitative or contamination was involved. To rule out contamination, the growth was subcultured into chloramphenicol-supplemented MSM medium. The rod-shaped cells remained, making it likely they were untransformed N-forms of PDC 134 able to propagate without xylose. In an attempt to remove the rod-shaped cells, the growth was subcultured into media containing MSM and 75 μ g/mL of ampicillin. The media was highly turbid within 4 days, and microscopic investigation of the growth displayed only the spherical cells (Figure 6.2C). After testing, these cells showed osmotic lysis upon addition to water, an insensitivity to peptidoglycan-inhibiting antibiotics, and hypersensitivity to dap. As these are previously demonstrated qualities of *B. subtilis* L-forms, the spherical cells are believed to be L-forms. Frozen stocks were made in the same manner as the N-form stocks.

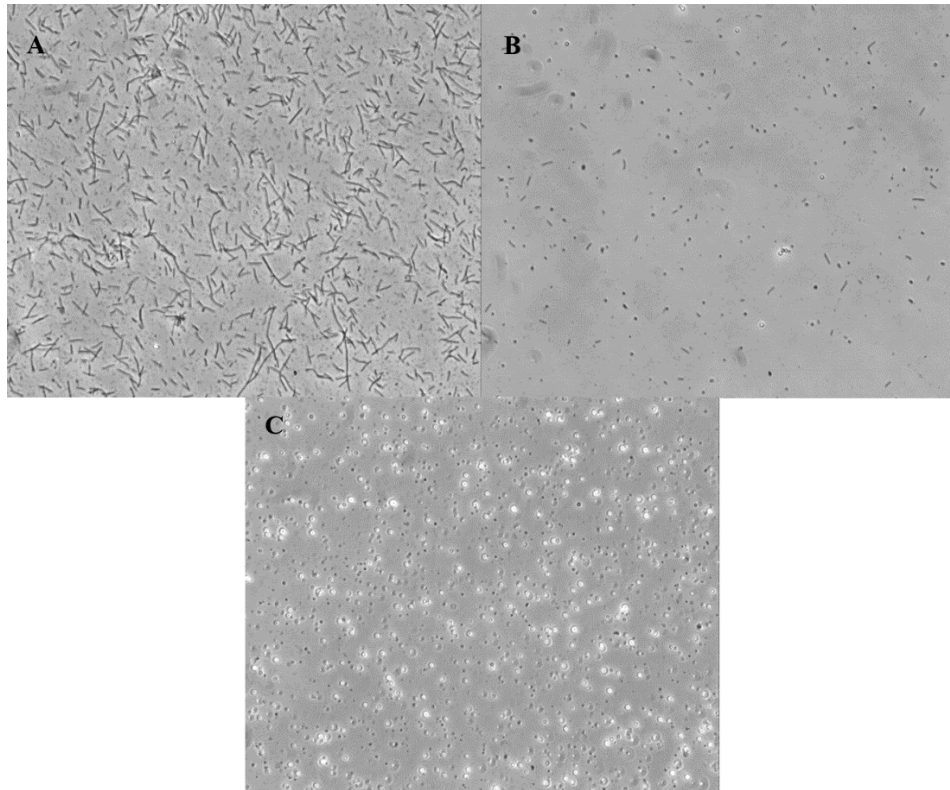


Figure 6.2: (A) One colony of PDC 134 N-forms grown in LB broth supplemented with 0.5% xylose, and 20 µg/mL chloramphenicol. (B) PDC 134 N-forms subcultured in MSM LB broth (C) PDC 134 N- and L-forms subcultured into MSM LB broth supplemented with 75 µg/mL ampicillin, giving a pure L-form culture.

6.2.3 Determining the antibacterial activity of antibiotics

The procedure for determining the minimum inhibitory concentration of the antibiotics has been described in a preceding chapter (see section 2.2.4)

6.2.4 Determining the antibacterial activity of daptomycin in the presence of other antibiotics

The antibiotic combinations were tested for antibacterial activity by broth dilution in a 96-well plate. Dap was added to wells at varying concentration above and below its MIC. The secondary antibiotic (which up- or down-regulates peptidoglycan precursors) was then added to the same wells at a fixed concentration above its MIC on N-form cells; this ensures the antibiotic is thoroughly affecting its antibacterial target and consequently changing the abundance of its associated peptidoglycan precursor. On the plate, the combinations were repeated 6 times, across all the concentrations. As a control, on the

same plate as the multiple antibiotic assay, an MIC with dap alone was completed. The concentrations of dap used are the same as the other multiple antibiotic assay. Each concentration is repeated 3 times on the plate. For all tests, the growth medium was MSM LB supplemented with 5 mM Ca²⁺. Each well was inoculated with PDC 134 L-forms and incubated at 30 °C for 3 days. Bacterial growth in each well was evaluated visually by turbidity.

6.3 Results

6.3.1 The difference in antibacterial activity between *B. subtilis* L-forms and N-forms

The transition to L-form allows cells to propagate freely without peptidoglycan as long as they are osmotically stabilized by the growth medium. Propagation in the cell wall deficient state is known to dramatically lower the sensitivity of the cells to antibiotics which affect the synthesis of the cell wall; including those discussed in the introduction (section 6.1). To verify that these antibiotics, which will be used to up- or down-regulate peptidoglycan precursors do not kill the L-forms, their antibacterial activities were determined (Table 6.3). As expected, the antibiotics have vastly increased MICs. However, laspartomycin is an exception. That its MIC on the L-forms is high is unexpected. Laspartomycin blocks the production of lipid I and lipid II by sequestering undecaprenol; this should have no effect on the bacteria.²⁹ This is an interesting result and should be evaluated with further tests.

The MICs of the chosen antibiotics were also determined on PDC 134 N-forms. The N-form cells, unlike the L-forms, continue to rely on peptidoglycan to survive. The MIC establishes a concentration of antibiotic which effectively inhibits its respective antibacterial target in the bacteria. Inhibition of the antibiotic's antibacterial target indicates the abundance of the peptidoglycan precursor associated with its mechanism of action has been effectively up- or down-regulated.

In the multiple antibiotic MIC assays, concentrations above the N-form MIC value can then be used on the L-forms; the L-form cells themselves will not die due to their inherent insensitivity to these mechanisms of action, however, the abundance of a particular peptidoglycan precursor is ensured to be effectively regulated. The activity of dap can then be tested without the presence of the affected precursor. All N-form MICs were similar to the *B. subtilis* strain ATCC 1046, which does not transition to L-form.

Table 6.3: MIC ($\mu\text{g/mL}$) of various antibiotics on *B. subtilis* ATCC 1046 and PDC 134 L-forms and N-forms.

Antibiotic	<i>B. subtilis</i> strain		
	ATCC 1046	PDC 134 (N-form)	PDC 134 (L-form)
Dap ^a	0.75	0.5–0.75	0.075
Ampicillin	2.5–5	2.5–5	>125
Cycloserine	80–120	80–120	>220
Fosfomycin	80–120	80–120	>200
Nisin	5–7	2.5–5	3.0
Vancomycin	0.15–0.175	0.15–0.20	≥ 10
Laspartomycin	4	4	1.5

^a5 mM Ca^{2+}

6.3.2 The reliance of daptomycin and nisin on *B. subtilis* PDC 134 peptidoglycan precursors

It quickly became apparent the original method of regulating peptidoglycan precursors with antibiotics would not be as straight forward as expected. This is due to the method in which the PDC 134 strain inhibits its peptidoglycan synthesis to transition from N-form to L-form. PDC 134 has a xylose-dependent promoter upstream of the *murE* operon, whose genes products are enzymes required for the very early steps in peptidoglycan synthesis. Consequently, in the L-form bacteria little or no peptidoglycan precursors are being synthesized when under normal growth conditions (xylose is absent from the growth medium). Due to this, the MIC of dap alone on the L-forms is analogous to dap in the presence of an early peptidoglycan synthesis inhibitor such as cycloserine or fosfomycin – which would have down-regulated lipid I and lipid II, and left undecaprenol free in the membrane.

When the activity of dap was tested alone on the L-form bacteria under normal growth conditions, its activity increased 10-fold (0.075 $\mu\text{g/mL}$ vs 0.75 $\mu\text{g/mL}$). Since the L-forms lack lipid I and lipid II, this demonstrates that interaction with those peptidoglycan precursors is not fundamental to dap's mechanism of action. As a control against low background production of peptidoglycan precursors by the L-forms, the activity of dap in the presence of cycloserine was determined (Table 6.4). The addition of cycloserine would down-regulate any potentially remaining lipid I and lipid II production. The results determined that the presence of cycloserine has no change on the MIC of dap. This corroborates that the presence of the precursors is not fundamental to dap activity.

Table 6.4: MIC ($\mu\text{g/mL}$) of dap in the presence of peptidoglycan precursor modulating antibiotics and 5 mM calcium, on *B. subtilis* PDC 134 L-forms. Media used is MSM and LB.

Secondary Antibiotic	Antibiotic Concentration		MIC	
	Secondary	Dap	Combination	Dap Control
Cycloserine	200	0–0.175	0.075	0.075

Despite not being fundamental to activity, the lipid I or lipid II precursor could mediate increased membrane binding and activity, such as in the case of lipid II and nisin. Dap’s activity must therefore be tested in their presence. The biosynthesis of the peptidoglycan precursors was up-regulated through the use of xylose. Normally, introduction of xylose into the growth medium permits transition to the N-form, as peptidoglycan is freely produced. For that reason, the growth medium was additionally supplemented with ampicillin. Ampicillin will allow for synthesis of lipid I and lipid II, but block peptidoglycan cross-linking and consequently inhibit full reversion to a walled state. L-forms grown on this medium did not revert, as determined by microscopy. However, there are potential complications. Research with *E. coli* has shown an unexpected decrease in lipid I and lipid II with use of penicillin; this was in contrast to use of moenomycin, which increased the peptidoglycan precursors.¹³⁶ The concentrations used by the authors were 641 $\mu\text{g/mL}$ and 500 $\mu\text{g/mL}$, respectively. The β -lactam concentration used by the authors is a nearly 6.5-fold increase in concentration compared to the media used here with *B. subtilis*. Furthermore, in contrast to *E. coli*, the *B. subtilis* L-forms are not being lysed over the experiment timescale. The differences in bacterial species, and antibiotic concentration, bring into question the significance of these findings to this research. Ultimately, the results show dap’s activity is unchanged in the presence of supposedly increased lipid I and lipid II concentrations (Table 6.5). Dap is therefore unlikely to interact with these precursors in any way.

Table 6.5: MIC ($\mu\text{g/mL}$) of dap on *B. subtilis* PDC 134 L-forms, in the presence of media with differing composition, but always supplemented with 5 mM Ca^{2+} . The media utilized is composed of MSM, and LB or MSM, Amp (100 $\mu\text{g/mL}$), 0.5% xylose, and LB.

Antibiotic	Growth medium	
	MSM media	Amp, Xylose, MSM media
Dap	0.075	0.075

In the opposite situation to lipid I and lipid II, is the lipid carrier undecaprenol phosphate. Undecaprenol phosphate is not synthesized by gene products within the *murE* operon, therefore it

remains in the L-form membrane. Moreover, it is entirely free in the membrane under xylose-free conditions as no lipid I or II is being transferred to the carrier. If dap, like its laspartomycin-like lipopeptide counterparts, binds to this precursor a portion of the initial 10-fold increase in dap activity on L-forms could be due to the unrestricted access of dap to undecaprenol. To test this, laspartomycin was to be used – it binds to undecaprenol and would consequently block the binding of dap. However, unexpectedly, the initial MIC tests using laspartomycin with the L-forms showed an increased MIC compared to the N-forms (1.5 $\mu\text{g}/\text{mL}$ vs 4 $\mu\text{g}/\text{mL}$). The L-forms are capable of peptidoglycan-free growth, therefore, the sequestration of undecaprenol should not kill the bacteria.²⁹ Unfortunately, due to this the reliance of dap upon undecaprenol was not tested. However, that the L-forms die to laspartomycin is intriguing and should be followed up with other studies.

In order to validate the tests done with dap and the L-forms under xylose-free and peptidoglycan precursor synthesizing conditions (xylose, ampicillin), nisin was used as a control. However, initial tests show that nisin, despite its known lipid II binding mechanism, may not be a useful control within this experimental set up. The MIC assay of nisin on PDC 134 N-forms and L-forms give results which are comparable to each other (2.5-5 $\mu\text{g}/\text{mL}$ vs 3 $\mu\text{g}/\text{mL}$). L-forms lack lipid II, therefore the activity of nisin should be significantly decreased as it cannot efficiently initiate pore formation. Nisin can produce lipid II-independent pores but it has only been shown on model membranes and required 1,000-fold increased antibiotic concentration.¹³⁷ A separate group, Wolf *et al.*¹³⁸, encountered the same problem with nisin on PDC 134 L-forms. They proposed that nisin may be binding to a secondary target molecule; they pointed to a precursor of wall teichoic acid biosynthesis, which is flipped to the outer membrane using undecaprenol and has recently been shown to bind nisin.^{138,139} However, this is inadequate as its synthesis requires the enzymes within the suppressed *murE* operon.¹³⁹

Nevertheless, when nisin is used under precursor synthesizing conditions (xylose, ampicillin), the expected result is seen (Table 6.6). Attempting to up-regulate lipid II caused a decrease in nisin's activity; however, the increase in activity is not large, which does not bode well for the sensitivity of the assay. Despite the success in this assay, that nisin's activity is not inhibited under conditions which should have no production of its target molecule, lipid II, render it an invalid control for the assays overall.

Table 6.6: MIC ($\mu\text{g/mL}$) of nisin on *B. subtilis* PDC 134 L-forms, in the presence of media with differing composition. The media utilized is composed of MSM, and LB or MSM, Amp (100 $\mu\text{g/mL}$), 0.5% xylose, and LB.

Antibiotic	Growth medium	
	MSM LB	Amp, Xylose, MSM LB
Nisin	3.0	2.5

6.4 Discussion

The multiple antibiotic MIC assay on L-forms resulted in some potentially promising results for the reliance of dap on lipid I and lipid II precursors; however, the control needed to validate them does not function as expected. Nisin's activity is not inhibited under conditions which should have no production of its target molecule, lipid II. Consequently, no conclusions from the data can be made. Whether the assay could be recovered with the choice of a different control antibiotic is uncertain.

Perhaps the most significant result from the attempts at the assay is the death of the L-forms to laspartomycin. No known mechanism of action accounts for this effect. First, the functionally-related lipopeptides such as amphomycin should be attempted. This will distinguish whether the effect occurs only by laspartomycin, or all its related antibiotics.

Ultimately, the dap's reliance on peptidoglycan precursors can be answered by a recent paper from Kleijn *et al.* (2016)²⁹. The research group performed a multitude of tests to characterize the mechanism of action of laspartomycin and used dap as the comparator; below are is a brief overview of their results for dap:

1. Addition of dap to *S. aureus* does not cause accumulation of the cytoplasmic lipid II precursor UDP-MurNAc-pentapeptide. This indicates no inhibition of upstream peptidoglycan precursor synthesis is happening, such as sequestration of undecaprenol.
2. A thin-layer chromatography (TLC) binding assay did not show stable complex formation when dap was incubated with undecaprenol phosphate or lipid II.
3. Direct addition of purified lipid I, lipid II, UDP-MurNAc-pentapeptide, UDP-GlcNAc, or undecaprenol phosphate at high concentrations to antibacterial activity assays does not antagonize the activity of dap.

Consequently, dap has been shown not to rely on peptidoglycan precursors for antibacterial affect.

6.5 Conclusion

To conclude, the findings from the chapters will be briefly summarized. Chapter 2 details the characterization of an acyl-linked dimer of dap. The dimer was found to undergo a mechanism of action identical to that of dap on model membranes. However, on bacteria its antibacterial activity is reduced due to sequestration into the peptidoglycan layer; furthermore, the dimerization affects the activity in some secondary manner. Consequently, dimerization is not a suitable method for increasing dap's activity. Future work with the dimer is unlikely due to the manner of its inactivation, however, research into the process of oligomerization remains important.

Chapter 3 details the characterization of additional synthetic analogs of dap, including dap-E12-W13 and dap-E12-Y13. The dap-E12-W13 analog is amongst the most active dap analogs characterized by research groups so far. The high antibacterial activity and simplified synthetic procedure make it a viable candidate for the role as the base scaffold in the generation of a combinatorial analog library. The dap-E12-Y13 analog's antibacterial activity is low unless calcium concentration is significantly increased; the amino acids in positions 12 and 13 appear to affect dap's calcium affinity. Future work involves establishing the process for the synthetic library and the characterization of additional analogs to further develop the structure-activity relationships of dap.

Chapter 4 details the characterization of LPG-mediated dap resistance. Overall, the mechanism of resistance is reminiscent of CL-mediated resistance; LPG appears to inhibit the translocation of dap oligomers across the membrane. The inhibition of translocation may occur due to LPG stabilizing the membrane. This would arise from the electrostatic interaction of LPG with PG; however, the data is not sufficient for a comprehensive explanation. Future work includes the examination of membranes with a larger range of LPG concentrations. This would corroborate the findings found here and allow for more in-depth tests.

Chapter 5 contains the investigation into the role of PS in dap-induced toxicity. Due to the lack of significant dap interaction with a PS-containing membrane at physiological calcium concentrations, PS is unlikely to be involved in toxicity. The need for future work is uncertain. Chapter 6 details the investigation into the reliance of dap's antibacterial activity on peptidoglycan precursors. Due to complications with the experimental assay and control, no data was able to be validated. The complications resulted from the *B. subtilis* PDC 134 strain utilized. Future work with a modified assay or different experimental setup is warranted.

Permissions

Figure 1.14: Reprinted from *Biochimica et Biophysica (BBA) – Biomembranes*, 1838, Zhang, T., Muraih, J. K., MacCormick, B., Silverman, J., and Palmer, M., Daptomycin forms cation- and size-selective pores in model membranes, 2425–2430, Copyright 2016, with permission from Elsevier.

Figure 1.15: This research was originally published in *The Journal of Biological Chemistry*. Zhang, T., Muraih, J. K., Tishbi, N., Herskowitz, J., Victor, R. L., Silverman, J., Uwumarenogie, S., Taylor, S. D., Palmer, M., and Mintzer, E. Cardiolipin prevents membrane translocation and permeabilization by daptomycin. *J. Biol. Chem.* 2014; 289:11584-91. © the American Society for Biochemistry and Molecular Biology.

Figure 1.16: This research was originally published in *The Journal of Biological Chemistry*. Zhang, T., Muraih, J. K., Tishbi, N., Herskowitz, J., Victor, R. L., Silverman, J., Uwumarenogie, S., Taylor, S. D., Palmer, M., and Mintzer, E. Cardiolipin prevents membrane translocation and permeabilization by daptomycin. *J. Biol. Chem.* 2014; 289:11584-91. © the American Society for Biochemistry and Molecular Biology.

References

- (1) World Health Organization. (1977) The selection of essential drugs: report of a WHO expert committee. *Tech. Rep. Ser. no 615*. Geneva: World Health Organization.
- (2) Laing, R., Waning, B., Gray, A., Ford, N., and t'Hoën, E. (2003) 25 years of the WHO essential medicines lists: progress and challenges. *Lancet* *361*, 1723–29.
- (3) Quick, J. D., Hogerzeil, H. V., Velasquez, G., and Rago, L. (2002) Twenty-five years of essential medicines. *Bull. World Health Organ.* *80*, 913–914.
- (4) World Health Organization. (2015) WHO Model List of Essential Medicines (April 2015). Geneva: World Health Organization.
- (5) Lee, E. H., Nicolas, M. H., Kitzis, M. D., Pialoux, G., Collatz, E., and Gutmann, L. (1991) Association of two resistance mechanisms in a clinical isolate of *Enterobacter cloacae* with high-level resistance to imipenem. *Antimicrob. Agents Chemother.* *35*, 1093–1098.
- (6) Srinivasan, A., Dick, J. D., and Perl, T. M. (2002) Vancomycin resistance in staphylococci. *Clin. Microbiol. Rev.* *15*, 430–8.
- (7) World Health Organization. (2015) Global action plan on antimicrobial resistance. Geneva: World Health Organization.
- (8) Jones, T., Yeaman, M. R., Sakoulas, G., Yang, S.-J., Proctor, R., Sahl, H.-G., Schrenzel, J., Xiong, Y. Q., and Bayer, A. S. (2008) Failures in clinical treatment of *Staphylococcus aureus* infection with daptomycin are associated with alterations in surface charge, membrane phospholipid asymmetry, and drug binding. *Antimicrob. Agents Chemother.* *52*, 269–78.
- (9) Mangili, A., Bica, I., Snyderman, D. R., and Hamer, D. H. (2005) Daptomycin-Resistant, Methicillin-Resistant *Staphylococcus aureus* Bacteremia. *Clin. Infect. Dis.* *40*, 1058–1060.
- (10) Gradmann, C. (2011) Magic bullets and moving targets: Antibiotic resistance and experimental chemotherapy, 1900-1940. *Dynamis* *31*, 305–321.
- (11) Aminov, R. I. (2010) A Brief History of the Antibiotic Era: Lessons Learned and Challenges for the Future. *Front. Microbiol.* *1*, 1–7.
- (12) Fleming, A. (1929) On the antibacterial action of cultures of a penicillium, with special reference to their use in the isolation of *B. influenzae*. *Br. Journal Exp. Pathol.* *10*, 226–236.

- (13) Silver, L. L. (2011) Challenges of antibacterial discovery. *Clin. Microbiol. Rev.* 24, 71–109.
- (14) Bérdy, J. (2012) Thoughts and facts about antibiotics: Where we are now and where we are heading. *J. Antibiot. (Tokyo)*. 65, 441–441.
- (15) Debono, M., Barnhart, M., Carrell, C. B., Hoffmann, J. a, Occolowitz, J. L., Abbott, B. J., Fukuda, D. S., Hamill, R. L., Biemann, K., and Herlihy, W. C. (1987) A21978C, a complex of new acidic peptide antibiotics: isolation, chemistry, and mass spectral structure elucidation. *J. Antibiot. (Tokyo)*. 40, 761–777.
- (16) Baltz, R. H. (2008) Renaissance in antibacterial discovery from actinomycetes. *Curr. Opin. Pharmacol.* 8, 557–63.
- (17) Alanis, A. J. (2005) Resistance to Antibiotics: Are We in the Post-Antibiotic Era? *Arch. Med. Res.* 36, 697–705.
- (18) Palmer, M., Chan, A., Dieckmann, T., and Honek, J. (2012) *Biochemical Pharmacology* 1st ed. Wiley & Sons, New Jersey, NY.
- (19) Wood, J. M. (2015) Bacterial responses to osmotic challenges. *J. Gen. Physiol.* 145, 381–388.
- (20) Brown, E. D., Vivas, E. I., Walsh, C. T., and Kolter, R. (1995) MurA (MurZ), the enzyme that catalyzes the first committed step in peptidoglycan biosynthesis, is essential in *Escherichia coli*. *J. Bacteriol.* 177, 4194–7.
- (21) Marquardt, J. L., Brown, E. D., Lane, W. S., Haley, T. M., Ichikawa, Y., Wong, C. H., and Walsh, C. T. (1994) Kinetics, stoichiometry, and identification of the reactive thiolate in the inactivation of UDP-GlcNAc enolpyruvoyl transferase by the antibiotic fosfomycin. *Biochemistry* 33, 10646–10651.
- (22) Madigan, M. T., Martinko, J. M., Stahl, D. A., and Clark, D. P. (2012) *Brock Biology of Microorganisms* (Espinoza, D., and Cook, K., Eds.) 13th ed. Pearson: Benjamin Cummings, San Francisco, CA.
- (23) Patel, S. S., Balfour, J. A., and Bryson, H. M. (1997) Fosfomycin tromethamine. A review of its antibacterial activity, pharmacokinetic properties and therapeutic efficacy as a single-dose oral treatment for acute uncomplicated lower urinary tract infections. *Drugs* 53, 637–656.
- (24) Neuhaus, F. C., and Lynch, J. L. (1964) the Enzymatic Synthesis of D-Alanyl-D-Alanine. III. On the Inhibition of D-Alanyl-D-Alanine Synthetase By the Antibiotic D-Cycloserine. *Biochemistry* 3,

471–480.

- (25) Clark, V. L., and Young, F. E. (1977) Inducible resistance to D-cycloserine in *Bacillus subtilis* 168. *Antimicrob. Agents Chemother.* 11, 871–876.
- (26) Prosser, G. A., and de Carvalho, L. P. S. (2013) Kinetic mechanism and inhibition of *Mycobacterium tuberculosis* D-alanine:D-alanine ligase by the antibiotic D-cycloserine. *FEBS J.* 280, 1150–66.
- (27) Noda, M., Kawahara, Y., Ichikawa, A., Matoba, Y., Matsuo, H., Lee, D. G., Kumagai, T., and Sugiyama, M. (2004) Self-protection mechanism in D-cycloserine-producing *Streptomyces lavendulae*. Gene cloning, characterization, and kinetics of its alanine racemase and D-alanyl-D-alanine ligase, which are target enzymes of D-cycloserine. *J. Biol. Chem.* 279, 46143–46152.
- (28) Tanaka, H., Iwai, Y., Oiwa, R., Shinohara, S., Shimizu, S., Oka, T., and Omura, S. (1977) Studies on Bacterial Cell Wall Inhibitors. II. Inhibition of Peptidoglycan Synthesis In Vivo and In Vitro by Amphomycin. *Biochim. Biophys. Acta* 497, 633–640.
- (29) Kleijn, L. H. J., Oppedijk, S. F., 't Hart, P., van Harten, R. M., Martin-Visscher, L. A., Kemmink, J., Breukink, E., and Martin, N. I. (2016) Total Synthesis of Laspartomycin C and Characterization of its Antibacterial Mechanism of Action. *J. Med. Chem.* 59, 3569–3574.
- (30) Walsh, C. T., Fisher, S. L., Park, I. S., Prahalad, M., and Wu, Z. (1996) Bacterial resistance to vancomycin: five genes and one missing hydrogen bond tell the story. *Chem. Biol.* 3, 21–28.
- (31) Levine, D. P. (2006) Vancomycin: A History. *Clin. Infect. Dis.* 42, S5–12.
- (32) Allison, L. A. (2012) *Fundamental Molecular Biology* 2nd ed. John Wiley & Sons, New Jersey, NY.
- (33) Alberts, B., Johnson, A., Lewis, J., Raff, M., Roberts, K., and Walter, P. (2008) *Molecular Biology of the Cell* 5th ed. Garland Science: Taylor & Francis Group, New York, NY.
- (34) Wolfe, A. D., and Hahn, F. E. (1965) Mode of action of chloramphenicol IX. Effects of chloramphenicol upon a ribosomal amino acid polymerization system and its binding to bacterial ribosome. *Biochim. Biophys. Acta - Nucleic Acids Protein Synth.* 95, 146–155.
- (35) Ettayebi, M., Prasad, S. M., and Morgan, E. a. (1985) Chloramphenicol-erythromycin resistance mutations in a 23S rRNA gene of *Escherichia coli*. *J Bacteriol* 162, 551–557.

- (36) Yunis, A. A. (1988) Chloramphenicol: relation of structure to activity and toxicity. *Annu. Rev. Pharmacol. Toxicol.* 28, 83–100.
- (37) Strahl, H., and Hamoen, L. W. (2010) Membrane potential is important for bacterial cell division. *Proc. Natl. Acad. Sci. U. S. A.* 107, 12281–6.
- (38) Breukink, E., Wiedemann, I., van Kraaij, C., Kuipers, O. P., Sahl, H., and de Kruijff, B. (1999) Use of the cell wall precursor lipid II by a pore-forming peptide antibiotic. *Science* 286, 2361–2364.
- (39) Breukink, E., and de Kruijff, B. (2006) Lipid II as a target for antibiotics. *Nat. Rev. Drug Discov.* 5, 321–323.
- (40) Shin, J. M., Gwak, J. W., Kamarajan, P., Fenno, J. C., Rickard, A. H., and Kapila, Y. L. (2015) Biomedical Applications of Nisin. *J. Appl. Microbiol.* 1–17.
- (41) Tenover, F. C. (2006) Mechanisms of Antimicrobial Resistance in Bacteria. *Am. J. Med.* 119.
- (42) Zavascki, A. P., Goldani, L. Z., Li, J., and Nation, R. L. (2007) Polymyxin B for the treatment of multidrug-resistant pathogens: A critical review. *J. Antimicrob. Chemother.* 60, 1206–1215.
- (43) Lambert, P. A. (2005) Bacterial resistance to antibiotics: Modified target sites. *Adv. Drug Deliv. Rev.* 57, 1471–1485.
- (44) Wright, G. D. (2005) Bacterial resistance to antibiotics: Enzymatic degradation and modification. *Adv. Drug Deliv. Rev.* 57, 1451–1470.
- (45) Fillgrove, K. L., Pakhomova, S., Newcomer, M. E., and Armstrong, R. N. (2003) Mechanistic Diversity of Fosfomycin Resistance in Pathogenic Microorganisms. *J. Am. Chem. Soc.* 125, 15730–15731.
- (46) Tsuruoka, T., and Yamada, Y. (1975) Characterization of spontaneous fosfomycin (phosphonomycin)-resistant cells of *Escherichia coli* B in vitro. *J. Antibiot. (Tokyo)*. 28, 906–911.
- (47) Jardetzky, O. (1963) Studies on the Mechanism of Action of Chloramphenicol. *J. Biol. Chem.* 238, 2498–2508.
- (48) Zhou, H., Fang, J., Tian, Y., and Lu, X. Y. (2013) Mechanisms of nisin resistance in Gram-positive bacteria. *Ann. Microbiol.* 64, 413–420.
- (49) D’Costa, V. M., Mukhtar, T. a, Patel, T., Koteva, K., Waglechner, N., Hughes, D. W., Wright, G. D., and De Pascale, G. (2012) Inactivation of the lipopeptide antibiotic daptomycin by hydrolytic

mechanisms. *Antimicrob. Agents Chemother.* 56, 757–64.

(50) Davlieva, M., Zhang, W., Arias, C. a, and Shamoo, Y. (2013) Biochemical characterization of cardiolipin synthase mutations associated with daptomycin resistance in enterococci. *Antimicrob. Agents Chemother.* 57, 289–96.

(51) Friedman, L., Alder, J. D., and Silverman, J. a. (2006) Genetic changes that correlate with reduced susceptibility to daptomycin in *Staphylococcus aureus*. *Antimicrob. Agents Chemother.* 50, 2137–45.

(52) Zhang, T., Muraih, J. K., Tishbi, N., Herskowitz, J., Victor, R. L., Silverman, J., Uwumarenogie, S., Taylor, S. D., Palmer, M., and Mintzer, E. (2014) Cardiolipin prevents membrane translocation and permeabilization by daptomycin. *J. Biol. Chem.* 289, 11584–91.

(53) Strieker, M., and Marahiel, M. A. (2009) The structural diversity of acidic lipopeptide antibiotics. *ChemBioChem* 10, 607–616.

(54) Eisenstein, B. I., Oleson, F. B., and Baltz, R. H. (2010) Daptomycin: from the mountain to the clinic, with essential help from Francis Tally, MD. *Clin. Infect. Dis.* 50, S10–5.

(55) Baltz, R. H. (2009) Daptomycin: mechanisms of action and resistance, and biosynthetic engineering. *Curr. Opin. Chem. Biol.* 13, 144–51.

(56) Baltz, R. H., Miao, V., and Wrigley, S. K. (2005) Natural products to drugs: daptomycin and related lipopeptide antibiotics. *Nat. Prod. Rep.* 22, 717–741.

(57) Debono, M., Abbott, B. J., Molloy, R. M., Fukuda, D. S., Hunt, A. H., Daupert, V. M., Counter, F. T., Ott, J. L., Carrell, C. B., Howard, L. C., Boeck, L. D., and Hamill, R. L. (1988) Enzymatic and Chemical Modification of Lipopeptide Antibiotic A21978C: The Synthesis and Evaluation of Daptomycin (LY146032). *J. Antibiot. (Tokyo)*. XLI, 1093–1105.

(58) Oleson, F. B., Berman, C. L., Kirkpatrick, J. B., Regan, K. S., Lai, J., and Tally, F. P. (2000) Once-Daily Dosing in Dogs Optimizes Daptomycin Safety. *Antimicrob. Agents Chemother.* 44, 2948–2953.

(59) Fowler, V. G., Boucher, H. W., Corey, R., Abrutyn, E., Karchmer, A. W., Rupp, M. E., Levine, D. P., Chambers, H. F., Tally, F. P., Vigliani, G. A., Cabell, C. H., Link, A. S., DeMeyer, I., Filler, S. G., Zervos, M., Cook, P., Parsonnet, J., Bernstein, J. M., Price, C. S., Forrest, G. N., Fatkenheuer, G., Gareca, M., Rehm, S. J., Brodt, H. R., Tice, A., and Cosgrove, S. E. (2006) Daptomycin versus

standard therapy for bacteremia and endocarditis caused by *Staphylococcus aureus*. *N. Engl. J. Med.* 355, 653–665.

(60) Silverman, J. A., Mortin, L. I., Vanpraagh, A. D. G., Li, T., and Alder, J. (2005) Inhibition of daptomycin by pulmonary surfactant: in vitro modeling and clinical impact. *J. Infect. Dis.* 191, 2149–52.

(61) Tanaka, H., Oiwa, R., Matsukura, S., and Omura, S. (1979) Amphomycin inhibits phospho-N-acetylmuramyl-pentapeptide translocase in peptidoglycan synthesis of *Bacillus*. *Biochem. Biophys. Res. Commun.* 86, 902–908.

(62) Robbel, L., and Marahiel, M. a. (2010) Daptomycin, a bacterial lipopeptide synthesized by a nonribosomal machinery. *J. Biol. Chem.* 285, 27501–8.

(63) Counter, F. T., Allen, N. E., Fukuda, D. S., Hobbs, J. N., Ott, J., Ensminger, P. W., Mynderse, J. S., Preston, D. A., and Wu, C. Y. E. (1990) A54145, A New Lipopeptide Antibiotic Complex: Microbiological Evaluation. *J. Antibiot. (Tokyo)*. XLIII, 616–622.

(64) Miao, V., Brost, R., Chapple, J., She, K., Gal, M.-F. C.-L., and Baltz, R. H. (2006) The lipopeptide antibiotic A54145 biosynthetic gene cluster from *Streptomyces fradiae*. *J. Ind. Microbiol. Biotechnol.* 33, 129–40.

(65) Allen, N. E., Hobbs, J. N., and Alborn, W. E. (1987) Inhibition of peptidoglycan biosynthesis in gram-positive bacteria by LY146032. *Antimicrob. Agents Chemother.* 31, 1093–1099.

(66) Lakey, J., and Lea, E. (1986) The role of acyl chain character and other determinants on the bilayer activity of A21978C an acidic lipopeptide antibiotic. *Biochim. Biophys. Acta (BBA)- Biomembranes* 859, 219–226.

(67) Drop, L. J., and Laver, M. B. (1975) Low Plasma Ionized Calcium and Response to Calcium Therapy in Critically Ill Man. *Anesthesiology* 43, 300–306.

(68) Jung, D., Rozek, A., Okon, M., and Hancock, R. E. W. (2004) Structural Transitions as Determinants of the Action of the Calcium-Dependent Antibiotic Daptomycin. *Chem. Biol.* 11, 949–957.

(69) Hachmann, A.-B. A.-B., Angert, E. R., and Helmann, J. D. (2009) Genetic Analysis of Factors Affecting Susceptibility of *Bacillus subtilis* to Daptomycin. *Antimicrob. Agents Chemother.* 53, 1598–609.

- (70) Hachmann, A. B., Sevim, E., Gaballa, A., Popham, D. L., Antelmann, H., and Helmann, J. D. (2011) Reduction in membrane phosphatidylglycerol content leads to daptomycin resistance in *Bacillus subtilis*. *Antimicrob. Agents Chemother.* 55, 4326–4337.
- (71) Lakey, J. H., and Ptak, M. (1988) Fluorescence indicates a calcium-dependent interaction between the lipopeptide antibiotic LY146032 and phospholipid membranes. *Biochemistry* 27, 4639–4645.
- (72) Silverman, J. A., Perlmutter, N. G., Howard, M., and Shapiro, H. M. (2003) Correlation of daptomycin bactericidal activity and membrane depolarization in *Staphylococcus aureus*. *Antimicrob. Agents Chemother.* 47, 2538–2544.
- (73) Muraih, J. K., Pearson, A., Silverman, J., and Palmer, M. (2011) Oligomerization of daptomycin on membranes. *Biochim. Biophys. Acta* 1808, 1154–1160.
- (74) Muraih, J. K., and Palmer, M. (2012) Estimation of the subunit stoichiometry of the membrane-associated daptomycin oligomer by FRET. *Biochim. Biophys. Acta* 1818, 1642–7.
- (75) Muraih, J. K., Harris, J., Taylor, S. D., and Palmer, M. (2012) Characterization of daptomycin oligomerization with perylene excimer fluorescence: stoichiometric binding of phosphatidylglycerol triggers oligomer formation. *Biochim. Biophys. Acta* 1818, 673–8.
- (76) Zhang, T., Taylor, S., Palmer, M., and Duhamel, J. Membrane binding and oligomer formation of the calcium-dependent lipopeptide antibiotic A54145: a quantitative study with pyrene excimer fluorescence. *Biophys. J.* (submitted).
- (77) Lam, H. Y., Zhang, Y., Liu, H., Xu, J., Wong, C. T. T., Xu, C., and Li, X. (2013) Total synthesis of daptomycin by cyclization via a chemoselective serine ligation. *J. Am. Chem. Soc.* 135, 6272–9.
- (78) Zhang, T., Muraih, J. K., Mintzer, E., Tishbi, N., Desert, C., Silverman, J., Taylor, S., and Palmer, M. (2013) Mutual inhibition through hybrid oligomer formation of daptomycin and the semisynthetic lipopeptide antibiotic CB-182,462. *Biochim. Biophys. Acta* 1828, 302–8.
- (79) Kano, K., and Fendler, J. H. (1978) Pyranine as a Sensitive pH Probe for Liposome Interiors and Surfaces. *Biochim. Biophys. Acta* 509, 289–299.
- (80) Zhang, T., Muraih, J. K., MacCormick, B., Silverman, J., and Palmer, M. (2014) Daptomycin forms cation- and size-selective pores in model membranes. *Biochim. Biophys. Acta - Biomembr.* 1838, 2425–2430.

- (81) Palmer, K. L., Daniel, A., Hardy, C., Silverman, J., and Gilmore, M. S. (2011) Genetic basis for daptomycin resistance in enterococci. *Antimicrob. Agents Chemother.* 55, 3345–56.
- (82) Ball, L., Goult, C. M., Donarski, J. A., Mickle, J., and Ramesh, V. (2004) NMR structure determination and calcium binding effects of lipopeptide antibiotic daptomycin. *Org. Biomol. Chem.* 22, 1872–1878.
- (83) Ho, S. W., Jung, D., Calhoun, J. R., Lear, J. D., Okon, M., Scott, W. R. P., Hancock, R. E. W., and Straus, S. K. (2008) Effect of divalent cations on the structure of the antibiotic daptomycin. *Eur. Biophys. J.* 37, 421–433.
- (84) Taylor, R. M., Butt, K., Scott, B., Zhang, T., Muraih, J. K., Mintzer, E., Taylor, S. D., and Palmer, M. Two successive calcium-dependent transitions mediate membrane binding and oligomerization of daptomycin and the related antibiotic A54145. *BBA Biomembr.* (submitted).
- (85) Nguyen, K. T., He, X., Alexander, D. C., Li, C., Gu, J.-Q., Mascio, C., Van Praagh, A., Mortin, L., Chu, M., Silverman, J. a, Brian, P., and Baltz, R. H. (2010) Genetically engineered lipopeptide antibiotics related to A54145 and daptomycin with improved properties. *Antimicrob. Agents Chemother.* 54, 1404–13.
- (86) Miao, V., Coëffet-Legal, M.-F., Brian, P., Brost, R., Penn, J., Whiting, A., Martin, S., Ford, R., Parr, I., Bouchard, M., Silva, C. J., Wrigley, S. K., and Baltz, R. H. (2005) Daptomycin biosynthesis in *Streptomyces roseosporus*: cloning and analysis of the gene cluster and revision of peptide stereochemistry. *Microbiology* 151, 1507–1523.
- (87) He, Y., Li, J., Yin, N., Herradura, P. S., Martel, L., Zhang, Y., Pearson, A. L., Kulkarni, V., Mascio, C., Howland, K., Silverman, J. a, Keith, D. D., and Metcalf, C. a. (2012) Reduced pulmonary surfactant interaction of daptomycin analogs via tryptophan replacement with alternative amino acids. *Bioorg. Med. Chem. Lett.* 22, 6248–51.
- (88) Nguyen, K. T., Ritz, D., Gu, J.-Q., Alexander, D., Chu, M., Miao, V., Brian, P., and Baltz, R. H. (2006) Combinatorial biosynthesis of novel antibiotics related to daptomycin. *Proc. Natl. Acad. Sci. U. S. A.* 103, 17462–7.
- (89) Lohani, C. R., Taylor, R., Palmer, M., and Taylor, S. D. (2015) Solid-Phase Total Synthesis of Daptomycin and Analogs. *Org. Lett.* 17, 748–751.
- (90) Lamp, K. C., Rybak, M. J., Bailey, E. M., and Kaatz, G. W. (1992) In vitro Pharmacodynamic

Effects of Concentration, pH, and Growth Phase on Serum Bactericidal Activities of Daptomycin and Vancomycin. *Antimicrob. Agents Chemother.* 36, 2709–2714.

(91) Sabol, K., Patterson, J. E., Lewis, J. S., Owens, A., Cadena, J., and Jorgensen, J. H. (2005) Emergence of daptomycin resistance in *Enterococcus faecium* during daptomycin therapy. *Antimicrob. Agents Chemother.* 49, 1664–1665.

(92) Silverman, J. A., Oliver, N., Andrew, T., Andrew, T. E. D., and Li, T. (2001) Resistance Studies with Daptomycin. *Antimicrob. Agents Chemother.* 45, 1799–1802.

(93) Dubrac, S., and Msadek, T. (2004) Identification of Genes Controlled by the Essential YycG / YycF Two-Component System of *Staphylococcus aureus*. *J. Bacteriol.* 186, 1175–1181.

(94) Bisicchia, P., Lioliou, E., Noone, D., Salzberg, L. I., Botella, E., Hübner, S., and Devine, K. M. (2010) Peptidoglycan metabolism is controlled by the WalRK (YycFG) and PhoPR two-component systems in phosphate-limited *Bacillus subtilis* cells. *Mol. Microbiol.* 75, 972–989.

(95) Randall, C. P., Mariner, K. R., Chopra, I., and O’Neill, A. J. (2013) The target of daptomycin is absent from *Escherichia coli* and other gram-negative pathogens. *Antimicrob. Agents Chemother.* 57, 637–639.

(96) Ernst, C. M., Staubitz, P., Mishra, N. N., Yang, S.-J., Hornig, G., Kalbacher, H., Bayer, A. S., Kraus, D., and Peschel, A. (2009) The bacterial defensin resistance protein MprF consists of separable domains for lipid lysinylation and antimicrobial peptide repulsion. *PLoS Pathog.* 5, 1–9.

(97) Kilelee, E., Pokorny, A., Yeaman, M. R., and Bayer, A. S. (2010) Lysyl-phosphatidylglycerol attenuates membrane perturbation rather than surface association of the cationic antimicrobial peptide 6W-RP-1 in a model membrane system: implications for daptomycin resistance. *Antimicrob. Agents Chemother.* 54, 4476–4479.

(98) Mishra, N. N., McKinnell, J., Yeaman, M. R., Rubio, A., Nast, C. C., Chen, L., Kreiswirth, B. N., and Bayer, A. S. (2011) In vitro cross-resistance to daptomycin and host defense cationic antimicrobial peptides in clinical methicillin-resistant *Staphylococcus aureus* isolates. *Antimicrob. Agents Chemother.* 55, 4012–4018.

(99) Oku, Y. (2004) Characterization of the *Staphylococcus aureus* mprF gene, involved in lysinylation of phosphatidylglycerol. *Microbiology* 150, 45–51.

(100) Peleg, A. Y., Miyakis, S., Ward, D. V., Earl, A. M., Rubio, A., Cameron, D. R., Pillai, S.,

- Moellering, R. C., and Eliopoulos, G. M. (2012) Whole genome characterization of the mechanisms of daptomycin resistance in clinical and laboratory derived isolates of *Staphylococcus aureus*. *PLoS One* 7, e28316.
- (101) Klieneberger, E. (1935) The Natural Occurrence of Pleuro-Pneumonia-Like Organisms in Apparent Symbiosis With *Streptobacillus Moniliformis* and Other Bacteria. *J. Pathol. Bacteriol.* 5.
- (102) Devine, K. M. (2012) Bacterial L-forms on tap: An improved methodology to generate *Bacillus subtilis* L-forms heralds a new era of research. *Mol. Microbiol.* 83, 10–3.
- (103) Edward, D. G., and Freundt, E. a. (1956) The classification and nomenclature of organisms of the pleuropneumonia group. *J. Gen. Microbiol.* 14, 197–207.
- (104) Allan, E. J., Hoischen, C., and Gumpert, J. (2009) Bacterial L-forms. *Adv. Appl. Microbiol.* 1st ed. Elsevier Inc.
- (105) Stieglmeier, M., Alves, R., and Schleper, C. (1992) The Prokaryotes: Volume IV (Balows, A., Hans G, T., Dworkin, M., Harder, W., and Schleifer, K.-H., Eds.) 2nd ed. Springer Science+Business Media, New York, NY.
- (106) Domingue, G. J., and Woody, H. B. (1997) Bacterial persistence and expression of disease. *Clin. Microbiol. Rev.* 10, 320–344.
- (107) Domínguez-Cuevas, P., Mercier, R., Leaver, M., Kawai, Y., and Errington, J. (2012) The rod to L-form transition of *Bacillus subtilis* is limited by a requirement for the protoplast to escape from the cell wall sacculus. *Mol. Microbiol.* 83, 52–66.
- (108) Leaver, M., Domínguez-Cuevas, P., Coxhead, J. M., Daniel, R. A., and Errington, J. (2009) Life without a wall or division machine in *Bacillus subtilis*. *Nature* 457, 849–53.
- (109) Sonenshein, A. L., Hoch, J. A., and Losick, R. (2002) *Bacillus subtilis* and its Closest Relatives: From Genes to Cells. ASM Press, Washington, D.C.
- (110) Leaver, M., and Errington, J. (2005) Roles for MreC and MreD proteins in helical growth of the cylindrical cell wall in *Bacillus subtilis*. *Mol. Microbiol.* 57, 1196–1209.
- (111) Duman, R., Ishikawa, S., Celik, I., Strahl, H., Ogasawara, N., Troc, P., Löwe, J., and Hamoen, L. W. (2013) Structural and genetic analyses reveal the protein SepF as a new membrane anchor for the Z ring. *Proc. Natl. Acad. Sci. U. S. A.* 110, E4601–10.

- (112) Hamoen, L. W., Meile, J. C., Jong, W. De, Noirot, P., Errington, J., De Jong, W., Noirot, P., and Errington, J. (2006) SepF, a novel FtsZ-interacting protein required for a late step in cell division. *Mol. Microbiol.* 59, 989–999.
- (113) Olson, F., Hunt, C., and Szoka, F. (1979) Preparation of Liposomes of Defined Size Distribution by Extrusion through Polycarbonate Membranes. *Biochim. Biophys. Acta* 557, 9–23.
- (114) Canepari, P., Boaretti, M., Del Mar Lleo, M., and Satta, G. (1990) Lipoteichoic acid as a new target for activity of antibiotics: Mode of action of daptomycin (LY146032). *Antimicrob. Agents Chemother.* 34, 1220–1226.
- (115) Thomas, K. J., and Rice, C. V. (2014) Revised model of calcium and magnesium binding to the bacterial cell wall. *BioMetals* 27, 1361–1370.
- (116) Mishra, N. N., and Bayer, A. S. (2012) Correlation of cell membrane lipid profiles with daptomycin resistance in methicillin-resistant *Staphylococcus aureus*. *Antimicrob. Agents Chemother.* 57, 1082–5.
- (117) Scott, W. R. P., Baek, S. Bin, Jung, D., Hancock, R. E. W., and Straus, S. K. (2007) NMR structural studies of the antibiotic lipopeptide daptomycin in DHPC micelles. *Biochim. Biophys. Acta - Biomembr.* 1768, 3116–3126.
- (118) Straus, S. K., and Hancock, R. E. W. (2006) Mode of action of the new antibiotic for Gram-positive pathogens daptomycin: comparison with cationic antimicrobial peptides and lipopeptides. *Biochim. Biophys. Acta* 1758, 1215–23.
- (119) Lohani, C. R., Taylor, R., Palmer, M., and Taylor, S. D. (2015) Solid-phase synthesis and in vitro biological activity of a Thr4→Ser4 analog of daptomycin. *Bioorg. Med. Chem. Lett.* 25, 5490–5494.
- (120) Eliopoulos, G. M., Thauvin, C., Gerson, B., and Moellering, R. C. (1985) In Vitro Activity and Mechanism of Action of A21978C1, a Novel Cyclic Lipopeptide Antibiotic. *Antimicrob. Agents Chemother.* 27, 357–362.
- (121) Goerke, J. (1998) Pulmonary surfactant: functions and molecular composition. *Biochim. Biophys. Acta* 1408, 79–89.
- (122) Chen, Y., Tang, C., Zhang, J., Gong, M., Su, B., and Qiu, F. (2015) Self-assembling surfactant-like peptide A6K as potential delivery system for hydrophobic drugs. *Int. J. Nanomedicine* 10, 847–

858.

(123) Grünewald, J., Sieber, S. a, Mahlert, C., Linne, U., and Marahiel, M. a. (2004) Synthesis and derivatization of daptomycin: a chemoenzymatic route to acidic lipopeptide antibiotics. *J. Am. Chem. Soc.* 126, 17025–31.

(124) Taylor, S. D., and Palmer, M. (2016) The Action Mechanism of Daptomycin. *Bioorg. Med. Chem.* (submitted).

(125) Yang, S.-J., Xiong, Y. Q., Dunman, P. M., Schrenzel, J., François, P., Peschel, A., and Bayer, A. S. (2009) Regulation of mprF in daptomycin-nonsusceptible *Staphylococcus aureus* strains. *Antimicrob. Agents Chemother.* 53, 2636–7.

(126) Rubio, A., Conrad, M., Haselbeck, R. J., G C, K., Brown-Driver, V., Finn, J., and Silverman, J. a. (2011) Regulation of mprF by antisense RNA restores daptomycin susceptibility to daptomycin-resistant isolates of *Staphylococcus aureus*. *Antimicrob. Agents Chemother.* 55, 364–7.

(127) Ernst, C. M., and Peschel, A. (2011) Broad-spectrum antimicrobial peptide resistance by MprF-mediated aminoacylation and flipping of phospholipids. *Mol. Microbiol.* 80, 290–9.

(128) Mishra, N. N., Bayer, A. S., Moise, P. a, Yeaman, M. R., and Sakoulas, G. (2012) Reduced susceptibility to host-defense cationic peptides and daptomycin coemerge in methicillin-resistant *Staphylococcus aureus* from daptomycin-naïve bacteremic patients. *J. Infect. Dis.* 206, 1160–7.

(129) den Kamp, J. A., Redai, I., and van Deenen, L. L. (1969) Phospholipid composition of *Bacillus subtilis*. *J Bacteriol* 99, 298–303.

(130) Merck. (2015) Cubicin (daptomycin for injection) prescribing information. Kenilworth, New Jersey.

(131) Ebashi, S., Toyokura, Y., Momoi, H., and Sugita, H. (1959) High creatine phosphokinase activity of sera with progressive muscular dystrophy. *J. Biochem.* 46, 103–104.

(132) Morita, S., and Terada, T. (2015) Enzymatic measurement of phosphatidylglycerol and cardiolipin in cultured cells and mitochondria. *Sci. Rep.* 5, 11737.

(133) Tomohiro, S., Kawaguti, A., Kawabe, Y., Kitada, S., and Kuge, O. (2009) Purification and characterization of human phosphatidylserine synthases 1 and 2. *Biochem. J.* 418, 421–429.

(134) Fadok, V. A., Voelker, D. R., Campbell, P. A., Cohen, J. J., Bratton, D. L., and Henson, P. M.

- (1992) Exposure of phosphatidylserine on the surface of apoptotic lymphocytes triggers specific recognition and removal by macrophages. *J. Immunol.* *148*, 2207–2216.
- (135) Ostash, B., and Walker, S. (2010) Moenomycin family antibiotics: chemical synthesis, biosynthesis, biological activity. *Nat. Prod. Rep.* *27*, 1594–1617.
- (136) Kohlrausch, U., and Holtje, J. V. (1991) Analysis of murein and murein precursors during antibiotic-induced lysis of *Escherichia coli*. *J. Bacteriol.* *173*, 3425–3431.
- (137) Hsu, S.-T. D., Breukink, E., Tischenko, E., Lutters, M. A. G., de Kruijff, B., Kaptein, R., Bonvin, A. M. J. J., and van Nuland, N. A. J. (2004) The nisin-lipid II complex reveals a pyrophosphate cage that provides a blueprint for novel antibiotics. *Nat. Struct. Mol. Biol.* *11*, 963–7.
- (138) Wolf, D., Domínguez-Cuevas, P., Daniel, R. a., and Mascher, T. (2012) Cell envelope stress response in cell wall-deficient L-forms of *Bacillus subtilis*. *Antimicrob. Agents Chemother.* *56*, 5907–15.
- (139) Müller, A., Ulm, H., Reder-Christ, K., Sahl, H.-G., and Schneider, T. (2012) Interaction of Type A Lantibiotics with Undecaprenol-Bound Cell Envelope Precursors. *Microb. Drug Resist.* *18*, 261–270.

Appendix A

Raw fluorescence figures

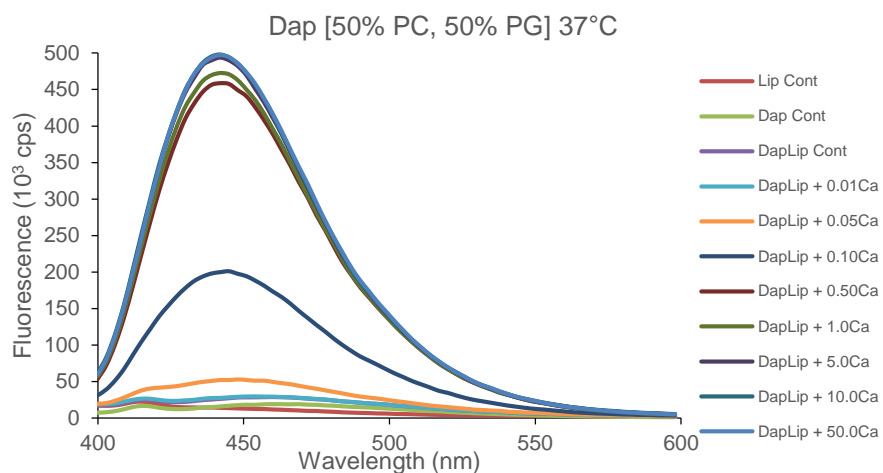


Figure 6.3: Fluorescence spectrum of dap in the presence of 50:50 PC:PG liposomes and increasing Ca²⁺ concentration (mM) at 37 °C. Legend: Lip refers to liposomes, Cont refers to control.

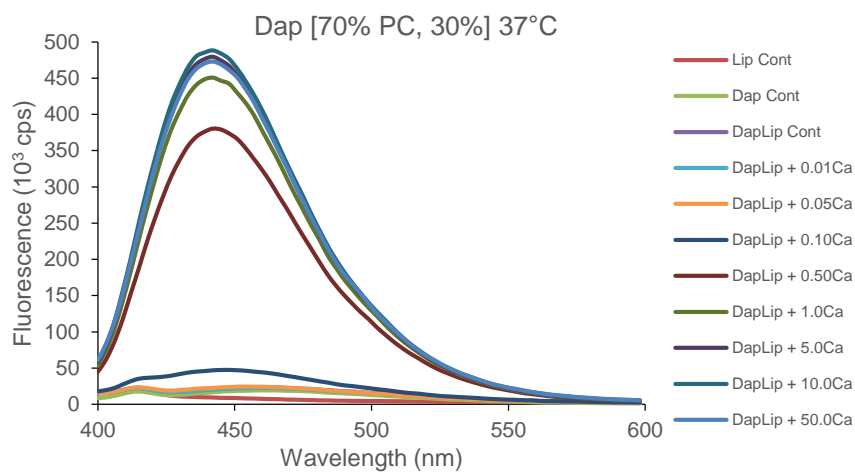


Figure 6.4: Fluorescence spectrum of dap in the presence of 70:30 PC:PG liposomes and increasing Ca²⁺ concentration (mM) at 37 °C. Legend: Lip refers to liposomes, Cont refers to control.

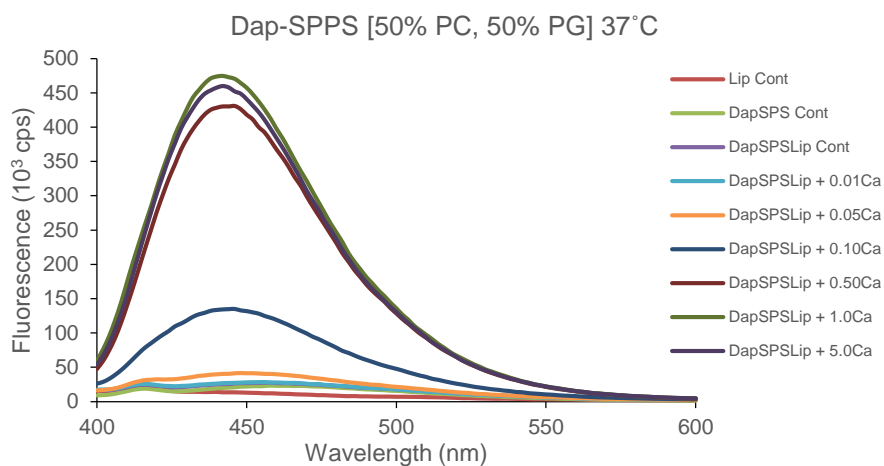


Figure 6.5: Fluorescence spectrum of solid-phase synthesis dap in the presence of 50:50 PC:PG liposomes and increasing Ca²⁺ concentration (mM) at 37 °C. Legend: Lip refers to liposomes, Cont refers to control.

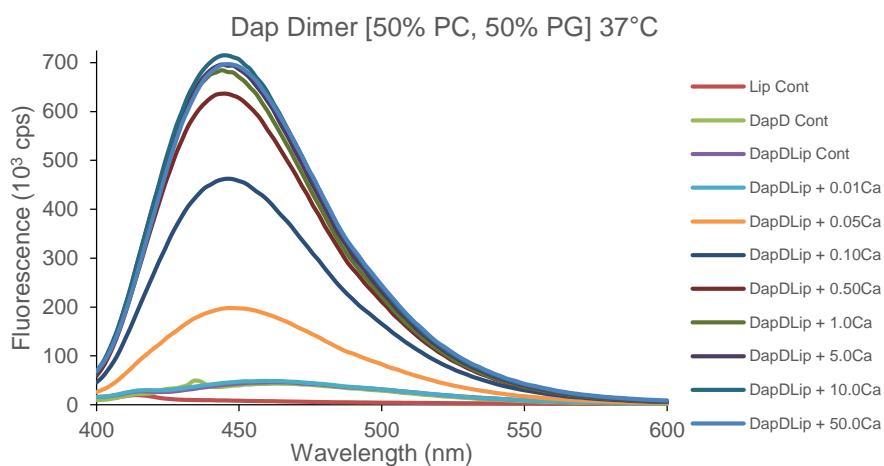


Figure 6.6: Fluorescence spectrum of dap dimer in the presence of 70:30 PC:PG liposomes and increasing Ca²⁺ concentration (mM) at 37 °C. Legend: Lip refers to liposomes, Cont refers to control.

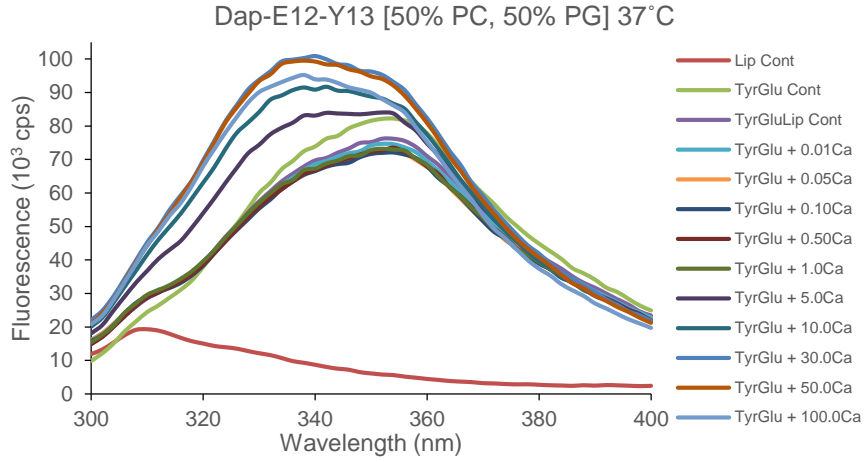


Figure 6.7: Fluorescence spectrum of dap-E12-Y13 in the presence of 50:50 PC:PG liposomes and increasing Ca²⁺ concentration (mM) at 37 °C. Legend: Lip refers to liposomes, Cont refers to control.

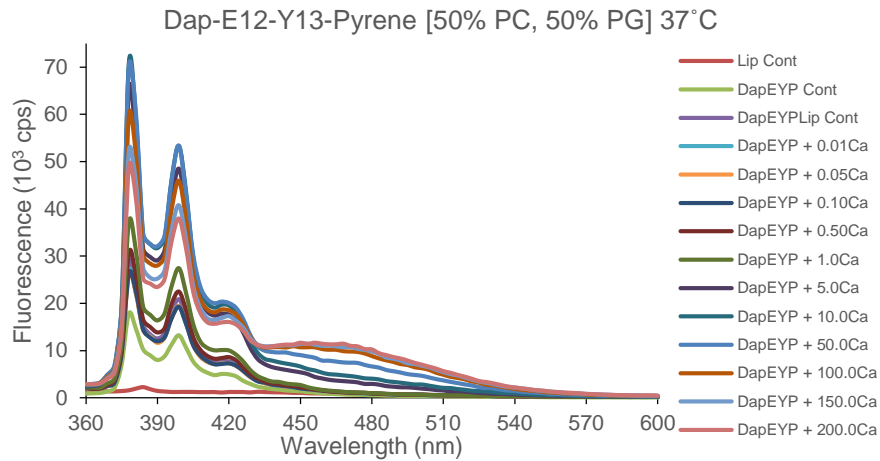


Figure 6.8: Fluorescence spectrum of dap-E12-Y13-pyrene in the presence of 50:50 PC:PG liposomes and increasing Ca²⁺ concentration (mM) at 37 °C. Legend: Lip refers to liposomes, Cont refers to control.

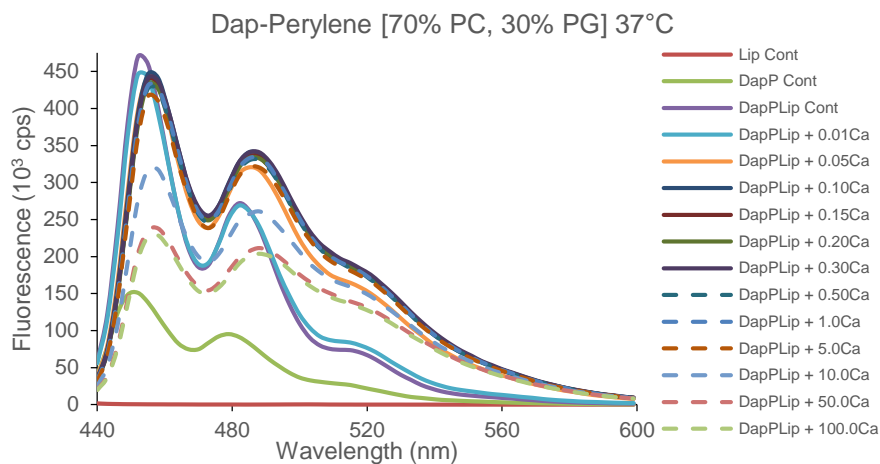


Figure 6.9: Fluorescence spectrum of dap-erylene in the presence of 70:30 PC:PG liposomes and increasing Ca²⁺ concentration (mM) at 37 °C. Legend: Lip refers to liposomes, Cont refers to control.

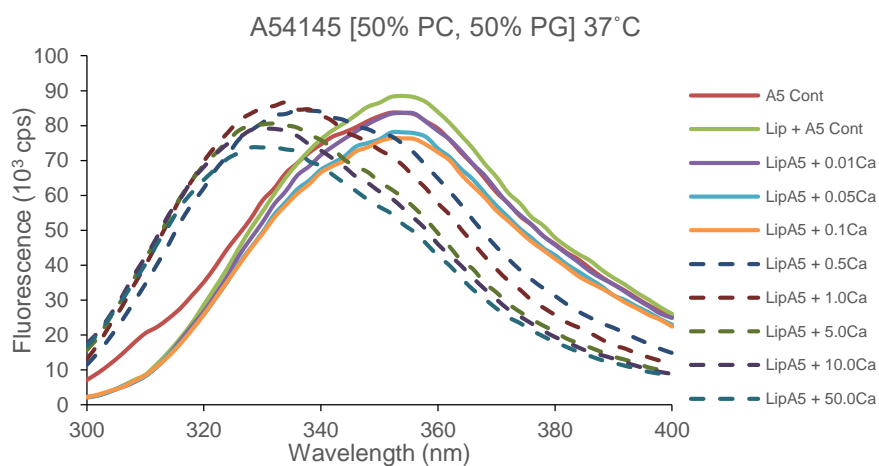


Figure 6.10: Fluorescence spectrum of A5 in the presence of 50:50 PC:PG liposomes and increasing Ca²⁺ concentration (mM) at 37 °C. Legend: Lip refers to liposomes, Cont refers to control.

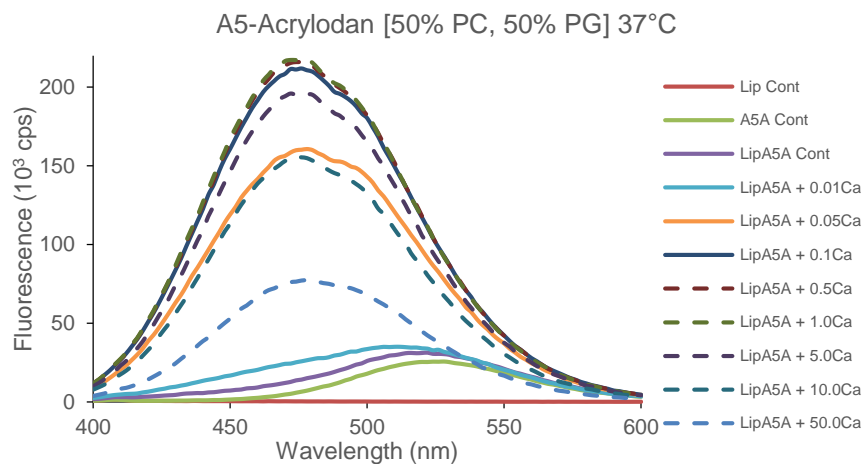


Figure 6.11: Fluorescence spectrum of A5-acrylodan in the presence of 50:50 PC:PG liposomes and increasing Ca²⁺ concentration (mM) at 37 °C. Legend: Lip refers to liposomes, Cont refers to control.

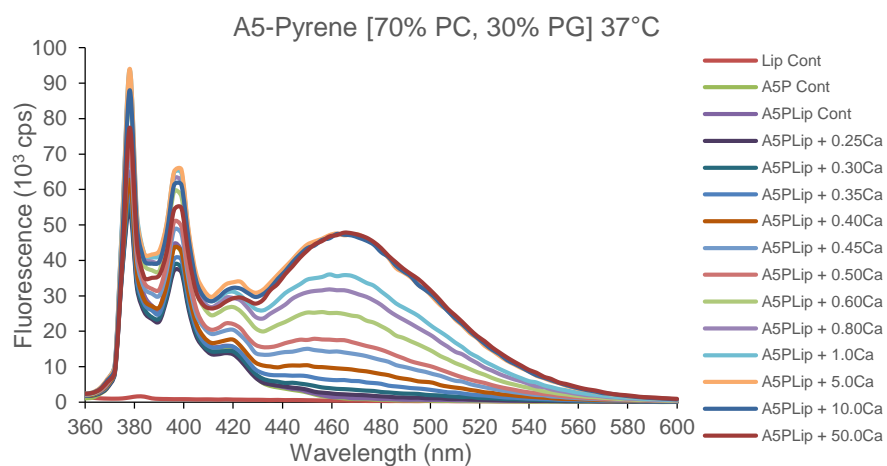


Figure 6.12: Fluorescence spectrum of A5-pyrene in the presence of 70:30 PC:PG liposomes and increasing Ca²⁺ concentration (mM) at 37 °C. Legend: Lip refers to liposomes, Cont refers to control.

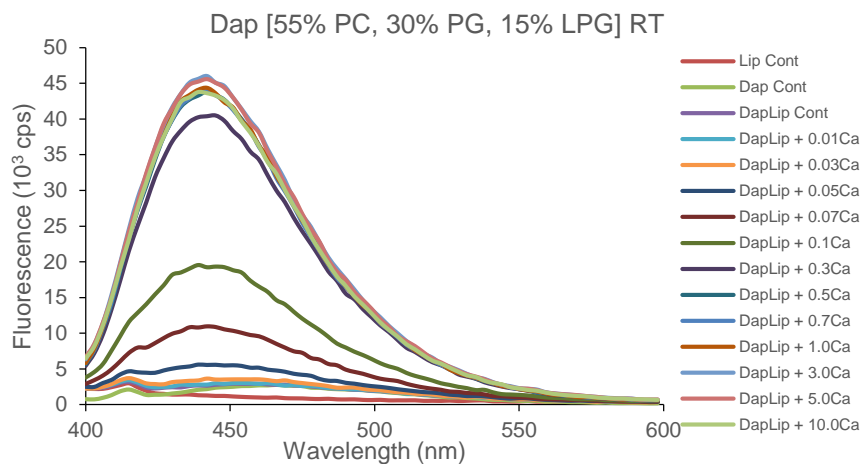


Figure 6.13: Fluorescence spectrum of dap in the presence of 55:30:15 PC:PG:LPG liposomes and increasing Ca^{2+} concentration (mM) under ambient conditions ($\sim 25^\circ\text{C}$). Performed on the day of membrane production. Legend: Lip refers to liposomes, Cont refers to control.

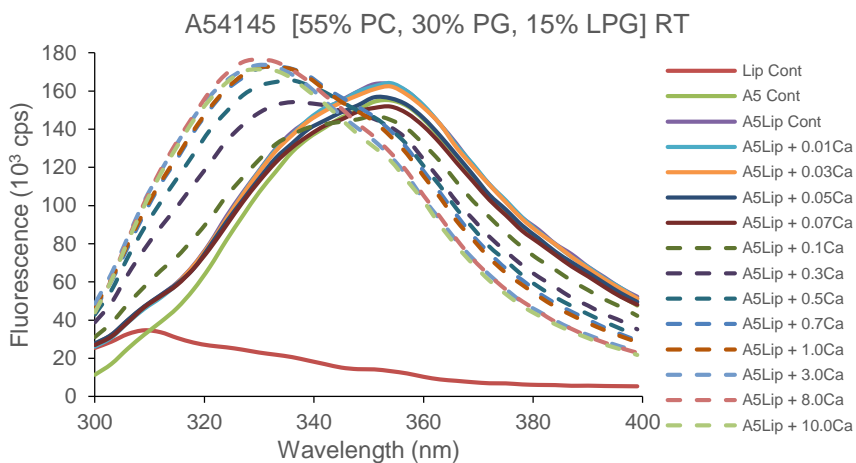


Figure 6.14: Fluorescence spectrum of A5 in the presence of 55:30:15 PC:PG:LPG liposomes and increasing Ca^{2+} concentration (mM) under ambient conditions ($\sim 25^\circ\text{C}$). Performed on the day of membrane production. Legend: Lip refers to liposomes, Cont refers to control.

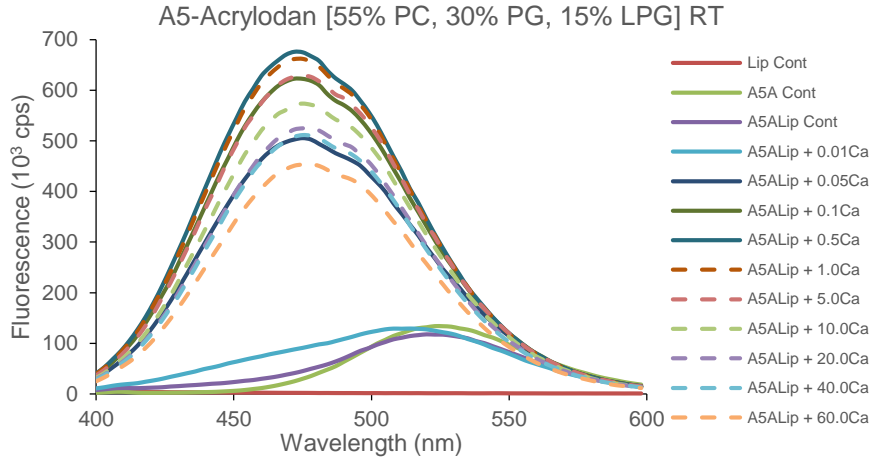


Figure 6.15: Fluorescence spectrum of A5-acrylodan in the presence of 55:30:15 PC:PG:LPG liposomes and increasing Ca²⁺ concentration (mM) under ambient conditions (~25 °C). Performed on the day of membrane production. Legend: Lip refers to liposomes, Cont refers to control.

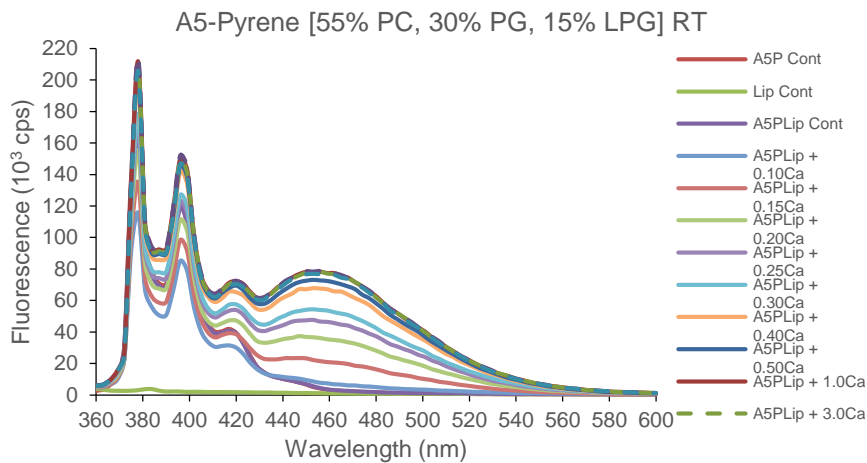


Figure 6.16: Fluorescence spectrum of A5-pyrene in the presence of 55:30:15 PC:PG:LPG liposomes and increasing Ca²⁺ concentration (mM) under ambient conditions (~25 °C). Performed on the day of membrane production. Legend: Lip refers to liposomes, Cont refers to control.

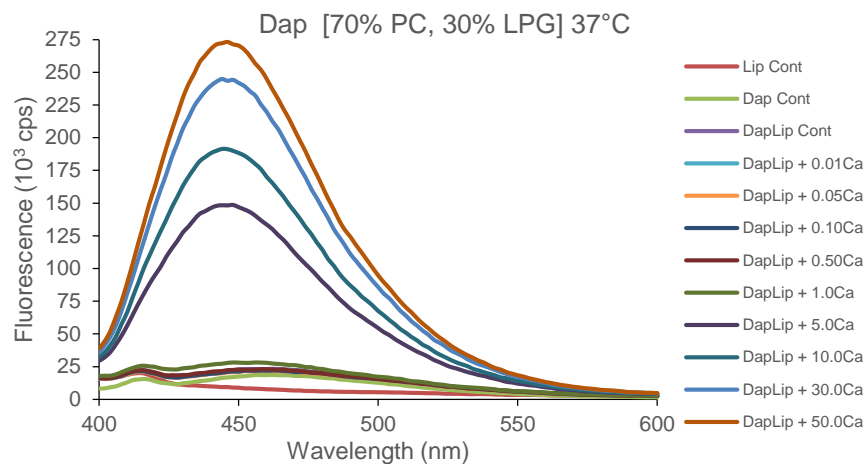


Figure 6.17: Fluorescence spectrum of dap in the presence of 70:30 PC:LPG liposomes and increasing Ca^{2+} concentration (mM) at 37 °C. Performed on the day of membrane production. Legend: Lip refers to liposomes, Cont refers to control.

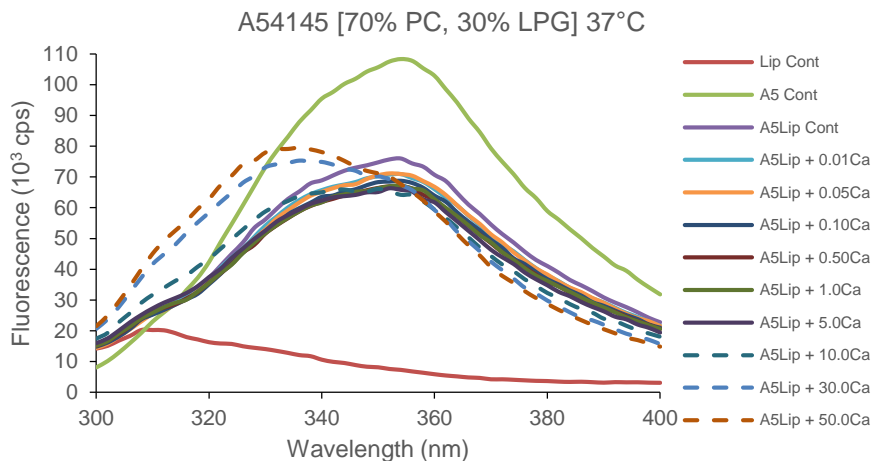


Figure 6.18: Fluorescence spectrum of A5 in the presence of 70:30 PC:LPG liposomes and increasing Ca^{2+} concentration (mM) at 37 °C. Performed on the day of membrane production. Legend: Lip refers to liposomes, Cont refers to control.

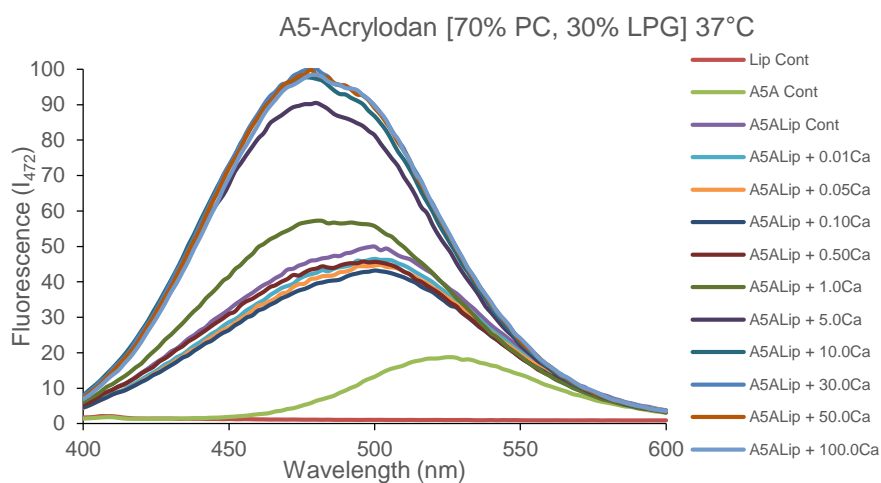


Figure 6.19: Fluorescence spectrum of A5-acrylodan in the presence of 70:30 PC:LPG liposomes and increasing Ca^{2+} concentration (mM) at 37 °C. Performed on the day of membrane production. Legend: Lip refers to liposomes, Cont refers to control.

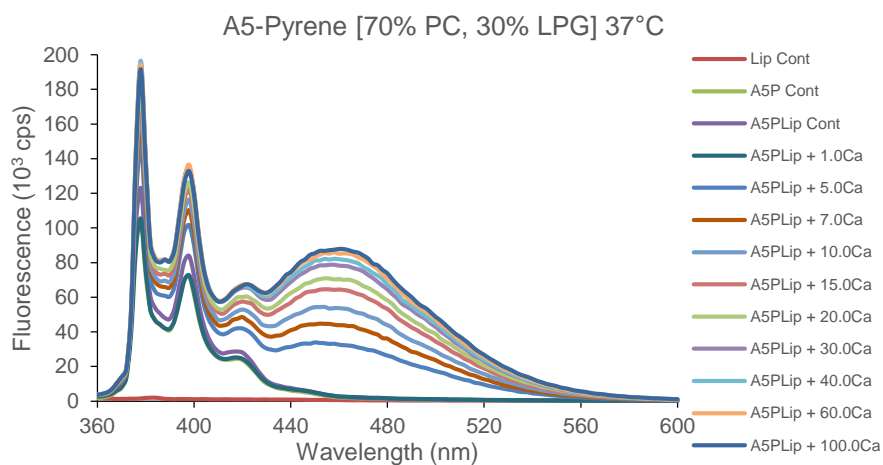


Figure 6.20: Fluorescence spectrum of A5-pyrene in the presence of 70:30 PC:LPG liposomes and increasing Ca^{2+} concentration (mM) at 37 °C. Performed on the day of membrane production. Legend: Lip refers to liposomes, Cont refers to control.

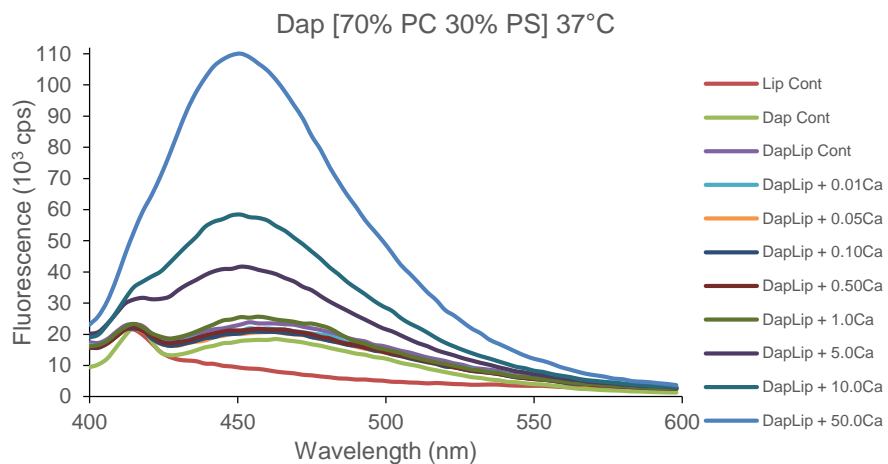


Figure 6.21: Fluorescence spectrum of dap in the presence of 70:30 PC:PS liposomes and increasing Ca^{2+} concentration (mM) at 37 °C. Legend: Lip refers to liposomes, Cont refers to control.

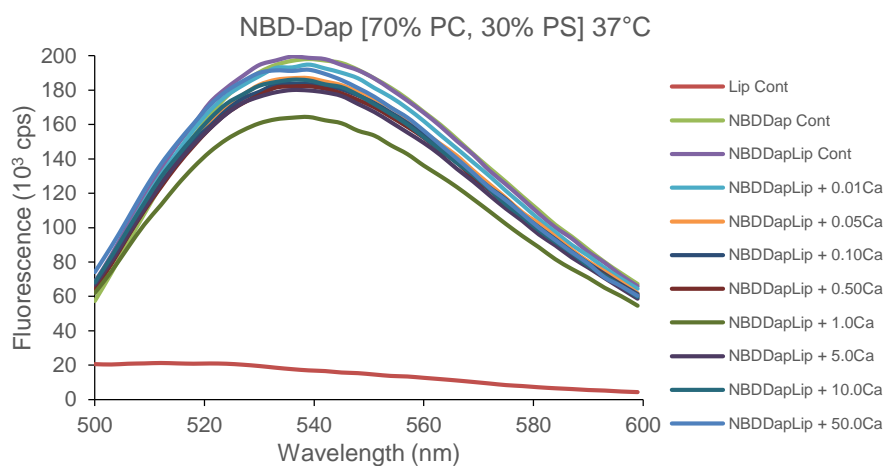


Figure 6.22: Fluorescence spectrum of NBD-dap in the presence of 70:30 PC:PS liposomes and increasing Ca^{2+} concentration (mM) at 37 °C. Legend: Lip refers to liposomes, Cont refers to control.

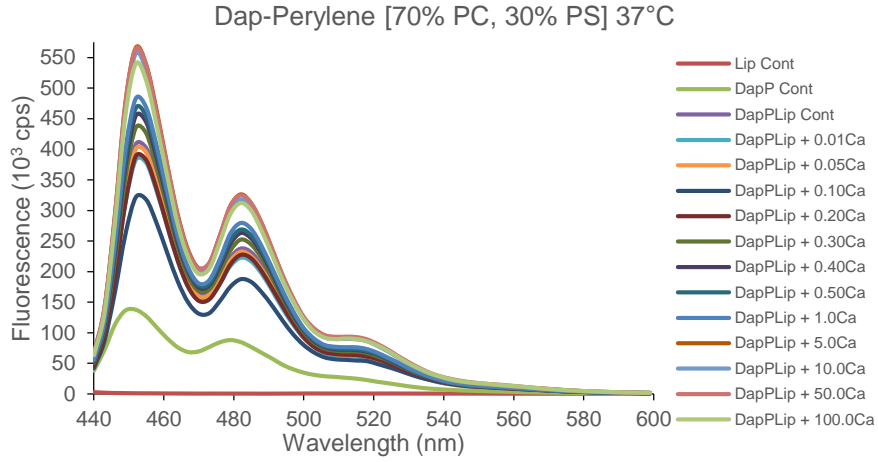


Figure 6.23: Fluorescence spectrum of dap-erylene in the presence of 70:30 PC:PS liposomes and increasing Ca²⁺ concentration (mM) at 37 °C. Legend: Lip refers to liposomes, Cont refers to control.

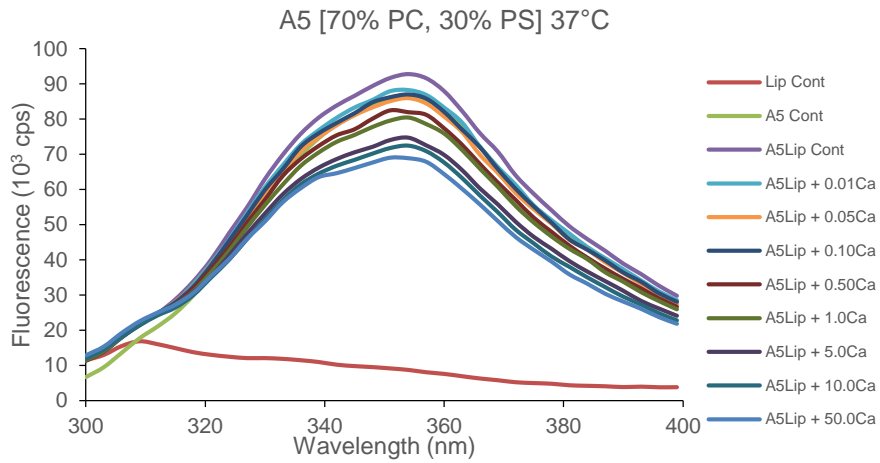


Figure 6.24: Fluorescence spectrum of A5 in the presence of 70:30 PC:PS liposomes and increasing Ca²⁺ concentration (mM) at 37 °C. Legend: Lip refers to liposomes, Cont refers to control.

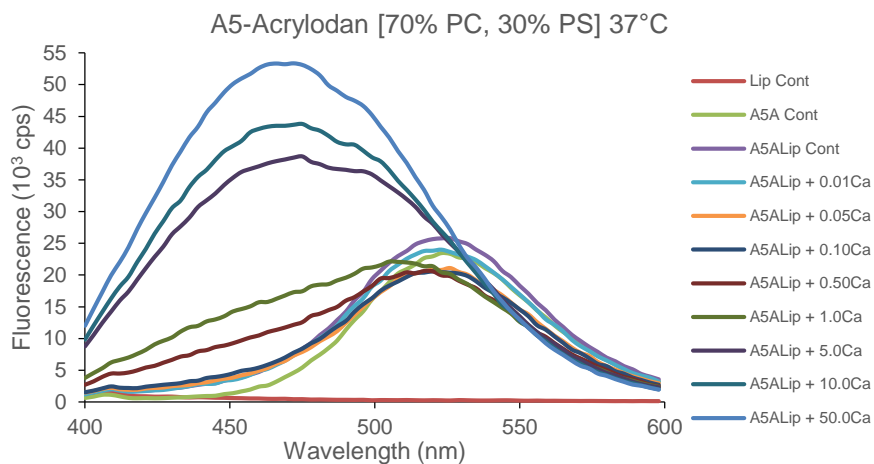


Figure 6.25: Fluorescence spectrum of A5-acrylodan in the presence of 70:30 PC:PS liposomes and increasing Ca²⁺ concentration (mM) at 37 °C. Legend: Lip refers to liposomes, Cont refers to control.

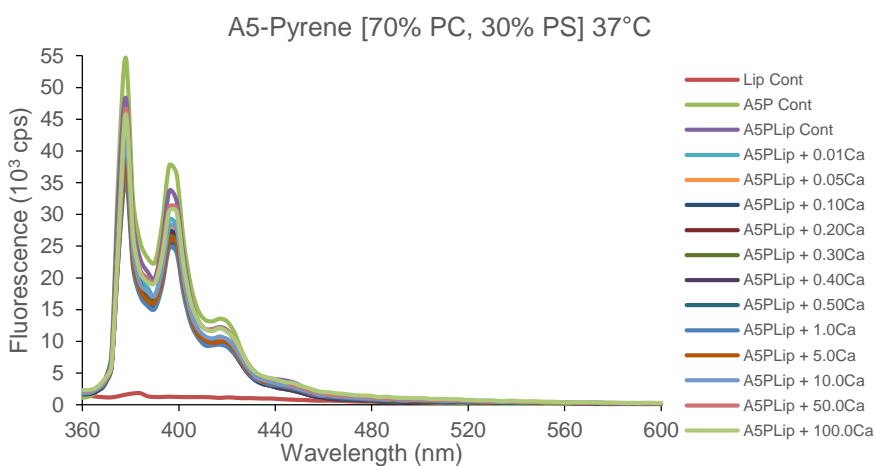


Figure 6.26: Fluorescence spectrum of A5-pyrene in the presence of 70:30 PC:PS liposomes and increasing Ca²⁺ concentration (mM) at 37 °C. Legend: Lip refers to liposomes, Cont refers to control.

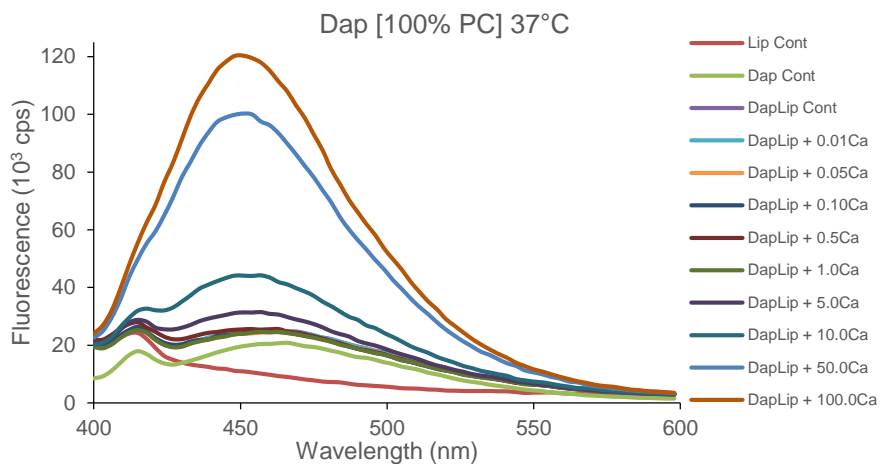


Figure 6.27: Fluorescence spectrum of dap in the presence of 100% PC liposomes and increasing Ca^{2+} concentration (mM) at 37 °C. Legend: Lip refers to liposomes, Cont refers to control.

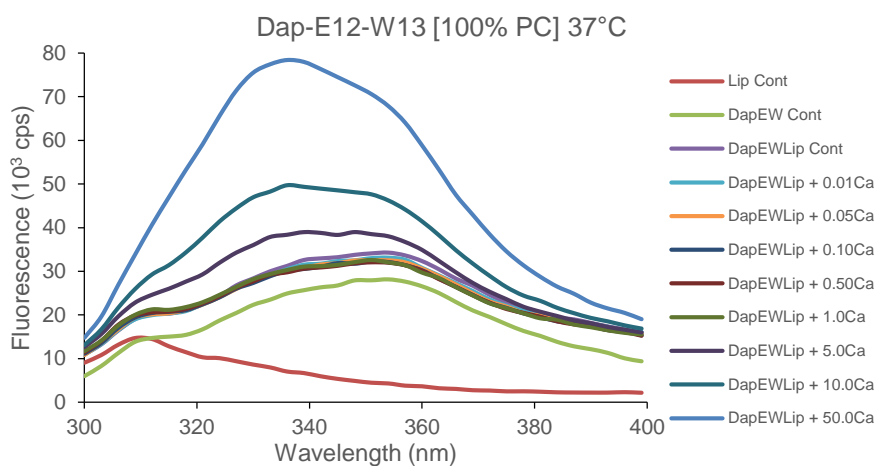


Figure 6.28: Fluorescence spectrum of dap-E12-W13 in the presence of 100% PC liposomes and increasing Ca^{2+} concentration (mM) at 37 °C. Legend: Lip refers to liposomes, Cont refers to control.

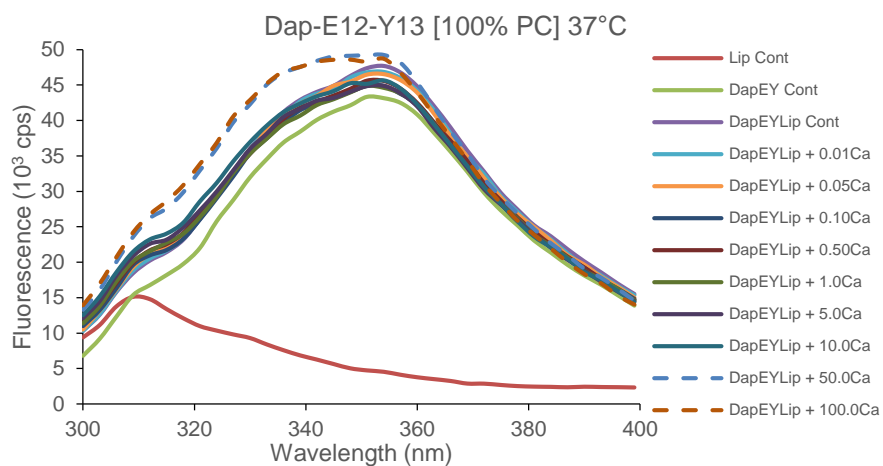


Figure 6.29: Fluorescence spectrum of dap-E12-Y13 in the presence of 100% PC liposomes and increasing Ca²⁺ concentration (mM) at 37 °C. Legend: Lip refers to liposomes, Cont refers to control.

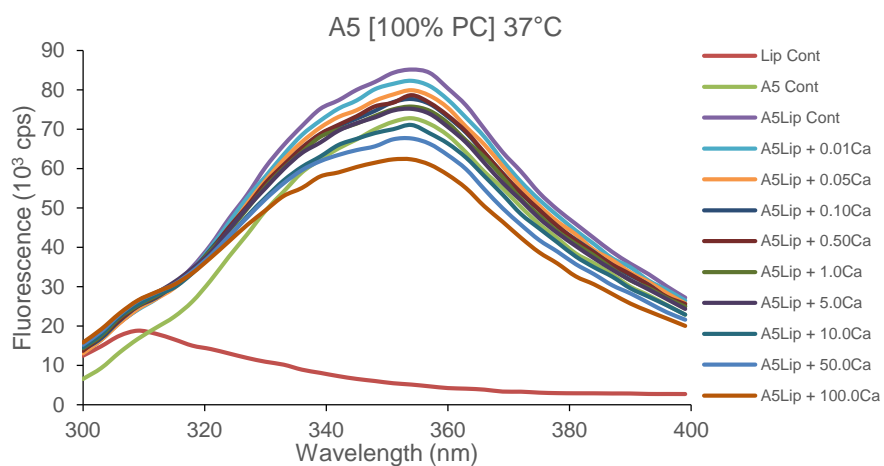


Figure 6.30: Fluorescence spectrum of A5 in the presence of 100% PC liposomes and increasing Ca²⁺ concentration (mM) at 37 °C. Legend: Lip refers to liposomes, Cont refers to control.

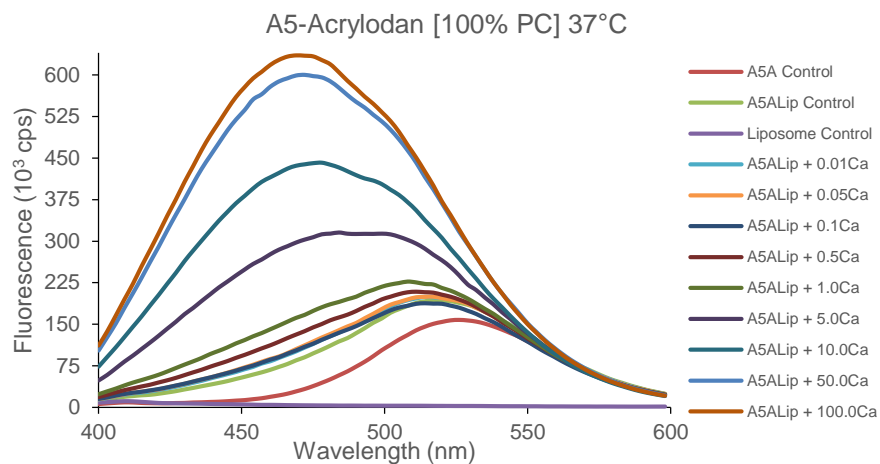


Figure 6.31: Fluorescence spectrum of A5-acrylodan in the presence of 100% PC liposomes and increasing Ca^{2+} concentration (mM) at 37 °C. Legend: Lip refers to liposomes, Cont refers to control.

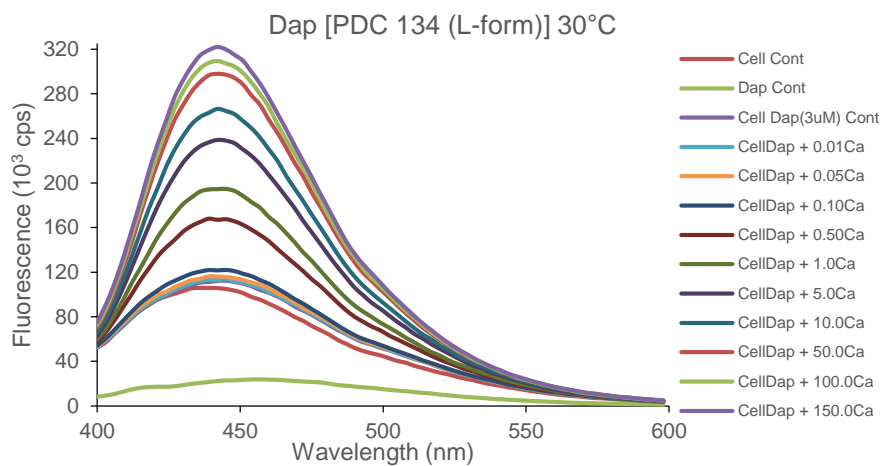


Figure 6.32: Fluorescence spectrum of dap in the presence *B. subtilis* PDC 134 L-forms ($\text{OD}_{600} = 0.8$) and increasing Ca^{2+} concentration (mM) at 30 °C. Legend: Lip refers to liposomes, Cont refers to control.

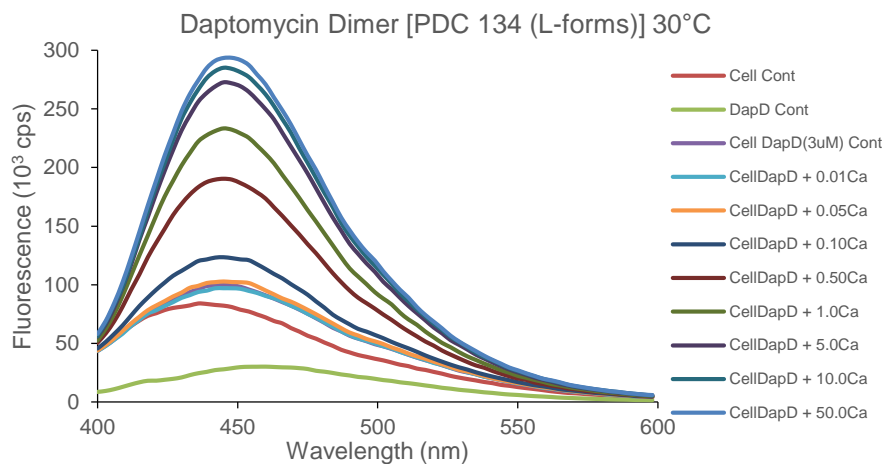


Figure 6.33: Fluorescence spectrum of dap dimer in the presence *B. subtilis* PDC 134 L-forms ($OD_{600} = 0.8$) and increasing Ca^{2+} concentration (mM) at 30 °C. Legend: Lip refers to liposomes, Cont refers to control.

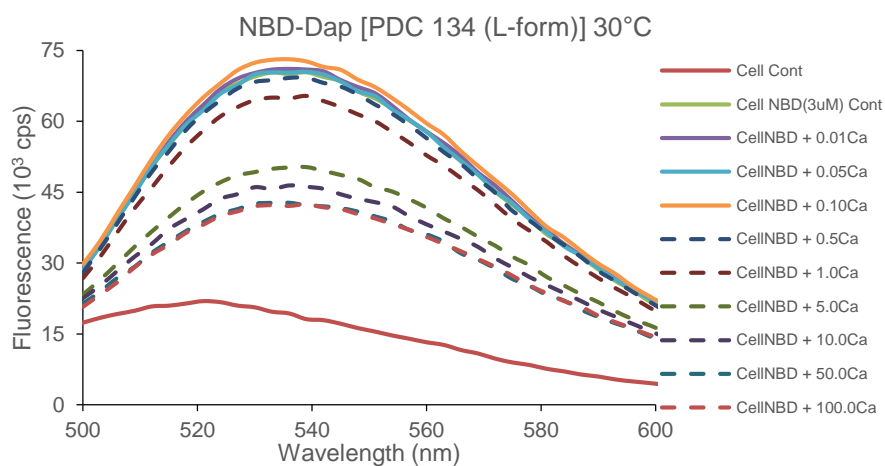


Figure 6.34: Fluorescence spectrum of NBD-dap in the presence *B. subtilis* PDC 134 L-forms ($OD_{600} = 0.8$) and increasing Ca^{2+} concentration (mM) at 30 °C. Legend: Lip refers to liposomes, Cont refers to control.

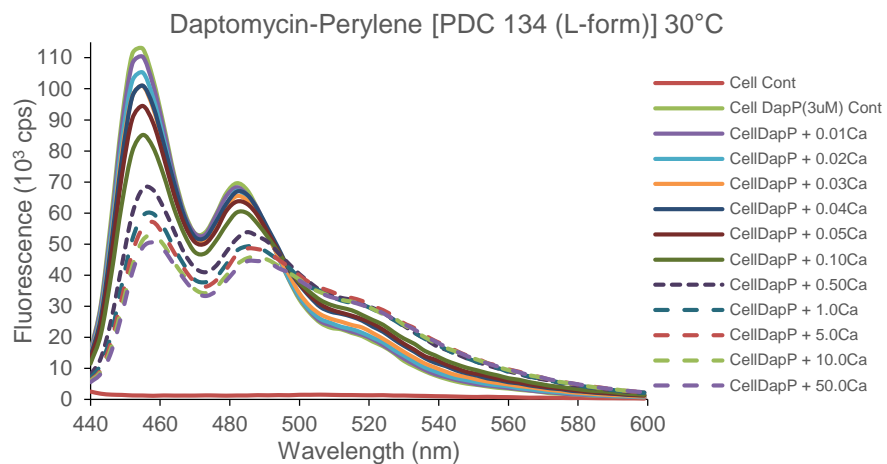


Figure 6.35: Fluorescence spectrum of dap-perylen in the presence *B. subtilis* PDC 134 L-forms ($OD_{600} = 0.8$) and increasing Ca^{2+} concentration (mM) at 30 °C. Legend: Lip refers to liposomes, Cont refers to control.

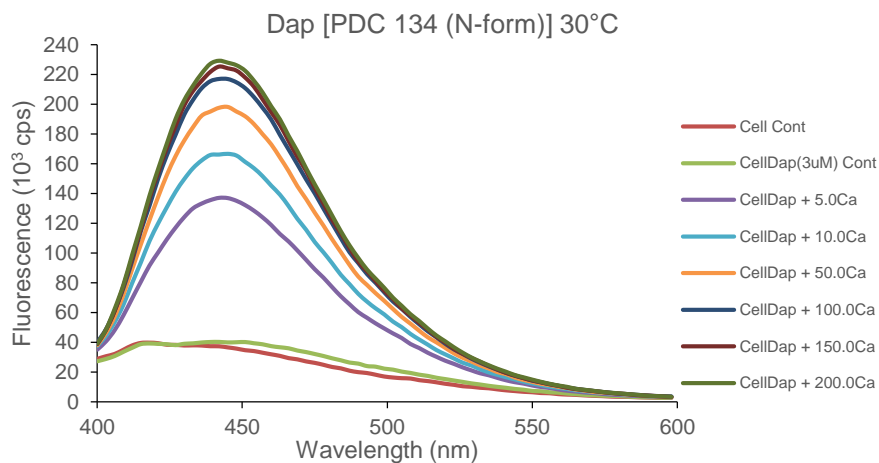


Figure 6.36: Fluorescence spectrum of dap in the presence *B. subtilis* PDC 134 N-forms ($OD_{600} = 0.4$) and increasing Ca^{2+} concentration (mM) at 30 °C. Legend: Lip refers to liposomes, Cont refers to control.

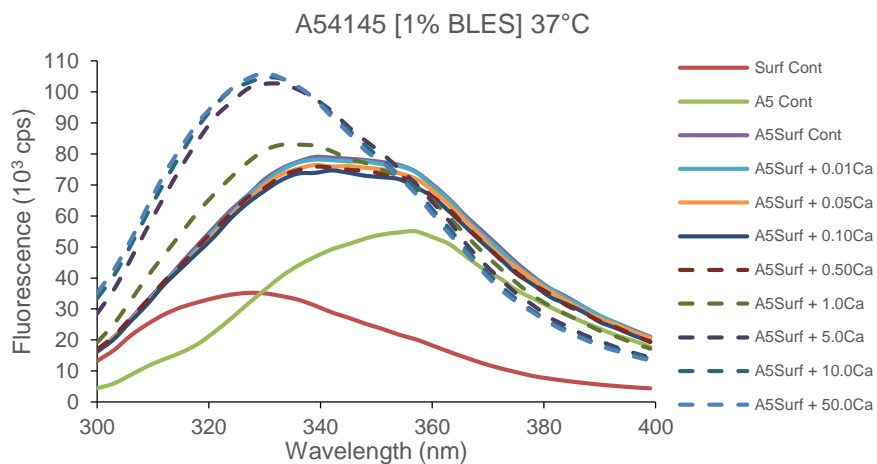


Figure 6.37: Fluorescence spectrum of A5 in the presence 1% BLES and increasing Ca^{2+} concentration (mM) at 30 °C. Legend: Lip refers to liposomes, Cont refers to control.

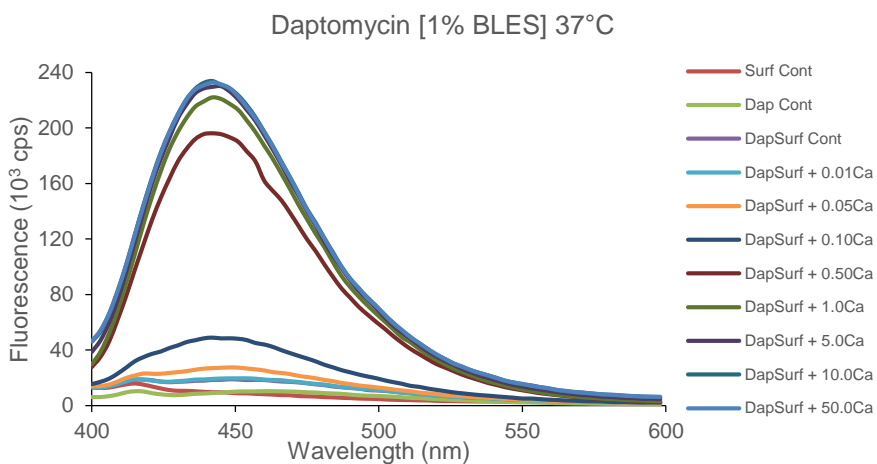


Figure 6.38: Fluorescence spectrum of dap in the presence of 1% BLES and increasing Ca^{2+} concentration (mM) at 30 °C. Legend: Lip refers to liposomes, Cont refers to control.

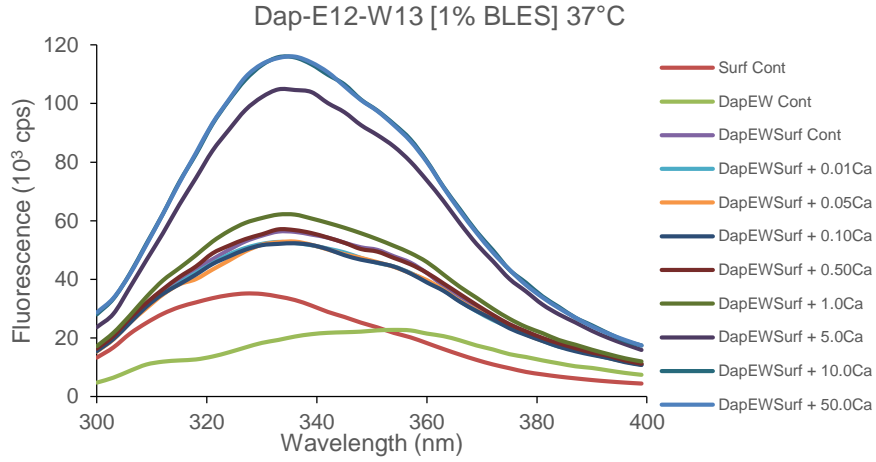


Figure 6.39: Fluorescence spectrum of dap-E12-W13 in the presence of 1% BLES and increasing Ca^{2+} concentration (mM) at 30 °C. Legend: Lip refers to liposomes, Cont refers to control.

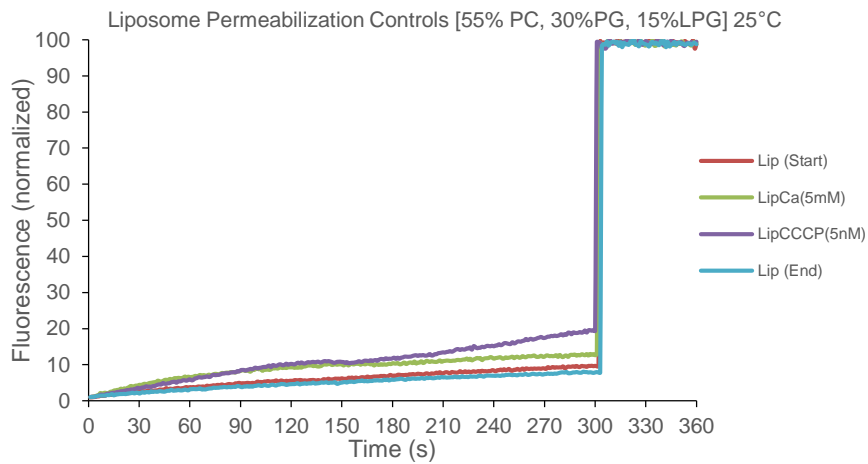


Figure 6.40: Liposome permeabilization test controls for the multiple lipopeptide analogs at 25 °C. Liposome controls were both at the start of the experiment and at the end. Ca^{2+} and CCCP alone raised the baseline a negligible amount. Fluorescence is normalized to the highest signal after Triton-X addition at 300s. Legend: Lip refers to liposomes

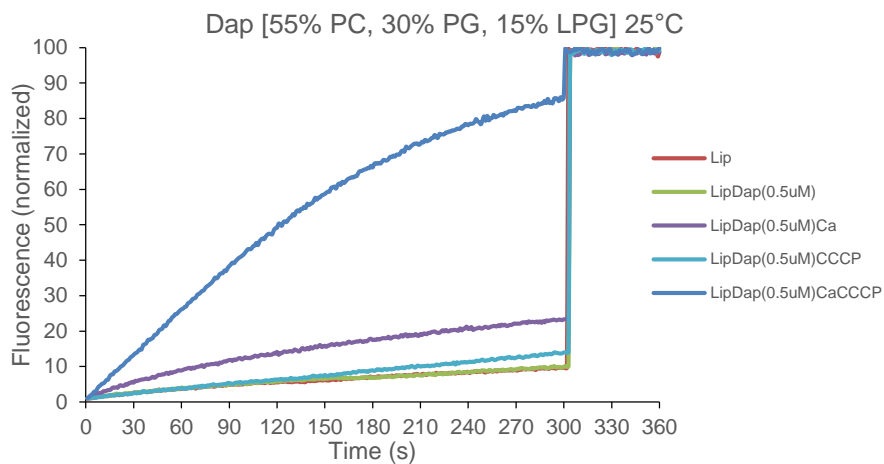


Figure 6.41: Liposome permeabilization test using dap in the presence of 5 mM Ca²⁺ and 5 nM CCCP at 25 °C. Controls include lipopeptide alone or in the presence of either Ca²⁺ or CCCP. The excitation and emission wavelengths are 460 nm and 510 nm, respectively. Fluorescence is normalized to the highest signal after Triton-X addition at 300s. Legend: Lip refers to liposomes, Cont refers to control.

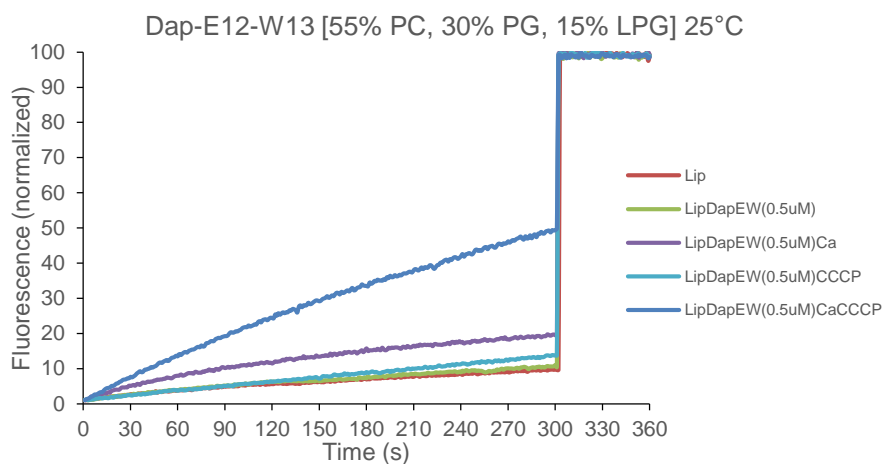


Figure 6.42 Liposome permeabilization test using dap-E12-W13 in the presence of 5 mM Ca²⁺ and 5 nM CCCP at 25 °C. Controls include lipopeptide alone or in the presence of either Ca²⁺ or CCCP. The excitation and emission wavelengths are 460 nm and 510 nm, respectively. Fluorescence is normalized to the highest signal after Triton-X addition at 300s. Legend: Lip refers to liposomes, Cont refers to control.

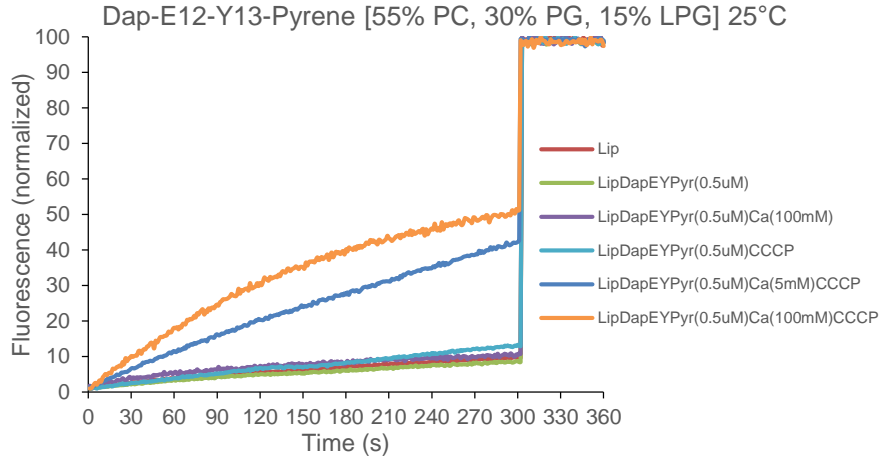


Figure 6.43 Liposome permeabilization test using dap-E12-Y13 in the presence of 5 (or 100) mM Ca^{2+} and 5 nM CCCP at 25 °C. Controls include lipopeptide alone or in the presence of either Ca^{2+} or CCCP. The excitation and emission wavelengths are 460 nm and 510 nm, respectively. Fluorescence is normalized to the highest signal after Triton-X addition at 300s. Legend: Lip refers to liposomes, Cont refers to control.

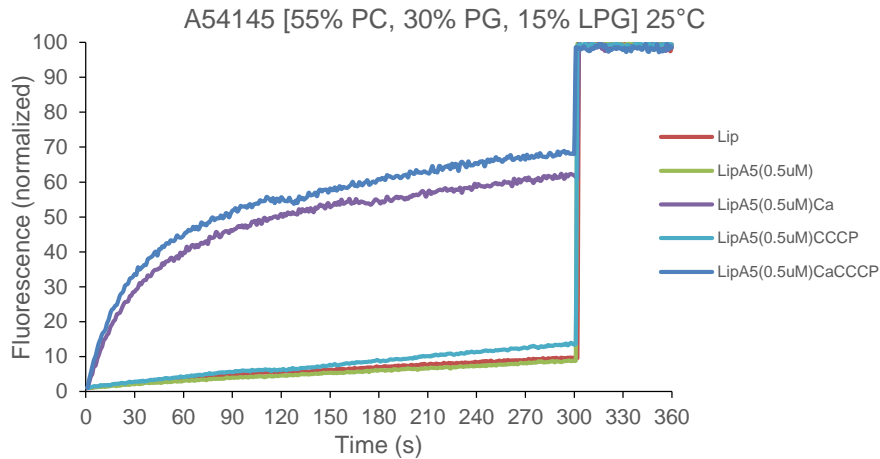


Figure 6.44 Liposome permeabilization test using A5 in the presence of 5 mM Ca^{2+} and 5 nM CCCP at 25 °C. Controls include lipopeptide alone or in the presence of either Ca^{2+} or CCCP. The excitation and emission wavelengths are 460 nm and 510 nm, respectively. Fluorescence is normalized to the highest signal after Triton-X addition at 300s. Legend: Lip refers to liposomes, Cont refers to control.

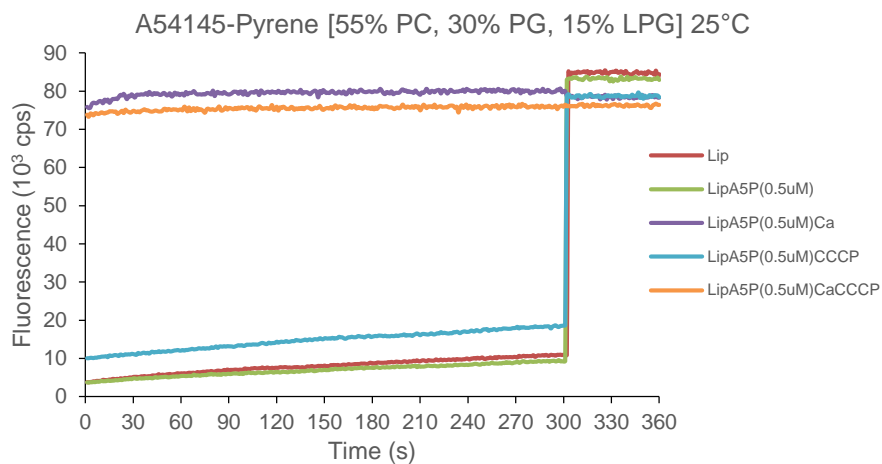


Figure 6.45 Liposome permeabilization test using A5-Pyrene in the presence of 5 mM Ca^{2+} and 5 nM CCCP at 25 °C. Controls include lipopeptide alone or in the presence of either Ca^{2+} or CCCP. The excitation and emission wavelengths are 460 nm and 510 nm, respectively. Fluorescence is not normalized due to the highest initial signal of A5-pyrene. Triton-X addition is continued at 300s. Legend: Lip refers to liposomes, Cont refers to control.